University of Alberta

A functional approach to profiling candidate genes in non model Brassicales

by

Peter James Mankowski

A thesis submitted to the Faculty of Graduate Studies and Research
in partial fulfillment of the requirements for the degree of

Master of Science
in
Systematics and Evolution

Biological Sciences

Spring 2013
Edmonton, Alberta

Dedication

This thesis is for everyone who struggles to pause and enjoy the view.

Abstract

Obtaining functional data is an essential component in understanding mechanisms underlying morphological variation. Virus-induced gene silencing (VIGS) is a reverse genetic technique for identifying the function of target loci through viral mediated transcript knockdown. Here we introduce this technique to two plant systems *Cleome violacea* (Cleomaceae) and *Erucaria erucarioides* (Brassicaceae) chosen for their morphological traits and phylogenetic position. In both species, a construct with a heterologous sequence and a construct with an endogenous sequence of the visual marker *PHYTOENE DESATURASE* (*PDS*) were incorporated into separate viral constructs for downregulation. Downregulation using a heterologous sequence produced a comparable fold change in transcript abundance to the endogenous sequence in both species however *C. violacea* was more susceptible to this process. Additional targets *FRUITFULL* (*FUL*) and a *TCP1* homologue were targeted for knockdown within *C. violacea* to extend the application of this technique. A protocol for VIGS application is now available to both species for optimization and future functional analysis.

Acknowledgements

I would like to thank my supervisor Jocelyn Hall who has always supported my academic career and with her guidance helped me to achieve my ambitious pursuits. I would also like to thank both of my committee members, Janice Cooke and Mike Deyholos who offered continuous concrete advice during the entirety of this project. I would like to thank Walid El Kayal whose unconditional mentoring and kindness served as a beacon during this journey.

I am truly indebted to both Kelsey Bernard and Melanie Patchell whose encouragement abilities are rivaled by no one. It has been an honor to work with them both. Thanks to my family who never fail to provide ongoing support in everything I set out to do.

Table of Contents

List of Tables

List of Figures

Chapter 1: Introduction to the methodology of virus-induced gene silencing (VIGS) and its profile as a transient RNAi technique

RNAi approach: Virus-induced gene silencing

A major question in evolutionary developmental genetics is understanding the basis of morphological diversity (Cronk et al., 2002; Kellogg, 2006; Friedman et al., 2008). In order to characterize the genetic changes responsible for morphological differences, researchers rely on a number of experimental approaches that generally entail a combination of phylogenetic analyses and molecular genetics of taxa with variation in traits of interest. To obtain the best picture of organismal diversity, many organisms need to be studied (Abzhanov et al., 2008). Often this is achieved by characterizing gene expression in related taxa with different morphologies. These comparative studies reveal conservation and deviation in gene-expression patterns associated with different morphologies. From there, genetic functional studies can test whether variation in the expression of a particular candidate gene is causally responsible for morphological differences. This last important step is often challenging when working with non-model organisms and may not always be practical with all species of interest.

Characterization of gene(s) requires functional data support. Determining the function of a gene allows for it's role to be established regarding a phenotype or trait. This pursuit is the basis of reverse genetics and encompasses the determination of a gene function to a known gene sequence. Reverse genetics is important for comparative research to assess the molecular mechanisms of novel morphological traits (Brakefield, 2011). When gene sequences with known functions have been established in model organisms, evaluating them in systems with different traits provides insight to both the premise of morphological novelty

and evidence for evolutionary development (Brakefield, 2011). Unfortunately, functional data is often lacking in species of interest.

The accessibility of reverse genetic techniques to non-model and emerging model taxa varies depending on the parameters of the technique and limitations of the target organism (Senthil-Kumar and Mysore, 2011; Huang et al., 2012). Establishing a methodology for a particular target system is often the first obstacle to using a reverse genetic methods in non-model organisms, especially those for which stable transformation approaches have not (or can not) be established.

Techniques such as transposon element knock down and hairpin induced RNAi are well established RNAi methods that have greatly contributed to functional analysis of genes within the genetic model *Arabidopsis* (Burch-Smith et al., 2004; Burch-Smith et al., 2006; Dinesh-Kumar et al., 2007; Purkayastha and Dasgupta, 2009; Becker and Lange, 2010). However, the applicability of these techniques stems from the plasticity of the *Arabidopsis* genome as well as a large previous body of genomic work (Liu et al., 2002a).

One technique that is rapidly becoming more accessible as a reverse genetic approach is virus-induced gene silencing (VIGS) (Ruiz et al., 1998; Baulcombe, 1999; Burch-Smith et al., 2004; Burch-Smith et al., 2006; Purkayastha and Dasgupta, 2009; Becker and Lange, 2010). VIGS is a technique which can be used to study loss-of-function mutations in plants through exploitation of their endogenous defense mechanism, post transcriptional gene silencing (PTGS), to block mRNA translation (Baulcombe, 1999). VIGS has been carried out on a wide range of plant systems including *Nicotiana tabacum*

(Solanaceae), *Pisum sativum* (Fabaceae), and *Arabidopsis thaliana* (Brassicaceae) (Kumagai et al., 1995; Ratcliff et al., 2001; Constantin et al., 2004). More recently a range of angiosperms have been utilized as VIGS targets: *Papaver somniferum* (Papaveraceae, core Eudicot) (Hileman et al., 2005); *Aquilegia formosa* (Ranunculaceae, basal Eudicot) (Kramer et al., 2007); *Glycine max* (Fabaceae, core Eudicot) (Igarashi et al., 2009); and *Zingiber officinal*e (Zingerberaceae, monocot) (Renner et al., 2009). Genes involved in flower development (Kramer and Jaramillo, 2003; Kramer et al., 2007; Sharma and Sharma, 2010), fruit development (Hileman et al., 2005) and pathogen response (Constantin et al., 2004) have all been subjected to VIGS demonstrating the diversity of application studies and functionality of this methodology.

VIGS entails the introduction of a recombinant viral vector (known as a construct) containing the gene sequence from the host being targeted for gene suppression (Baulcombe, 1999). This viral vector is integrated into the host cells where it is transcribed and produces dsRNA molecules. These dsRNA trigger PTGS and instigate the degradation of complementary mRNA transcripts preventing the expression of the homologous target gene (Figure 1.1). VIGS has been labeled as a rapid technique which is capable of correlating a known gene sequence with a mutant phenotype within a month's time (Lu et al., 2003; Burch-Smith et al., 2004). Although achievable, a large amount of coordination is required and nuances within experimental designs can extend this period.

VIGS functions upon the same cellular processes as other RNAi techniques (Baulcombe, 1999). PTGS is activated by the presence of a dsRNA

molecule (Baulcombe, 1999). These molecules are degraded by a selective endonuclease known as DICER which cuts the dsRNA molecules into small fragments known as small interfering RNA (siRNA) of 20-25 nucleotides in length (Donaire et al., 2008) (Figure 1.1). The siRNA molecules are then recruited by a protein complex known as RISC (RNA induced silencing complex) and melted into ssRNA fragments (Donaire et al., 2008). These fragments are held by a protein known as *ARGONAUTE* within the complex where they act as templates and complement with the endogenous transcripts of the cell (Donaire et al., 2008) (Figure 1.1). Therefore, the degree of sequence similarity between the endogenous mRNA and the transcribed viral dsRNA determines the efficacy of this process. If a match is found, the RISC complex signals it for degradation leading to the "knock down" of the gene originally replicated by the viral construct.

Many different viral strains have been used this assay, increasing the breadth of species that can be studied (Burch-Smith et al., 2004; Robertson, 2004; Godge et al., 2009; Becker and Lange, 2010). Originally, the PVX vector was used to silence genes in a few Solanaceae species (Ruiz et al., 1998; Liu et al., 2002a; Dinesh-Kumar et al., 2003). However, due to the specific nature of viral efficacy, additional viral strains have since been modified into viral constructs to target additional flowering plants (Burch-Smith et al., 2004). The viral vector chosen to complete a VIGS assay is dependent on the host organism as the virus must be able to infect and propagate throughout the plant (Ruiz et al., 1998; Dinesh-Kumar et al., 2003). Viruses such as TMW (tobacco mosaic virus), PVX

(potato virus X), CbLCV (cucumber) and TRV (tobacco rattle virus) are a select few of the virus strains available (Baulcombe, 1999; Ratcliff et al., 2001; Turnage et al., 2002; Burch-Smith et al., 2006). Originally, TMV was shown to be effective in the Brassicaceae species *Arabidopsis thaliana* (Baulcombe, 1999). More recent modifications to the virus TRV (strain pYL156) have created a strain that instigates more vigorous silencing due to a double 35S promoter and a ribozyme at the c-terminus (Ratcliff et al., 2001; Wang et al., 2006). VIGS viral vectors are unified by their standard Ti-Binary nature (Burch-Smith et al., 2004). In the case of TRV, two constructs, TRV1 and TRV2 are mixed together prior to infiltration to supply the necessary components for viral replication to take place (Ratcliff et al., 2001).

Exploitation of PTGS as a mechanism to downregulate gene expression requires a modification of a chosen viral strain into a recombinant construct followed by infection of the target species. VIGS therefore creates a simple workflow that involves the production of constructs that contribute to a viral library. Unlike other RNAi techniques the stability of the procedure occurs at the construct stage (Watson et al., 2005). Once assembled, a construct can be used repeatedly and depending on sequence similarity, on a range of target hosts. Because of these advantages, VIGS application was chosen as the method to establish functional data in two focal taxa. Due to the nature of VIGS, the methodology must be optimized for each new species of interest.

Overview of VIGS technique

The application of VIGS can be conceptually broken into three individual processes (Burch-Smith et al., 2004; Becker and Lange, 2010). The first is labeled construct design and encompasses obtaining the gene sequence of interest and developing a viral construct. The second process involves establishing a viral phenotype within focal species by inoculating then screening infected plants. Finally, the third stage involves supporting the phenotype with evidence of endogenous mRNA degradation, which traditionally has been done through reverse transcriptase PCR (RT-PCR) (Ruiz et al., 1998; Liu et al., 2002a; Liu et al., 2002b; Wang et al., 2006; Gould and Kramer, 2007). Recently, quantitative RT-PCR (qRT-PCR) has become a more reliable technique (Rotenberg et al., 2006; Gould and Kramer, 2007; Sharma et al., 2011).

This assay will determine how viral constructs are to be developed. Since VIGS can be used for a variety of purposes (genomic screening, evolutionary development etc.), the nature of the constructs can also vary. For example, if VIGS is used for a genome wide functional assay, cDNA or EST libraries may be incorporated into many individual viral vectors (Dong et al., 2007; Zhu et al., 2010). The majority of VIGS application falls within the scope of evolutionary developmental genetics and therefore utilizes ligation dependent vectors to create single gene targeting constructs (Burch-Smith et al., 2004). With this purpose established, viral construct inserts are usually designed with a specific candidate gene in mind. In these situations, genes are usually amplified, cloned, sequenced and then digested prior to ligation into the binary system ensuring the nature of silencing induced will be highly specific (Liu and Page, 2008).

For the purpose of downregulating an individual candidate gene for functional analysis, obtaining the sequence is required to initiate construct design. This can be readily done for species with published genomes, ESTs and sequence data. However, for most non-model organisms the gene sequence must first be obtained, often through an RT-PCR-based cloning strategy (Kramer et al., 1998; Kramer et al., 2003). Sequence information is essential for a successful VIGS application as it is required to confirm the identity of the sequence being associated with a mutant phenotype. Furthermore, the degree of sequence similarity between the construct and endogenous mRNA sequences influences the strength of the projected mutant phenotype (Thomas et al., 2001). Only 23 nucleotides of 100% sequence similarity is required to activate PTGS (Thomas et al., 2001). Thus, an insert as small as 23 nucleotides can be enough to carry out transcript silencing. However, most studies use constructs with longer target sequences, ranging from 200-1300 bp (Burch-Smith et al., 2004). Choosing a highly conserved region of a gene may silence other genes within the same gene family if they contain large amounts of sequence similarity (Burch-Smith et al., 2004). In order to ensure high penetrance of viral-based silencing, an insert sequence with multiple regions of identical 23 nucleotide segments is recommended (Liu and Page, 2008).

With the gene sequence known, primers are then designed to amplify the gene of interest for insertion into the viral vector system (Kramer and Jaramillo, 2003; Gould and Kramer, 2007; Sharma et al., 2011). Binary vector systems such as TRV require an insert to be placed into the multiple cloning site of one of the

two vectors (e.g. TRV2). This is commonly done using primers with amendable restriction enzyme sites that add the cut sites to the flanks of the amplified PCR products allowing for double digestion (Gould and Kramer, 2007; Sharma et al., 2011). Additionally, the viral vector can be double digested followed by ligation of the gene sequence into the system. Once successfully ligated, a completed viral construct must then be transformed into *Agrobacterium tumefaciens* for plant inoculation (Baulcombe, 1999).

The second phase of VIGS analysis involves growing and inoculating the plants being studied. Sufficient numbers must be grown for the multiple treatment groups typically used in these experiments: (1) control plants, which are simply transplanted, (2) mock treat plants, which are subjected to infiltration of empty viral constructs, and (3) treated plants which are subjected to infiltration by a viral construct containing a fragment of the gene target for silencing. In some cases, a positive treatment is also included in which the plants are exposed to a silencing construct previously shown to work (e.g. *PDS*) to provide a standard against another experimental construct (Sharma et al., 2011). Different plant maturities have been optimized for *Arabidopsis*, *Nicotiana* and tomato (Liu et al., 2002a; Dinesh-Kumar et al., 2003; Wang et al., 2006) with young seedlings producing the most efficacious results. However, optimal maturity will be species and question specific. For example, emerging model system *Aquilegia* requires vernalization (Kramer and Hodges, 2010). As such, VIGS experiments regarding floral development must be conducted on more mature plants (Kramer et al., 2003; Kramer et al., 2007; Sharma et al., 2011). Depending on the growth rate of

a species, coordinating when the seeds are sowed with the predicted construct assembly time may require seeds to be germinated in advance.

Once the construct assembly has been completed and the plants reach the appropriate stage, inoculation can be carried out. This process is highly dependent on the mechanism of inoculation chosen to infect the plants. Stabbing, syringe infection, floral dipping and vacuum infiltration have all been completed with varied results (Wang et al., 2006). Generally, vacuum infiltration is the most stable technique while the remaining procedures are easier to complete but effective on fewer organisms (Wang et al., 2006). However, some authors are concerned that vacuum infiltration and, its removal of seedlings from substrate, may have negative consequences for developmental studies (Wege et al., 2007).

Finally after mutant symptoms manifest, plant tissue is collected for RNA extraction and cDNA synthesis. Depending on the combination of the viral strain and silencing target, variable knock down penetrance can provide a range of phenotypes (Liu et al., 2002a; Burch-Smith et al., 2004; Rotenberg et al., 2006; Di Stilio et al., 2010). This characteristic of VIGS requires that a large number of individuals be screened for a mutant phenotype strong enough to provide information of the function of the gene target. Often, silenced individuals with similar symptoms are pooled into categorizes in the attempt to correlate phenotypic strength with mRNA transcript abundance (Rotenberg et al., 2006; Kramer et al., 2007; Di Stilio et al., 2010). Along with the silenced tissue, samples must be taken from both the negative control group (empty viral construct) and control (uninfected or wildtype) individuals. This is required for

comparative purposes in order to show that level of mRNA transcript abundance is reduced when compared to non-symptomatic individuals.

RT-PCR has been employed to compare relative RNA levels between viral infected and control specimens by normalizing the target gene against another reference gene that is constitutively expressed (Burch-Smith et al., 2004). More recent VIGS work has seen the employment of qRT-PCR for more rigous analysis of mRNA levels (Rotenberg et al., 2006; Sharma et al., 2011; Kawalek et al., 2012). qRT-PCR offers a method for comparison of transcript levels that is favored for its sensitivity and reliability as well as its ability to detect variation between samples (Brigneti et al., 2004; Rotenberg et al., 2006). The application of qRT-PCR requires a comprehensive experimental design that has been outlined in previous VIGS work (Livak and Schmittgen, 2001; Brigneti et al., 2004; Constantin et al., 2004; Ryu et al., 2004; Valentine et al., 2004; Rotenberg et al., 2006). The $2^{-\Delta\Delta Ct}$ method (Livak and Schmittgen, 2001) is most commonly used as an analysis method. $2^{-\Delta\Delta Ct}$ utilizes reference gene and candidate gene comparison to determine transcript fold changes within experimental groups. This is most likely the result of convenience and to reinforce the high throughput capability of VIGS, as the standard curve method requires a higher amount of time investment. However, application of the $2^{-\Delta\Delta Ct}$ method is dependent on the assumption that the amplification of the target and reference genes are equal within each sample. If this assumption is not met, it cannot be concluded that the relative differences between the detected genes accurately reflect differential

amounts of expression (Applied biosystems, 1998; Livak and scmittgen 2001; Zhang, Ruschhaupt and Biczok, 2012).

Both the relative standard curve method and the absolute standard curve method are possible alternatives to the $2^{-\Delta\Delta Ct}$ method that can be used to strengthen the evidence for transcript downregulation. As standard curve methods, both techniques require a standard curve to be initially produced for each reference and target genes from standard samples (e.g., plasmid DNA) (Applied Biosystems). A standard curve graph is then created by plotting the C_t values of the standard sample at multiple dilutions against known quantifications such as absorbance (A260) (Applied Biosystems). For absolute quantification, this curve is then used to directly assign a quantity to the unknown samples once their Ct is determined. For relative quantification, quantification is expressed relative to a calibrator sample similar to the $2^{-\Delta\Delta Ct}$ method (Applied Biosystems). Each unknown is quantified using a standard curve to obtain a value that can be divided by the quantity of the calibrator sample. Thus, the expression of the unknown samples is reported as a fold change (Applied Biosystems).

For each gene targeted for silencing, relative expression values must be determined under at least three experimental conditions (control, mock treated and treated) in order for transcript abundance to be associated with viral mediated PTGS. The gene *PHYTOENE DESATURASE* (*PDS*) is the established standard to assess the susceptibility of a plant species to VIGS (Kumagai et al., 1995; Ruiz et al., 1998). *PDS* is a gene involved in carotenoid biosynthesis (phytoene downstream target) and without its protection chlorophyll is destroyed by

photooxidation (Demmigadams and Adams, 1992). Silencing this gene results in an easily distinguishable white phenotype allowing for superifically assessment of penetrance before quantification of transcript knock down by qRT-PCR. Once *PDS* silencing has been established within focal species, other gene candidates can be chosen for functional knock down analysis.

Benefits to using VIGS

VIGS can be compared to other loss of function techniques for its ability to alter gene expression and determine its function (Burch-Smith et al., 2004). Both transposon activation and T-DNA insertions approaches create stable knock down phenotypes for functional analysis. However, these techniques are disadvantaged by their extensive time requirements. In order to observe a mutant phenotype, multiple generations of genetically modified lines must be crossed and grown to accumulate mutant progeny (Watson et al., 2005). Achieving a silenced phenotype within one generation increases efficiency of functional analysis as well as reduces the labour requirements spent screening progeny for mutant characteristics. Furthermore, VIGS' rapid timeframe for demonstrating a knock down phenotype allows this methodology to be used for screening purposes. Initially screening for a silenced phenotype will determine if a mutant phenotype is detectable prior to establishing a permanent mutant line (Becker and Lange, 2010). VIGS can establish if stable transformation for a line with a permanent phenotype is even viable.

The ability of VIGS to induce mutant phenotypes without stable transformation and generation of mutant lines is a unique characteristic to this loss

of function approach. Being able to produce a silenced phenotype within a single generation is beneficial for models with lengthy life cycles or for systems incapable of self crossing (Burch-Smith et al., 2004). Additionally, known embryo lethal genes can only be analyzed when knocked down in adult plants (Burch-Smith et al., 2004; Watson et al., 2005; Becker and Lange, 2010). Stable transformation techniques are incapable of studying these genes since mutated progeny will fail to germinate leaving VIGS as a promising alternative.

Many plant species are not amenable to stable genetic transformation techniques as the majority of this techniques were first established on model organisms included *Nicotiana tabacum* and *Arabidopsis thaliana*. These model organisms are easily crossable, highly susceptible to transformation (e.g. callus formation) and reproduce within a short period of time (Becker and Lange, 2010). Becker and Lange (2010) note that VIGS can be used to overcome the demands of loss of function methodologies by its transient infection and dependence upon viral infection. As additional viruses continue to be modified into vectors for VIGS analysis, the range of species which can be subjected to VIGS will continue to increase (Burch-Smith et al., 2004; Purkayastha and Dasgupta, 2009).

Limitations to using VIGS

Some parameters of VIGS assays can be viewed as limitations and therefore reduce the desirably of utilizing VIGS as a reverse genetics tool (Burch-Smith et al., 2004). The first limitation is the inability to induce a stable knock out. If additional silenced phenotypes need to be collected (e.g. more biological replicates) the entire inoculation has to be repeated. Furthermore, because this

procedure reduces mRNA transcript levels but does not eliminate them, some genes will not produce visible phenotypes if the function of the target gene can be completed at reduced transcript levels (Wege et al., 2007).

The reliance of VIGS on viral infection can restrict its application (Purkayastha and Dasgupta, 2009). Some crop strains carry viral resistant genes which could inhibit the virus from propagating throughout the plant and provide a discernible phenotype (Purkayastha and Dasgupta, 2009). Also, the duration and tissue site of infection of the viral silencing is dependent on the chosen strain. For this reason, viruses are capable of being passed to progeny while others cannot. Each viral strain allows has its own degree of viable penetrance along with the variable penetrance found between infected individuals. This can complicate the characterization of a mutant phenotype and make it difficult to assess the impact of downregulation without qRT-PCR support (Wege et al., 2007). Furthermore, this gradient in penetrance can make it difficult to accumulate biological replicates with similar symptoms for categorization of phenotypic conditions that satisfy a defined group of biological replicates.

While these limitations are impairing, one additional limitation that is of greater concern to researchers of non-model organisms is the ability of VIGs to silence multiple transcripts if they share a conserved sequence (Watson et al., 2005). Without a sequenced genome or transcriptome, copies and highly conserved homologues can be unintentionally silenced allowing for a falsification of the strength or parameters of a mutation phenotype to be correlated with the silencing of a single gene of interest. This limitation however is not always

defined as such since silencing multiple conserved members of the same family (Allen et al., 2004) or multiple difference genes may be a desirable outcome.

Using VIGS to target Non Model Systems

The ability of VIGS to be utilized by emerging model systems makes it an ideal methodology for evolutionary developmental genetic research. Specifically, when used in conjunction with traditional evolutionary biology (e.g. phylogenetics) and comparative genetic studies, VIGS can contribute to the analysis of phenotypic variation and morphological diversity (Abzhanov et al., 2008). A number of species across land plants are emerging as model species (Kramer, 2009). However, a minimum of one functional tool must be applied to each new model system in order to link gene expression profiles with gene functions. With its continually expanding breath of applicability, VIGS provides a necessary functional analysis approach for either type of system.

Two groups of emerging systems have been chosen for VIGS application as the focus of this thesis. The tribe Brassiceae (Brassicaceae) is monophyletic and exhibits tremendous diversity in fruit forms (Hall et al., 2006; Hall et al., 2011). Due to its close phylogenetic position with the model organism *Arabidopsis*, examination of this tribe provides the opportunity to study differences in dispersal capabilities between close and otherwise morphologically similar Brassiceae relatives (Fig. 1.2). Many Brassiceae members display a novel fruit type known as heteroarthrocarpy (Hall et al., 2006) which entails the lateral division of siliques into two segments by a structure called the joint (Appel, 1999). The distal segment is always indehiscent, whereas the proximal segment

may or may not open to release seeds. Closely-related *Cakile lanceolata* and *Erucaria erucarioides* display two major forms of heteroarthrocarpy (Hall et al., 2006; Hall et al., 2011). *Cakile* fruits are fully indehiscent and the joint separates (abscises) at maturity such that the two segments disperse independently from one another as protected propagules (Fig. 1.3). *Erucaria* is partially indehiscent and the joint does not abscise at maturity (Hall et al., 2006) (Fig. 1.3).

Differences in expression patterns of valve margin position genes are consistent with anatomical hypotheses on the origin of heteroarthrocarpy. The fruit-patterning network in *Arabidopsis* (Fig. 1.4) (Dinneny and Yanofsky, 2004; Dinneny et al., 2005) is a powerful model for examining fruit variation in relatives. Fruits of *Arabidopsis* are dependent on the proper formation of three regions: (1) valves, which fall off fruit to release seeds, (2) replum, which is the persistent placental tissue, and (3) the valve-margin, which is a narrow band of cells between the valves and replum. The valve-margin is comprised of the cells that degrade to release the valves. Valve margin identity is determined by combined activities of *SHATTERPROOF1* (*SHP1*), *SHATTERPROOF2* (*SHP2*), *ALCATRAZ* (*ALC*), and *INDEHISCENT* (*IND*) (Dinneny and Yanofsky, 2004; Dinneny et al., 2005; Avino et al., 2012). The position of the valve is determined by two additional genes, *FRUITFULL* (*FUL*) and *REPLUMLESS* (*RPL*), which are expressed in the valves and replum, respectively (Dinney and Yanofsky, 2004; Dinneny et al., 2005). Both *FUL* and *RPL* prevent the expression of the valve margin identity genes, thereby positioning the placement of the valve margin.

This network serves as a model to predict how changes in gene expression made lead to modifications in fruit morphology observed in Brassiceae. Basically, heteroarthrocarpy entails the re-positioning of the valve margin to only the proximal or bottom portion of heteroarthrocarpic fruits (Hall et al., 2006). We have identified a total of 12 homologous loci from both species (Avino et al., 2012), representing all components of the pathway described in *Arabidopsis*. All twelve loci were assessed for their spatial and temporal expression patterns using *in situ* hybridization at various maturity states starting with young buds to post-fertilization mature fruit (Avino et al., 2012). From *Cakile* the homologous of *ClALC*, *ClRPL*, *ClFUL1*, *ClFUL2*, *ClSHP1* and *ClSHP2* were studied. From *Erucaria* the homologues of *EeALC, EeRPL, EeFUL1, EeFUL2* and *EeIND* were identified and studied comparatively with the non-heteroarthrocarpic species *Arabidopsis thaliana*.

From the species *Erucaria erucarioides*, the loci *EeFUL1* and *EeFUL2* were of particular interest due to their divergence expression compared to *FUL* (Avino et al. 2012). *EeFUL1* was found within the valves of the developing fruit specifically within the proximal inner mesocarp layer and end*b* layer (Avino et al., 2012). This reduced expression pattern is parallel with the dehiscent regions of the mature fruit and suggests that the expression of these loci is associated with the maintenance of dehiscence. Because *EeFUL1* valve expression is only in proximal portion of fruit when compared to *Arabidopsis*, it has been proposed that the change in regional expression contributed to the establishment of heteroarthrocarpy (Avino et al., 2012). The *EeFUL1* profile has been interpreted

to support the hypothesis that the valves within this fruit type are dissociated from the replum and that only the proximal region fully matures as an ovary (Avino et al., 2012; Hall et al., 2006). The distal segment lacking in *EeFUL1* expression is incapable of dehiscing and therefore associates *EeFUL1* expression with the separate dehiscence profiles of the proximal and distal fruit segments. By downregulating *EeFUL1* by means of VIGS within partially indehiscent *E. erucarioides* we hypothesized that the ability of the joint to abscise will be lost. The resulting mutant phenotype will thereby support joint morphology as a result of relocalization of distal valve margin tissue through differential *FUL* expression compared to that of fully dehiscent non-heteroarthrocarpic fruit (e.g. *Arabidopsis thaliana*). Ideally, we will further support the role of this locus in the maintenance of heteroarthrocarpy and the conservation of the genes associated with valve margin identity within the Brassieae by contributing functional data along with the previous the expression analysis.

Within the species *Cakile lanceolata* only *ClALC*, *CLSHP1* and *ClSHP2* where detected with in suit hybridization (Avino et al., 2012). It has been proposed that *SHP1/2* play redundant roles in the development and maturation of the ovary wall as these loci have very similar expression profiles (Avino et al., 2012). The absence of both *ClSHP1* and *ClSHP2* from the mature valve tissue of the *Cakile* fruit is believed to be associated with a completely indehiscent morphology supporting and suggestive of their requirement for development of a joint that can abscise as a result of functional valve margin tissue (Avino et al., 2012, Hall et al., 2006). Future work targeting both of these genes for functional

analysis will better elucidate the regulation of this fruit morphology. Ultimately, understanding the genetic basis of this morphological variation between both species will provide insight on the evolution of plant dispersal.

Cleomaceae is the sister family to the Brassicaceae and offers another excellent focus for evolutionary development genetic inquiries (Fig. 1.2). This family displays a great deal of morphological variation compared to the Brassicaceae, especially regarding flowers. In particular, the monosymmetric (zygomorphic) flowers of Cleomaceae species represent an opportunity to investigate the basis of floral symmetry through comparative evolutionary developmental work with members of the Brassicaceae (Patchell et al., 2011). Importantly, genomic resources are being developed for this group (Schranz and Mitchell-Olds, 2006; Schranz et al., 2007). Callus formation followed stable *Agrobacterium* transformation has been successful in two species, *Cleome gynandra* and *Cleome spinosa* (Newell et al., 2010; Tsai et al., 2012). Once VIGS has been successfully established as a tool applicable to Cleomaceae species, gene knock down will complement this group with a transient functional analysis approach. Establishing this technique will allow for homologues of relative model organisms to be targeted within these non model species for knock down.

My Masters project aims to outline a methodology that will be used to better understand the genetic basis of two important traits associated with plant propagation, heteroarthrocarpy and monosymmetry. It is my goal to establish the use of VIGS on non model Brassiceae to provide support for individual gene functions within the heteroarthrocarpic fruit patterning network. Additionally,

VIGS functional assays will be conducted to outline the developmental premise of the Cleomaceae floral symmetry network.

Figures

Figure 1.1. Overview of the mechanism of action of VIGS inoculation and the resulting viral systemic spread (Modified from Becker and Lange, 2010). A cDNA fragment is used to make a viral pTRV2 construct which is paired with pTRV1 for seedling inoculation mediated by Agrobacterium. The viral construct is replicated endogenously to produce a dsRNA molecule that triggers the post-transcriptional gene silencing (PTGS) response and activates the enzyme DICER. The double stranded RNA molecule is cleaved in siRNA molecules that are recruited by ARGONAUTE as templates for identification and degradation of complementary transcripts.

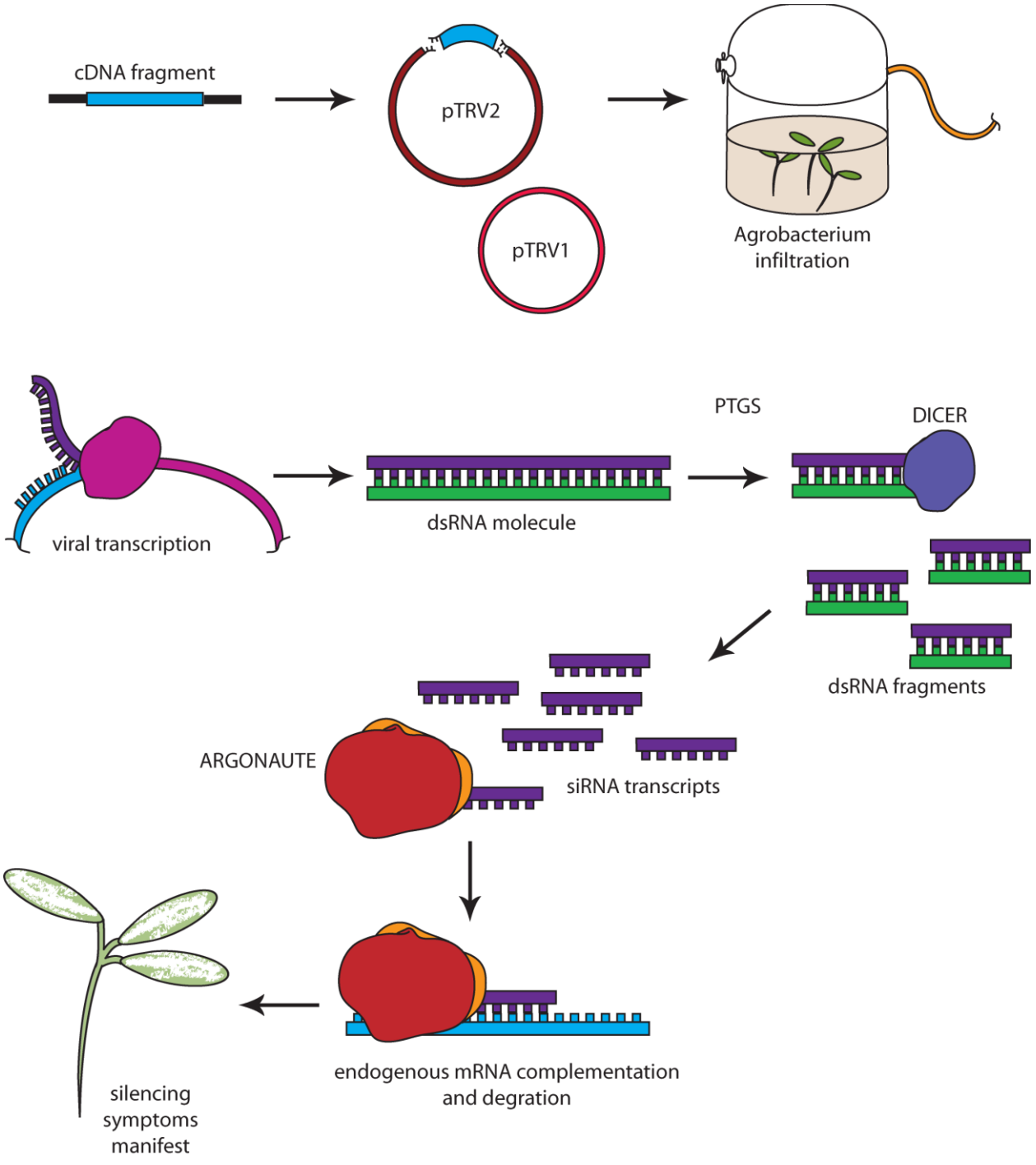
cDNA fragment
pTRV2
pTRV1
Agrobacterium
infiltration
viral transcription
dsRNA molecule
PTGS
DICER
dsRNA fragments
ARGONAUTE
siRNA transcripts
endogenous mRNA complementation
and degration
silencing
symptoms
manifest

Figure 1.2. Schematic of the phylogenetic relationships between the focal families Cleomaceace and Brassiceaeae. Relative placement of focal taxa *Cleome violacea*, *Erucaria erucarioides* and *Arabidopsis thaliana* have been indicated with labeled arrows. The remainder of the order Brassicales serves as the outgroup for this schematic.

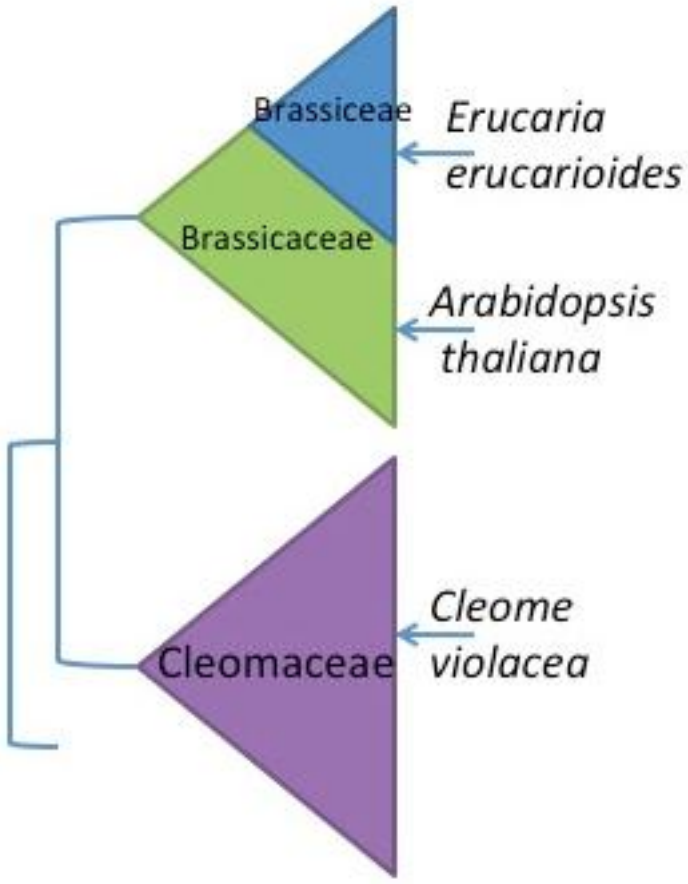

Figure 1.3. Photographic data of the heteroarthrocarpic fruit morphology. (A) Fruits of *Erucaria erucarioides* have a dehiscent proximal (bottom) segment, whereas fruits of (B) *Cakile lanceolata* are completely indehiscent. Arrowhead is joint, which only abscises in *Cakile lanceolata*. Scale-bars = 0.5 cm (reprinted with permission from Hall et al., 2006).

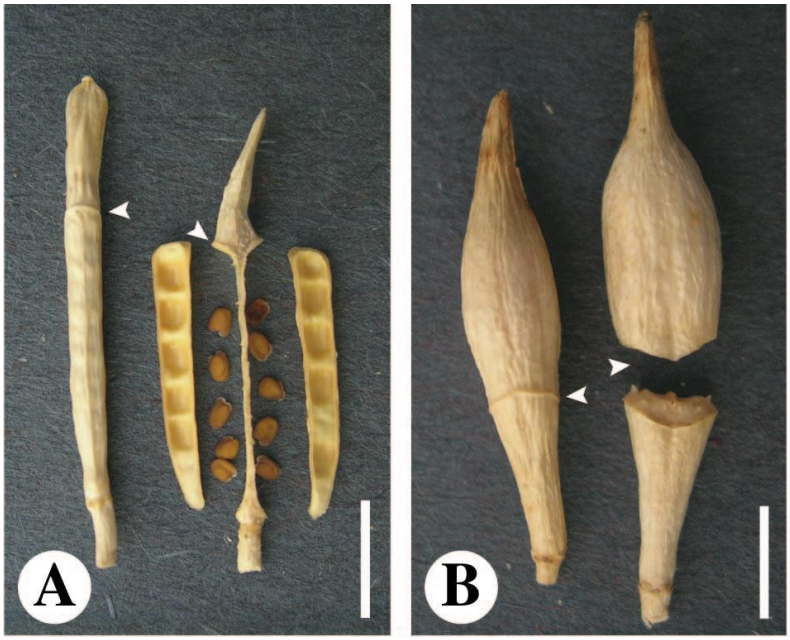

Figure 1.4. Comparison of the network of identified loci involved in valve margin development between focal taxa, including summary of gene expression data (reprinted with permission from Avino et al., 2012).

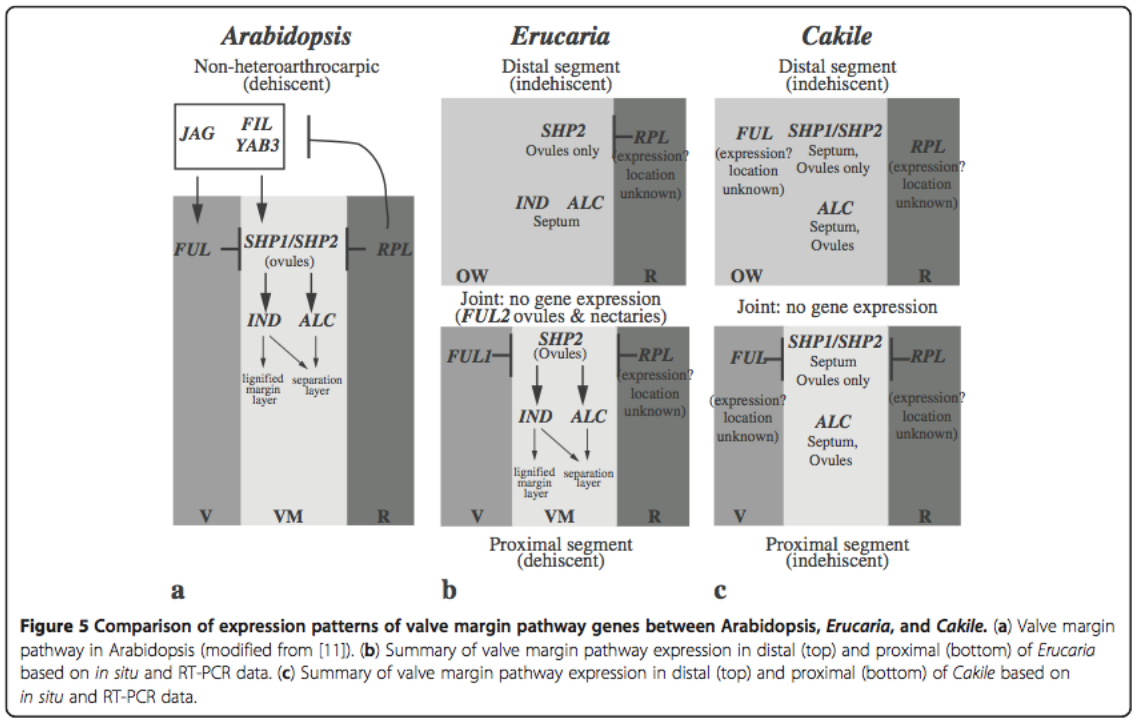

Figure 5 Comparison of expression patterns of valve margin pathway genes between Arabidopsis, *Erucaria*, and *Cakile*. (**a**) Valve margin pathway in Arabidopsis (modified from [11]). (**b**) Summary of valve margin pathway expression in distal (top) and proximal (bottom) of *Erucaria* based on *in situ* and RT-PCR data. (**c**) Summary of valve margin pathway expression in distal (top) and proximal (bottom) of *Cakile* based on *in situ* and RT-PCR data.

Literature Cited

Abzhanov, A., Extavour, C.G., Groover, A., Hodges, S.A., Hoekstra, H.E., Kramer, E.M., and Monteiro, A. (2008). Are we there yet? Tracking the development of new model systems. Trends in Genetics **24,** 353-360.

Allen, E., Xie, Z.X., Gustafson, A.M., Sung, G.H., Spatafora, J.W., and Carrington, J.C. (2004). Evolution of microRNA genes by inverted duplication of target gene sequences in *Arabidopsis thaliana*. Nature Genetics **36,** 1282-1290.

Appel, O. (1999). The so-called 'beak', a character in the systematics of Brassicaceae? . Botanische Jahrbücher für Systematik Pflanzengeschichte und Pflanzengeographie **121,** 85-98.

Avino, M., Kramer, E.M., Donohue, K., Hammel, A.J., and Hall, J.C. (2012). Understanding the basis of a novel fruit type in Brassicaceae: conservation and deviation in expression patterns of six genes. EvoDevo **3,** 20.

Baulcombe, D.C. (1999). Fast forward genetics based on virus-induced gene silencing. Current Opinion in Plant Biology **2,** 109-113.

Becker, A., and Lange, M. (2010). VIGS - genomics goes functional. Trends in Plant Science **15,** 1-4.

Brakefield, P.M. (2011). Evo-devo and accounting for Darwin's endless forms. Philosophical Transactions of the Royal Society B-Biological Sciences **366,** 2069-2075.

Brigneti, G., Martin-Hernandez, A.M., Jin, H., Chen, J., Baulcombe, D.C., Baker, B., and Jones, J.D. (2004). Virus-induced gene silencing in *Solanum* species. Plant Journal **39,** 264-272.

Burch-Smith, T.M., Anderson, J.C., Martin, G.B., and Dinesh-Kumar, S.P. (2004). Applications and advantages of virus-induced gene silencing for gene function studies in plants. Plant Journal **39,** 734-746.

Burch-Smith, T.M., Schiff, M., Liu, Y., and Dinesh-Kumar, S.P. (2006). Efficient virus-induced gene silencing in *Arabidopsis*. Plant Physiology **142,** 21-27.

Constantin, G.D., Krath, B.N., MacFarlane, S.A., Nicolaisen, M., Johansen, I.E., and Lund, O.S. (2004). Virus-induced gene silencing as a tool for functional genomics in a legume species. Plant Journal **40,** 622-631.

Cronk, Q.C.B., Bateman, R.M., and Hawkins, J.A. (2002). Developmental genetics and plant evolution. (London, UK: Taylor and Francis).

Demmigadams, B., and Adams, W.W. (1992). Photoprotection and other responses of plants to high light stress. Annual Review of Plant Physiology and Plant Molecular Biology **43,** 599-626.

Di Stilio, V.S., Kumar, R.A., Oddone, A.M., Tolkin, T.R., Salles, P., and McCarty, K. (2010). Virus-induced gene silencing as a tool for comparative functional studies in *Thalictrum*. Plos One **5,** 1-9.

Dinesh-Kumar, S.P., Anandalakshmi, R., Marathe, R., Schiff, M., and Liu, Y. (2003). Virus-induced gene silencing. Methods in Molecular Biology **236,** 287-294.

Dinesh-Kumar, S.P., Burch-Smith, T., Liu, Y., Schiff, M., Dong, Y., Zhu, X., and Mamillapalli, P. (2007). Virus-induced gene silencing (VIGS) for gene function studies in plants. Phytopathology **97,** S145-S145.

Dinneny, J.R., and Yanofsky, M.F. (2004). Drawing line and borders: how the dehiscent fruit of *Arabidopsis* is patterned. Bioessays **27,** 42-49.

Dinneny, J.R., Weigel, D., and Yanofsky, M.F. (2005). A genetic framework for fruit patterning in *Arabidopsis thaliana*. Development **132,** 4687-4696.

Donaire, L., Barajas, D., Martinez-Garcia, B., Martinez-Priego, L., Pagan, I., and Llave, C. (2008). Structural and genetic requirements for the biogenesis of tobacco rattle virus-derived small interfering RNAs. Journal of Virology **82,** 5167-5177.

Dong, Y., Burch-Smith, T.M., Liu, Y., Mamillapalli, P., and Dinesh-Kumar, S.P. (2007). A ligation-independent cloning tobacco rattle virus vector for high-throughput virus-induced gene silencing identifies roles for *NbMADS4-1* and *-2* in floral development. Plant Physiology **145,** 1161-1170.

Friedman, W.E., Barrett, S.C.H., Diggle, P.K., Irish, V.F., and Hufford, L. (2008). Whither plant evo-devo? New Phytologist **178,** 468-471.

Godge, M.R., Purkayastha, A., Dasgupta, I., and Kumar, P.P. (2009). Virus-induced gene silencing for functional analysis of selected genes. Plant Cell Reports **28,** 335-335.

Gould, B., and Kramer, E.M. (2007). Virus-induced gene silencing as a tool for functional analyses in the emerging model plant *Aquilegia* (columbine, Ranunculaceae). Plant Methods **3,** 6.

Hall, J.C., Tisdale, T.E., Donohue, K., and Kramer, E.M. (2006). Developmental basis of an anatomical novelty: heteroarthrocarpy in *Cakile lanceolata* and *Erucaria erucarioides* (Brassicaceae). International Journal of Plant Sciences **167,** 771-789.

Hall, J.C., Tisdale, T.E., Donohue, K., Wheeler, A., Al-Yahya, M.A., and Kramer, E.M. (2011). Convergent evolution of a complex fruit structure in the tribe Brassiceae (Brassicaceae). American Journal of Botany **98,** 1989-2003.

Hileman, L.C., Drea, S., de Martino, G., Litt, A., and Irish, V.F. (2005). Virus-induced gene silencing is an effective tool for assaying gene function in the basal eudicot species *Papaver somniferum* (opium poppy). Plant Journal **44,** 334-341.

Huang, C.J., Qian, Y.J., Li, Z.H., and Zhou, X.P. (2012). Virus-induced gene silencing and its application in plant functional genomics. Science China-Life Sciences **55,** 99-108.

Igarashi, A., Yamagata, K., Sugai, T., Takahashi, Y., Sugawara, E., Tamura, A., Yaegashi, H., Yamagishi, N., Takahashi, T., Isogai, M., Takahashi, H., and Yoshikawa, N. (2009). Apple latent spherical virus vectors for reliable and effective virus-induced gene silencing among a broad range of

plants including tobacco, tomato, *Arabidopsis thaliana*, cucurbits, and legumes. Virology **386,** 407-416.

Kawalek, A., Dmochowska-Boguta, M., Nadolska-Orczyk, A., and Orczyk, W. (2012). A new BSMV-based vector with modified beta molecule allows simultaneous and stable silencing of two genes. Cellular & Molecular Biology Letters **17,** 107-123.

Kellogg, E.A. (2006). Progress and challenges in studies of the evolution of development. Journal of Experimental Botany **57,** 3505-3516.

Kramer, E.M. (2009). Chapter 4. New model systems for the study of developmental evolution in plants. Current Topics in Developmental Biology **86,** 67-105.

Kramer, E.M., and Jaramillo, M.A. (2003). The role of *APETALA3* and *PISTILLATA* homologs in the production of novel floral morphologies. Developmental Biology **259,** 456-456.

Kramer, E.M., and Hodges, S.A. (2010). *Aquilegia* as a model system for the evolution and ecology of petals. Philosophical Transactions of the Royal Society B-Biological Sciences **365,** 477-490.

Kramer, E.M., Dorit, R.L., and Irish, V.F. (1998). Molecular evolution of genes controlling petal and stamen development: Duplication and divergence within the *APETALA3* and *PISTILLATA* MADS-box gene lineages. Genetics **149,** 765-783.

Kramer, E.M., Di Stilio, V.S., and Schluter, P.M. (2003). Complex patterns of gene duplication in the *APETALA3* and *PISTILLATA* lineages of the Ranunculaceae. International Journal of Plant Sciences **164,** 1-11.

Kramer, E.M., Holappa, L., Gould, B., Jaramillo, M.A., Setnikov, D., and Santiago, P.M. (2007). Elaboration of B gene function to include the identity of novel floral organs in the lower eudicot *Aquilegia*. Plant Cell **19,** 750-766.

Kumagai, M.H., Donson, J., Dellacioppa, G., Harvey, D., Hanley, K., and Grill, L.K. (1995). Cytoplasmic inhibition of carotenoid biosynthesis with virus-derived RNA. Proceedings of the National Academy of Sciences of the United States of America **92,** 1679-1683.

Liu, E., and Page, J.E. (2008). Optimized cDNA libraries for virus-induced gene silencing (VIGS) using tobacco rattle virus. Plant Methods **4,** 5.

Liu, Y., Schiff, M., and Dinesh-Kumar, S.P. (2002a). Virus-induced gene silencing in tomato. Plant Journal **31,** 777-786.

Liu, Y.L., Schiff, M., Marathe, R., and Dinesh-Kumar, S.P. (2002b). Tobacco Rar1, *EDS1* and *NPR1*/*NIM1* like genes are required for N-mediated resistance to tobacco mosaic virus. Plant Journal **30,** 415-429.

Livak, K.J., and Schmittgen, T.D. (2001). Analysis of relative gene expression data using real-time quantitative PCR and the $2^{-\Delta\Delta C}_{T}$ method. Methods **25,** 402-408.

Lu, R., Martin-Hernandez, A.M., Peart, J.R., Malcuit, I., and Baulcombe, D.C. (2003). Virus-induced gene silencing in plants. Methods **30,** 296-303.

Newell, C.A., Brown, N.J., Liu, Z., Pflug, A., Gowik, U., Westhoff, P., and Hibberd, J.M. (2010). Agrobacterium tumefaciens-mediated transformation of *Cleome gynandra* L., a C-4 dicotyledon that is closely related to *Arabidopsis thaliana*. Journal of Experimental Botany **61,** 1311-1319.

Patchell, M.J., Bolton, M.C., Mankowski, P., and Hall, J.C. (2011). Comparative floral development in Cleomaceae reveals two distinct pathways leading to monosymmetry. International Journal of Plant Sciences **172,** 352-365.

Purkayastha, A., and Dasgupta, I. (2009). Virus-induced gene silencing: A versatile tool for discovery of gene functions in plants. Plant Physiology and Biochemistry **47,** 967-976.

Ratcliff, F., Martin-Hernandez, A.M., and Baulcombe, D.C. (2001). Technical Advance. Tobacco rattle virus as a vector for analysis of gene function by silencing. Plant Journal **25,** 237-245.

Renner, T., Bragg, J., Driscoll, H.E., Cho, J., Jackson, A.O., and Specht, C.D. (2009). Virus-Induced Gene Silencing in the culinary ginger (*Zingiber officinale*): An effective mechanism for down-regulating gene expression in tropical monocots. Molecular Plant **2,** 1084-1094.

Robertson, D. (2004). VIGS vectors for gene silencing: Many targets, many tools. Annual Review of Plant Biology **55,** 495-519.

Rotenberg, D., Thompson, T.S., German, T.L., and Willis, D.K. (2006). Methods for effective real-time RT-PCR analysis of virus-induced gene silencing. Journal of Virology Methods **138,** 49-59.

Ruiz, M.T., Voinnet, O., and Baulcombe, D.C. (1998). Initiation and maintenance of virus-induced gene silencing. Plant Cell **10,** 937-946.

Ryu, C.M., Anand, A., Kang, L., and Mysore, K.S. (2004). Agrodrench: a novel and effective agroinoculation method for virus-induced gene silencing in roots and diverse Solanaceous species. Plant Journal **40,** 322-331.

Schranz, M.E., and Mitchell-Olds, T. (2006). Independent ancient polyploidy events in the sister families Brassicaceae and Cleomaceae. Plant Cell **18,** 1152-1165.

Schranz, M.E., Song, B.H., Windsor, A.J., and Mitchell-Olds, T. (2007). Comparative genomics in the Brassicaceae: a family-wide perspective. Current Opinion in Plant Biology **10,** 168-175.

Senthil-Kumar, M., and Mysore, K.S. (2011). New dimensions for VIGS in plant functional genomics. Trends in Plant Science **16,** 656-665.

Sharma, B., Guo, C., Kong, H., and Kramer, E.M. (2011). Petal-specific subfunctionalization of an *APETALA3* paralog in the Ranunculales and its implications for petal evolution. New Phytol **191,** 870-883.

Sharma, S., and Sharma, R.K. (2010). Seed physiological aspects of pushkarmool (*Inula racemosa*), a threatened medicinal herb: response to storage, cold stratification, light and gibberellic acid. Current Science **99,** 1801-1806.

Thomas, C.L., Jones, L., Baulcombe, D.C., and Maule, A.J. (2001). Size constraints for targeting post-transcriptional gene silencing and for RNA-directed methylation in *Nicotiana benthamiana* using a potato virus X vector. Plant Journal **25,** 417-425.

Tsai, Y.T., Chen, P.Y., and To, K.Y. (2012). Plant regeneration and stable transformation in the floricultural plant *Cleome spinosa*, a C-3 plant closely related to the C-4 plant *C. gynandra*. Plant Cell Reports **31,** 1189-1198.

Turnage, M.A., Muangsan, N., Peele, C.G., and Robertson, D. (2002). Geminivirus-based vectors for gene silencing in *Arabidopsis*. Plant Journal **30,** 107-114.

Valentine, T., Shaw, J., Blok, V.C., Phillips, M.S., Oparka, K.J., and Lacomme, C. (2004). Efficient virus-induced gene silencing in roots using a modified tobacco rattle virus vector. Plant Physiology **136,** 3999-4009.

Wang, C.C., Cai, X.Z., Wang, X.M., and Zheng, Z. (2006). Optimisation of tobacco rattle virus-induced gene silencing in *Arabidopsis*. Functional Plant Biology **33,** 347-355.

Watson, J.M., Fusaro, A.F., Wang, M., and Waterhouse, P.M. (2005). RNA silencing platforms in plants. FEBS Letters **579,** 5982-5987.

Wege, S., Scholz, A., Gleissberg, S., and Becker, A. (2007). Highly efficient virus-induced gene silencing (VIGS) in california poppy (*Eschscholzia californica*): An evaluation of VIGS as a strategy to obtain functional data from non-model plants. Annals of Botany **100,** 641-649.

Zhu, X., Pattathil, S., Mazumder, K., Brehm, A., Hahn, M.G., Dinesh-Kumar, S.P., and Joshi, C.P. (2010). Virus-induced gene silencing offers a functional genomics platform for studying plant cell wall formation. Molecular Plant **3,** 818-833.

Chapter 2 Virus-induced gene silencing as a tool for functional studies in relatives of *Arabidopsis thaliana*

Introduction

A number of new model organisms are emerging across angiosperms as a powerful approach to investigate the evolution of morphological diversity (Abzhanov et al., 2008; Kramer, 2009). These taxa are chosen for their phylogenetic position as well as their morphological innovations, typically not present in model species. Close relatives of model species offer an excellent opportunity to study both conservation and divergence in genetic programs underlying variation, while allowing researchers to use the vast genetic knowledge of model species to formulate hypotheses. For example, within Brassicaceae, the family that houses *Arabidopsis thaliana*, there is tremendous variation in fruit morphology (Koch et al., 2003; Mummenhoff et al., 2009; Franzke et al., 2011). Thus, examination of species with variable fruit morphologies will lead to a better understanding of differences underlying seed dispersal (Hall, in press). However, floral morphology is remarkable similar across the 3000 plus species in Brassicaceae (Koch et al., 2003) and, as such, does not permit the study of floral diversity (but see Busch and Zachgo, 2007; Busch et al., 2012). Fortunately, members of Cleomaceae, sister family to Brassicaceae, exhibit tremendous variation in floral form and are known for their monosymmetric flowers (Endress, 1992; Hall et al., 2002; Iltis et al., 2011; Patchell et al., 2011), a trait of clear importance to plant-pollinator interactions (Cubas, 2004).

We propose the development of two species as emerging models, *Cleome violacea* (Cleomaceae) and *Erucaria erucarioides* (Brassicaceae), both of which

exhibit traits not present in *Arabidopsis*. The fruits of *E. erucarioides* display variable dehiscence and segmentation (termed heteroarthrocarpy), which dramatically alters how seeds are dispersed when compared to *Arabidopsis.* Moreover, a range of complementary studies, including phylogenetic (Hall et al., 2011), developmental (Hall et al., 2006), and comparative gene expression (Avino et al., 2012) inquiries, provide a strong foundation for understanding mechanisms underlying differences in fruit morphology. *Cleome violacea* offers perhaps greater potential for a new macroevolutionary model as there is a larger community of researchers interested in a range of attributes of this taxon. Floral development studies provide insight into how and when these flowers become monosymmetric (Karrer, 1991; Erbar and Leins, 1997; Patchell et al., 2011). In addition, members of the family are the closest relative to *Arabidopsis* with C-4 photosynthesis (Brown et al., 2005; Marshall et al., 2007; Voznesenskaya et al., 2007; Feodorova et al., 2010). The family has also undergone an independent polyploidy event from Brassicaceae and has been of interest to comparative genomic researchers (Schranz and Mitchell-Olds, 2006; Barker et al., 2009). Thus, both focal species are well suited for additional evolutionary developmental investigations and are need development of functional methodologies.

Emerging macroevolutionary models are established to elucidate mechanisms by which novel morphological traits arise (Abzhanov et al., 2008). Once selected, new systems are subjected to comparative gene expression work in conjunction with functional or transgene assays to define the cause of variation for a specific trait (Abzhanov et al., 2008). Developing these two species as

emerging model systems requires the appropriate complement of tools and resources for comparative work to occur (Abzhanov et al., 2008; Di Stilio, 2011). For macroevolutionary models, gene sequences must be obtained and subjected to phylogenetic analysis, expression studies must be carried out (e.g. *in situ* hybridization) and functional assay techniques must support the expression data (Abzhanov et al., 2008). These three approaches in coordination can establish gene profiles which can be used to propose the origin or process responsible for a novel morphology (Abzhanov et al., 2008).

Functional analysis of gene candidates has been identified as a major limiting factor in establishing new model systems (Abzhanov et al., 2008; Di Stilio et al., 2010). Many concrete characteristics of potential model plants are of importance for functional analyses making few plants susceptible to this process (Burch-Smith et al., 2004). Life cycle duration, reproducibility and subjectivity to transformation are just a few of the determining factors which limit the species subject to functional work (Burch-Smith et al., 2004; Di Stilio et al., 2010). However, a recently developed technique known as virus-induced gene silencing (VIGS) has become a favorite of developmental-evolutionary biologists for its vast plant target range and rapid production of data (Burch-Smith et al., 2004; Purkayastha and Dasgupta, 2009; Becker and Lange, 2010; Di Stilio et al., 2010).

VIGS uses RNA interference to exploit the plant defense mechanism post-transcription gene silencing (PTGS) and prevent endogeneous mRNA from being translated (Ruiz et al., 1998; Baulcombe, 1999; Burch-Smith et al., 2004; Becker and Lange, 2010). VIGS provides the opportunity to knock down individual loci

in a relatively simple manner and determine specific gene functions through the resulting phenotype (Baulcombe, 1999; Gould and Kramer, 2007; Purkayastha and Dasgupta, 2009; Becker and Lange, 2010). This technique requires the use of a viral construct containing a fragment of the target loci to elicit the PTGS response (Ruiz et al., 1998; Baulcombe, 1999). Infection of the viral construct is mediated by *Agrobacterium* transformation followed by infiltration (Dinesh-Kumar et al., 2003). A modified Tobacco Rattle Virus (TRV) strain has been shown to be the most efficacious for silencing in brassicaceous species (Bachan and Dinesh-Kumar; Ratcliff et al., 2001; Wang et al., 2006; Donaire et al., 2008). Most commonly, the gene *PHYTOENE DESATURASE* (*PDS*) is initially silenced to determine the efficacy and optimize the technique in a newly chosen model (Liu et al., 2002a; Gould and Kramer, 2007; Wege et al., 2007; Di Stilio et al., 2010).

VIGS has become increasingly utilized for its favorable transient silencing capability and limited system requirements (Burch-Smith et al., 2004; Becker and Lange, 2010; Di Stilio, 2011). As a result, resources have been developed for increasing the ability to access VIGS components and incorporate the methodology to novel pursuits. Since the technique has been established and optimized on *Nicotiana tabacum* and *Arabidopsis thaliana*, complete constructs are now available for both species (Bachan and Dinesh-Kumar; Hayward et al.; Dinesh-Kumar et al., 2003; Burch-Smith et al., 2006b; Wang et al., 2006). Because VIGS is dependent on sequence similarity, phylogenetically similar species can be targeted for gene silencing using heterologous sequences (Fofana

et al., 2004; Senthil-Kumar et al., 2007). Thus, orthologues of genes from species with sequence data can be used to induce silencing in related species using VIGS (Senthil-Kumar et al., 2007). Previously, the *PDS* sequence from *Nicotiana benthamiana* was used to silence *PDS* in seven other species demonstrating the methodology as a viable tool for these additional systems (Senthil-Kumar et al., 2007). However, this approach as not yet been examined with relatives of *Arabidopsis* in order to test the viability of using constructs with *PDS* sequence from this species to identify additional species amenable to VIGS. Now with readily available constructs and published protocols, introducing VIGS to new models can be done faster than ever (Hayward et al.; Liu et al., 2002b; Dinesh-Kumar et al., 2003; Burch-Smith et al., 2006a). Being that the dependent factor is the degree of sequence similarity, choosing the species of close phylogenetic distance is advisable, especially if the sequence being targeted in the new system is not yet known (Senthil-Kumar et al., 2007).

VIGS protocols must be tailored for each new species. First, we introduced the methodology of VIGS to two relatives of *Arabidopsis* to establish these species for future comparative work: *C. violacea* (Cleomaceae) and *E. erucarioides* (Brassicaceae). Second, we tested whether *Arabidopsis PDS* constructs could be used as an efficient screen to determine how amenable these two relatives are to VIGS. By obtaining *Arabidopsis thaliana* pTRV2-*PDS* constructs from TAIR and introducing them into these new systems, VIGS was demonstrated to be an effective methodology for both species, albeit with greater success in *C. violacea*. Additionally, endogenous sequences from both species

were then used to produce pTRV2-*PDS* constructs to compare the penetrance and phenotype strength to the constructs containing a heterologous *AtPDS* sequence. Finally, *FRUITFULL* (*FUL*) constructs were developed to demonstrate silencing in fruits. *FUL* is critical for proper fruit patterning in *Arabidopsis* (Dinneny and Yanofsky, 2004; Dinneny et al., 2005) and comparative gene expression suggests it may be important for indehiscence and segmentation in *E. erucarioides* (Avino et al., 2012).

Methods

Construct design

Construct design and viral inoculation were carried out in accordance to previous VIGS work (Kramer and Gould, 2007; Kramer et al., 2007; Sharma et al., 2011). Each construct utilized was classified as either a heterologous construct (i.e. viral vectors containing a homologous gene fragment from a plant species other than the one being subjected to the treatment) or endogenous constructs (i.e. a viral vector containing a gene fragment from the plant species being treated). The viral vectors TRV1, TRV2, and the heterologous pTRV2-*AtPDS* were obtained from TAIR (Dinesh-Kumar original donor). Additionally, four endogenous constructs were generated: pTRV2-*EePDS*, pTRV2-*CvPDS*, pTRV2-*EeFUL* and pTRV2-*CvFUL*-*CvPDS*. Endogenous *PDS* constructs were designed for both *C. violacea* and *E. erucarioides* to compare results to heterologous constructs as well as determine VIGS susceptibility.

RNA was extracted from leaves using Concert Plant RNA Reagent kit (Invitrogen, Carlsbad, CA, USA), DNAse1 treated to remove DNA (Fermentas, Honover, MD, USA) and then further enriched with RNAeasy MiniKit (Qiagen, MD, USA). mRNA was purified from total RNA with the Dynabeads mRNA Purification Kit (Invitrogen, Carlsbad, CA, USA). cDNA was then synthesized from the mRNA using the SuperScript III reverse transcriptase (Invitrogen, Carlsbad, CA, USA) by priming with polyT primer (Kramer et al., 1998). Degenerate primers were designed from the *Arabidopsis thaliana PDS3* (AT4G14210; see table 2.1 for primer information and sequences) to obtain *PDS3* sequences from both focal taxa. Using the primers *PDS* Brassicales F and *PDS* Brassicales R (see table 2.1 for a complete primer list) a 768bp and 953bp fragment was amplified from *E. erucarioides* and *C. violacea*, respectively, to obtain the *PDS* coding sequence. These fragments were cloned into the TOPO-TA plasmid vector (Invitrogen, Carlsbad, CA, USA) according to manufacture instructions and sequenced using BigDye Terminator Sequencing (Applied Biosystems, Foster City, CA) with vector specific primers M13F (5'-GTA AAA CGA CGG CCA G-3') and M13R (5'-CAG GAA ACA GCT ATG AC-3') (Applied Biosystems, Foster City, CA). From these sequences, new primers were designed which amplified a fragment region in addition to adding XbaI and BamHI restriction sites to the 5' and 3' fragment ends (Table 2.1). For *E. erucarioides* the primer sets *PDS*-F2-XbaI and Ee*PDS* R2-BamHI were used to obtain a 444bp region (Appendix 2). For *C. violacea* the primers *PDS*-F2-XbaI and Cv-*PDS*-R2-BamHI were used to obtain a 429bp region (Appendix 1). Both

fragments were then cloned into the TOPO-TA plasmid (Invitrogen). Using both XbaI and BamHI restriction enzymes (New England BioLabs), the fragments were excised from the TOPO-TA vector and ligated into separate digested TRV2 vectors using T4 DNA ligase (PGem). Construct identity was confirmed using BigDye Terminator sequencing (Applied Biosystems, Foster City, CA) with primers which span the TRV2 cloning site, 156F (5'-TTACTCAAGGAAGCACGATGAGC-3') and156R (5'-GAACCGTAGTTTAATGTCTTCGGG-3'). Sequences were obtained with an ABI-3730 DNA Analyzer (Applied Biosystems, Foster City, California, USA) after being cleaned with a Performa DTR V# 96-well Short Plate Kit (Edge BioSystems, Gaithersburg, MD). Chromatograms were edited in Sequencher v. 4.10.1.

Constructs targeting *FUL* were produced to silence an additional candidate gene of interest. To produce the pTRV2-*EeFUL1* vector a 195bp fragment of the *E. erucarioides FUL* coding sequence was amplified from floral tissue cDNA using primers designed from the *EeFUL1* coding sequence (JX292966, Table 2.1). There are two copies of *EeFUL*, but only one shows valve-specific expression patterns (Avino et al., 2011), so this copy was chosen for VIG experiments. To produce the pTRV2-*CvFUL* vector a 195 fragment of the *C. violacea FUL* coding sequence was amplified from floral tissue cDNA using the previously designed *FUL* specific primers (*C. violacea,* unpublished transcriptome library). Primers were designed to amplify from the fifth exon to the eighth exon of the coding sequence to avoid silencing MADS box homologues

with a conserved domain sequence. The fragments were cloned into the TOPO-TA plasmid vector (Invitrogen) and sequenced using BigDye Terminator and vector specific primers M13F and M13R (Applied Biosystems, Foster City, CA) Sequencing. Using both XbaI and BamHI restriction enzymes, the fragments were excised from the TOPO-TA vector and ligated into separate digested TRV2 vectors to obtain both *FUL* constructs.

The pTRV2-*CvFUL* construct was further modified to produce a hybrid construct with the easily discernible silencing marker *PDS*, pTRV2-*CvFUL-CvPDS*. A second *C. violacea* fragment was amplified from the original TOPO-TA miniprep containing the *C. violacea PDS* sequence using primers which added BamHI and XhoI restriction enzyme sites to the flanks of the sequence (Table 2.1). This fragment was cloned into a TOPO-TA vector followed by double digestion using BamHI and XhoI restriction enzymes (New England Biolabs). The previously assembled pTRV2-*CvFUL* construct was also double digested with these enzymes after which the excised *PDS* fragment was ligated into the digested construct to assemble a hybrid pTRV2-*CvFUL-CvPDS* construct which was then sequenced for identity confirmation.

For purification and sequencing purposes, all ligated constructs were cloned into chemically competent *E. coli* (Invitrogen, Carlsbad, CA, USA) and plated onto LB media agar plates containing 50 ug/ml gentamycin, 50 ug/ml kanamycin and 25 ug/ml rifampycin. After overnight growth at 37^{o} C, colonies were PCR screening using 156F and 156R primers. Constructs were purified

(Qiagen Miniprep kit) followed by identity confirmation using BigDye Terminator sequencing (Applied Biosystems, Foster City, CA).

Preparation of *Agrobacterium tumefaciens*

Agrobacterium tumefaciens was chosen to mediate infection of the viral constructs into focal species. Chemically competent *Agrobacterium tumefaciens* were prepared for transformation as described (Weigel and Glazebrook, 2002). All of the following vectors were transformed into *Agrobacterium tumefaciens* strain GV3101::pMP90RK individually: pTRV2-*AtPDS*, pTRV2-*CvPDS*, pTRV2-*EePDS*, pTRV2-*CvFUL*, pTRV2-*EeFUL1*, TRV2, and TRV1. For transformation purposes, 10 µl of purified constructs were mixed with 250 µl of competent bacteria. Transformants were grown on selection media containing 50 mg/ml kanamycin, 50 mg/ml gentamycin and 25 mg/ml rifampycin for 4 days. Transformants were screened using primers 156F and 156R. Glycerol stocks were produced from positive transformants and stored at -80°C.

Plant materials

In preparation for vacuum infiltration *C. violacea* and *E. erucarioides* were sowed onto a 2:1 soil mixture of Sunshine Mix (SunGro) and Perlite (Tera-lite). Each tray of seeds contained 10 pots with approximately 10 seeds sown per 4-inch pot. Seedlings were watered daily to maintain high soil moisture. Rounds of VIGS inoculations were carried out using plants grown for 4-6 weeks at 24^{o}C under long day conditions (16 hours light, 8 hours dark) in the University of Alberta, Department of Biological Sciences, growth chambers.

Vacuum infiltration

Vacuum infiltration was chosen as the mechanism used to expose *C. violacea* and *E. erucarioides* plants to the VIGS constructs due to its previously reported ease and success rate (Wang et al., 2006; Becker and Lange, 2010). To prepare for infection, *Agrobacterium tumefaciens* containing TRV1, TRV2 or a ligated TRV2 gene construct were streaked onto LB media plates containing 50 mg/ml kanamycin, 50 mg/ml gentamycin and 25mg/ml rifampycin. Streaked plates were left at room temperature for 72 hours. Single colonies were pricked for liquid culture growth in liquid LB media (50 mg/ml kanamycin, 50 mg/ml gentamycin and 25mg/ml rifampycin). Each culture was serially inoculated until a final volume of 500 ml over a growing phase of 72 hours at room temperature with rapid agitation (275 rpm). Culture cells were then collected by centrifugation at 3200 g for 20 minutes at 4^{o}C. Cells were then resuspended in infiltration buffer (10 mM MES(2-(4-Morpholino)-Ethane Sulfonic Acid), 10 mM MgCl2, 0.1 M Acetosyringone (3'5'-Dimethozy-4'-hydrozyamcetophenone)) to a final OD_{600} = 2.0. Cultures were then left at room temperature for 3-4 hours.

Agrobacterium tumefaciens solutions containing TRV1 and TRV2 constructs were mixed in a 1:1 ratio and placed in a large open container. Silwet L-77 was added to the mixture at a concentration of 100 µl/L (Lehle Seeds, Round Rock, TX). Seedlings were removed from soil and rinsed by floating in water. Batches of 10-15 seedlings were placed into the mixture for two minutes under vacuum. Seedlings were then placed on paper towel to remove excess liquid and replanted into autoclaved soil consisting of the same mixture used to grow them. Plants were categorized based on the number of true leaves: small (S) with 0-3

true leaves, medium (M) with 4-6 true leaves, and large (L) with 7 or more true leaves. Treated plants were covered by clear plastic aerodomes for at least 2 days at 24^{o}C under long day conditions. Trials included between 119 and 213 of seedlings. A total of 916 (503 *C. violacea*; 413 *E. erucarioides*) seedlings were treated during 7 trials (Table 2.2 and 2.3).

Viral infection symptoms were displayed as early as 20 days after innoculation. Leaves of *C. violacea* that showed symptoms of photobleaching due to either pTRV2-*AtPDS* or pTRV2-*CvPDS* infection 40 days after inoculation were scored for their symptom strength then flash frozen in liquid nitrogen at -80 ^{o} C (Figure 2.1). Similarly, *E. erucarioides* leaves that showed photobleaching from either pTRV2-*AtPDS* or pTRV2-*EePDS* infection were also scored and collected at this time (See Figure 2.2). For both species photobleaching was scored on a gradient with leaves being classified as either pale, variegated or strongly photobleached. Categorization was done by visual inspection in rough accordance with percentage of white leaf tissue present: pale (<50%), variegated (<80%), strong (>80%). Within this gradient, pTRV2-*AtPDS* and pTRV2-*EePDS* were able to induce silencing within both the pale and variegated categories. Only Cv*PDS*-TRV2 produced photobleaching within the variegated and strong ranges. Leaf tissues were also collected at this time from control and mock treated plants. Records of viral penetrance and plant mortality were kept throughout the post inoculation period (Table 2.2).

Fruits of *C. violacea* infected with pTRV2-*CvFUL*-*CvPDS* that showed atypical developmental symptoms after 30 days were scored for their degree of

silenced phenotype (Figure 2.3). Silenced fruit were identified by multiple infected symptoms including the presence of white valve tissue from *PDS* silencing, stunted fruit length, and valve tissue appressed to the interior ovules. These symptoms have been previously described in *Arabidopsis thaliana* and were used to predict the effects of silencing *CvFUL* within *C. violacea* (Gu et al., 1998). Whole fruits were collected as previously done with leaf tissue. Heteroarthrocarpic *E. erucarioides* fruits failed to show atypical development when infected with pTRV2-*EeFUL1*. As such, no samples were taken and the species was not investigated further with regards to this construct.

Photographic data was collected using a handheld digital camera (Canon DS126181) and NIS Elements BR 3.0 Imaging software. Images were prepared for figure assembly using Adobe Photoshop CS2 and then compiled using Adobe Illustrator CS2.

RNA extraction and cDNA synthesis

Plant tissue was collected in 1.5ml tubes (Eppendorf) from plants subjected to VIGS and immediately flash frozen with liquid nitrogen. Samples ranged from 50 mg to 100 mg in weight. Each sample was ground using a Mixer Mill MM 400 (Retsch, Haan, Germany). Samples were placed in the Mixer Mill twice for 30 seconds at 25 RPM. RNA was then extracted from each sample using a modified protocol of the Chang et al. (1993) CTAB method according to the specifications of Pavy et al. (2008) and El Kayal et al. (2011). In addition, two modifications were made to the Pavy et al. (2008) protocol: the LiCL-EDTA solution (7.5 M LiCl and 50 mM EDTA) added to the extraction mixture was

done so in a ratio of 1:2 and the final precipitated RNA samples were resuspended in DEPC water. Each RNA extract was quantified using a nanodrop prior to cDNA synthesis. cDNA pools from floral and leaf extractions were produced using a Superscript III Reverse Transcriptase kit (Invitrogen).

Expression analysis of VIGS-treated plants

Quantitative reverse transcriptase polymerase chain reaction (qRT-PCR) was carried out to compare relative transcript levels between control and viral conditions using the the $2^{-\Delta\Delta Ct}$ method. The $2^{-\Delta\Delta Ct}$ method is a comparative approach for analyzing fold changes in a gene of interest (Livak and Schmittgen, 2001). This method is therefore dependent on a stably expressed reference gene to quantify relative transcript levels. Numerous reference genes have been previously reported as remaining stably expressed across VIGS treatment groups (TRV infected, mock-treated, control) (Rotenberg et al., 2006). Two genes were chosen as potential endogenous references, *ELONGATION FACTOR 1-α* (*EF1-α*) and *FBOX1*. Primers were then designed to target these genes for qRT-PCR analysis using Primer Express 3.0 (Applied Biosystems, Carlsbard, CA, USA). Simultaneously, primers were designed to detect downregulated targets, *PDS3* and *CvFUL*. The degree of sequence similarity between *E. erucarioides* and *C. violacea PDS* allowed for the same primer sets to be used for both species (See table 2.4 for complete primers list, Appendix 1 and 2).

Primers were first assessed for their efficiency. cDNA pools were diluted by a factor of 1/4 twice to create three concentrations within a dilution series. A primer optimization run was completed to confirm that all primer sets could be

used. C_t values for each primer were plotted against the log value of each concentration for each gene to produce a standard curve (Appendix 3). The slope of each dilutions series was then calculated for each primer set to determine their efficiency and if they were viable for the $2^{-\Delta\Delta Ct}$ method (Appendix 4). Primer efficiency was calculated using the formula $E_x = 10^{(-1/slope)}-1$ as outline by the TaqMan Gene expression assay manual (Applied Biosystems). The efficiency of the reference gene and target gene primer sets must be approximately equal to one another to proceed with the $2^{-\Delta\Delta Ct}$ method.

Both reference genes were quantified within a sample from each treatment group (e.g. pTRV2-*AtPDS*, untreated etc.) to ensure consistent expression between the various species and their organs. This was done to support the expression of these reference genes as consistent standards for relative comparison against VIGS targeted loci. The C_t valve was calculated based on for three technical replicates of 11 samples, representing various treatment groups. A sample standard deviation of the C_t valves as used to evaluate the degree of variation between treatments. A lower the standard deviation implies a more consistent expression of the reference gene. A standard deviation of 2.765 was obtained for *EF1-α*. *FBOX1* was eliminated as a reference gene due to inconsistency between samples (data not shown). Therefore qRT-PCR analysis was carried out using *EF1-α* as the reference control.

cDNA samples were prepared from both silenced and control samples after CTAB RNA extraction was performed as outlined above. qRT-PCR reactions were carried out in 10 µl reactions using SYBR Green master mix

(0.25x SYBR Green, 0.1x ROX, 0.3U Platinum Taq Polymerase (Invitrogen, Carlsbad, CA, USA) and 0.2 mM dNTPs) with 20 ng of cDNA and 300 nM of each primer. A Biomek 3000 (Beckman Instruments) robot was used to dispense reaction components into 384 well plates for qRT-PCR analysis. Plates were run using a 7900HT Fast Real-Time system (Applied Biosciences) then relative gene expression was calculated using the $2^{-\Delta\Delta Ct}$ method against endogenous *EF1-α* expression. Three technical replicates were carried out per sample with at least 3 (range 3-5) biological replicates for each condition.

Scanning electron microscopy of *C. violacea* fruit

Scanning electron microscopy (SEM) was used to examine fruits of both untreated *C. violacea* and pTRV2-*CvFUL*-*CvPDS* treated fruits. Untreated and treated fruit were collected at the same time as tissue was collected for RNA extraction and qRT-PCR. SEM was conducted as described in Patchell et al. (2011).

Results

Downregulation of *PDS* using heterologous and endogenous constructs

We first targeted both species for *PDS* to determine whether VIGS is a technique applicable to these taxa. *PDS* has previously been established as a preliminary target for silencing in undocumented systems for its easily discernible phenotype. Assembled *Arabidopsis thaliana* pTRV2-*PDS* construct are readily available and prove a potential resource for screening VIGS in closely related taxa.

Both *C. violacea* and *E. erucarioides* were inoculated with the pTRV2-*AtPDS* construct, although *C. violacea* was noticeably more susceptible. Multiple rounds of VIGS were carried out including an average of 72 *C. violacea* seedlings and 60 *E. erucarioides* seedlings per round (Table 2.2). Initially, all trial data was pooled to determine the variation between construct types with respect to seedling mortality and silencing penetrance (Table 2.2). Then, to better examine the efficacy of the VIGS silencing constructs, the VIGS rounds were divided into their original individual trials to create samples of similar treatment groups that were used for statistical analysis (Table 2.3). One-tailed student *t*-test comparisons were completed between the untreated group and each VIGS construct for each treatment size (small, medium or large) (Table. 2.3). The treatment group pTRV2-*CvPDS*-*CvFUL* was excluded from these statistical comparisons since only one round of this construct was completed.

The seedling total mortality rate for the 503 plants of *C. violacea* was 33.7% including TRV2-*AtPDS* treated and mock treatment groups. For small seedlings only pTRV2-*CvPDS* (T_{ST} =6.085, P = 0.0002) and pTRV2-*CvTCP* (T_{ST} = 6.035, P = 0.0009) had significantly higher mortality rates than the untreated group. Significantly higher morality rates were also seen for medium pTRV2-*CvPDS* (T_{ST} = 2.968, P = 0.010) and pTRV2-*CvTCP* (T_{ST} = 2.175, P = 0.033) as well as large pTRV2-*CvPDS* (T_{ST} = 2.599, P = 0.018) individuals. Symptoms of viral infection and silencing became visible after average 20 days post inoculation. Of the survivor plants treated for silencing with pTRV2-*AtPDS*, 51.9% showed some degree of silencing as of 30 days (Table 2.2). However, this

silencing efficiency failed to significantly differ than the untreated group since this percentage was combined from less than 20% silencing rates from each population (small, medium and large) (Table 2.3). Mock-treated (empty pTRV2 vector) *C. violacea* plants developed contorted stems and curled leaves. These symptoms are believed to be the result of the viral infection as they were not observed in the control group (untreated). *Cleome violacea* plants targeted by the pTRV2-*AtPDS* construct displayed a gradient of both penetrance and silencing strength (Figure 2.1 A-E). The amount of tissue that produced photobleached leaves varied per individual from a few leaves to the entire plant. Treated leaves of individuals were categorized into three groups: no photobleaching, pale photobleaching (Figure 2.1 A, C) and variegated (Figure 2.1 B, D-E). Both pale and variegated photobleaching was speckled in appearance. Pale was used to categorize leaves with less than 50% speckled coverage. Variegated leaves displayed more than 50% photobleaching across the leaf.

Of the 413 *E. erucarioides* seedlings inoculated with the pTRV2-*AtPDS* construct throughout all trials, 33.7% mortality was observed for treated and mock treated groups (Table 2.4). For all three treatment sizes (small, medium and large) the mortality rate of pTRV2-*AtPDS* treated *E. erucarioides* was not significantly different from the untreated populations (Table 2.5). Similar to *C. violacea*, photobleaching was observed approximately 20 days after inoculation. However, the silencing phenotype observed was less pronounced in *E. erucarioides* than *C. violacea* with only 5.3% of treated survivor plants showing any photobleached symptoms (Table 2.4). Again, this failed to be significantly

different that the untreated populations (Table 2.5). When photobleaching was observed, it manifested at a single site on the individual (Figure 2.2), rather than the more systemic phenotype observed in *C. violacea* (Figure 2.1). Treated individuals were classified into the same three groups as the *C. violacea* pTRV2-*AtPDS* treatment: no photobleaching, pale photobleaching (Figure 2.2 B) and variegated photobleaching (Figure 2.2 D-E). Leaves classified as pale photobleaching displayed partially white-pink areas. The pink tones observed are likely due to anthocyanin pigments being revealed by the degradation of chlorophyll (Di Stilio et al., 2010). Variegated photobleaching of *E. erucarioides* was only observed in the stems of the individuals and was characterized by consistent white tissue (Figure 2.2 C-D). Unlike *C. violacea,* mock-treated *E. erucarioides* did not show any symptoms discernible from the control group (Figure 2.1K and Figure 2.2 A).

After the pTRV2-*AtPDS* construct was shown to induce some degree of silencing in both focal species, endogenous constructs were assembled for comparison. *Cleome violacea* and *E. erucarioides* plants were inoculated with pTRV2-*CvPDS* and pTRV2-*EePDS* constructs respectively to induce photobleaching under the same conditions as the pTRV2-*AtPDS* treatments (Figure 2.1 F-J, N and 2.2 E-G, I). *Cleome violacea* silencing symptoms emerged after 20 days when treated with the pTRV2-*CvPDS* construct with a 63.3% total silencing efficacy of the survivors (Table 2.2). Both medium (T_{ST} = 3.952, P =0.003) and large (T_{ST} = 3.054, P =0.009) *C. violacea* treatment groups showed significantly higher silencing efficiencies than the untreated populations (Table

2.3). For comparative purposes, photobleached leaves were characterized using a similar gradient as designated for the pTRV2-*AtPDS* silenced individuals. An additional category, strong photobleaching (>80%), was established to classify leaves which were approximately entirely photobleached (Figure 2.1 G, I, J). No leaves resembled the pale *AtPDS* group previously described as pale and therefore leaves were labeled as either variegated or strongly photobleached. *Erucaria erucarioides* plants subjected to pTRV2-*EePDS* constructs displayed photobleaching symptoms in a similar manner to pTRV2-*AtPDS* targeted individuals. A total silencing efficiency of 10.7% was observed (Table 2.4) which was failed to be significantly different than the untreated *E. erucarioides* silencing rates (Table 2.5). Photobleaching occurred at a single site of the plant with a similar penetrance and strength as observed with the previous construct (Figure 2.2 E-G, I). Silenced tissue was classified using the same two categories, pale and variegated. However, variegated photobleaching was expanded to include leaves in addition to stems which displayed white tissue for at least 50% of the leaf (Figure 2.2 F, G).

To confirm that silencing occurred due to a reduction in the abundance of *PDS* transcript levels, qRT-PCR analysis was performed using the $2^{-\Delta\Delta Ct}$ method on each experimental group. These experiments demonstrated that a heterologous construct can be used to induce transcript downregulation (Figure 2.3), in a comparable manner to the transcript degradation observed when an endogenous construct was used in *C. violacea* (Figure 2.4). A ten-fold reduction in *PDS* transcript abundance was observed in both pale and variegated silenced *C.*

violacea leaf tissue when targeted by the pTRV2-*AtPDS* construct. The *CvPDS* targeted samples however noted smaller fold change compared to the *AtPDS* treatment despite the stronger photobleaching observed. *Cleome violacea* leaves with variegated symptoms displayed a 3-fold reduction in transcript abundance while strongly silenced pTRV2-*CvPDS* targeted leaves displayed a 5-fold reduction in transcript abundance. Control samples and tissue from groups which did not display photobleaching symptoms displayed consistent *PDS* transcript abundance within the error margin.

Unlike *C. violacea*, qRT-PCR analysis of *E. erucarioides* samples targeted by either the endogenous or heterologous construct produced a similar degree of transcript degradation (Figure 2.5). Samples targeted by *AtPDS* displayed a fold reduction in the relative *PDS* transcript abundance for the pale samples. Tissue classified as pale displayed a moderate reduction of 70% transcript abundance. *Erucaria erucarioides* samples classified as variegated photobleaching displayed a fold change similar to untreated and control treatments. Samples targeted by the endogenous pTRV2-*EePDS* construct demonstrated degradation fold change values that were consistent with the photographic data. A reduction of 90% *PDS* transcript abundance was shown in the pale category and a 2-fold reduction was detected from the variegated pTRV2-*EePDS* treated sample.

Downregulation of *C. violacea FRUITFULL* using hybrid construct

Cleomaceae exhibits a very similar fruit type to typical siliques of *Arabidopsis*. Siliques of Brassicaceae are two-valved capsule with a persistent placental tissue (replum) connected by a thin membranous septum that divides the

ovary into two locules. Fruits of Cleomaceae are also two-valved, dry capsules that have a replum, however these fruits lack the septum. To establish whether *C. violacea* would be a good model for examining fruit evolution, we targeted a fruit patterning gene, *FUL*. A hybrid construct was developed containing both a fragment of the *CvFUL* and *CvPDS* sequence for simultaneous silencing. Including *CvPDS* in the viral construct provided a visual marker making facilitating the detection of *FUL* knock-downs.

Cleome violacea seedlings were subjected to inoculation with the pTRV2-*CvFUL-CvPDS* construct. Photobleaching symptoms arose within the same timeframe as the previous *PDS* constructs in the leaves however, the plants had not yet produced fruits (Figure 2.6 E-G). Fruits were collected as early as 30 days after inoculation when they were close to maturity. Control fruits were collected at the same time to ensure a consistency in developmental state (Figure 2.6 J, K and Fig 2.7 A,B). A total silencing efficacy of 25.7% was observed in the pTRV2-*CvFUL-CvPDS* treated *C. violacea* population (table 2.2). Previous documentation of *Arabidopsis ful* mutants was used to compare the symptoms of the *C. violacea FUL* mutants along with the indication of white fruit tissue due to *CvPDS* downregulation. *ful* mutants produced fruits stunted in length and further analysis with SEM revealed that the fruits displayed irregular replum patterning (Gu et al., 1998). Here, *CvFUL-CvPDS* mutant fruits were found to be white and curled with valves highly appressed to the seeds creating a ribbed appearance (Figure 2.6 A-D and Figure 2.7 C, D). SEM data demonstrates the constriction of valve development as a result of smaller cell size shown by the higher density of

valve trichomes in pTRV2-*CvFUL*-*CvPDS* fruit (Figure 2.8 B, E). Furthermore, these fruits showed various degrees of stunting in length (Figure 2.6 A-D). Silenced fruits also displayed engorged repla noticeably raised compared to the valve regions (Figure 2.7 C-D and Figure 2.8 E). Silenced fruits had an average length of 4.400 ± 1.679 cm (n=10 fruits, ± sample variance) (Table 2.7). Untreated fruits however were on average 5.543 ± 0.241 cm in length (n=12 fruits) (Table 2.7). The width of the silenced fruit was on average was 0.147 ± 0.002 cm. Untreated fruit however had a width average of 0.131 ± 0.002 cm (Table 2.7). Length measurements were taken at from the end of the petiole to the apex of the fruit. Width was measured at the centre location as determined from the length measurement. A one-tailed *t*-test supports the length of pTRV2-*CvFUL*-*CvPDS* fruit to be significantly different than the untreated population (T_{ST} = 2.862, P =0.005) (Table 2.7). Only fruits which displayed all of these characteristics were classified as *CvFUL* silenced and collected for qRT-PCR analysis. Photobleached leaves from the pTRV2-*CvFUL*-*CvPDS* treatment were also collected since *FUL* transcription occurs within the leaves and would provide a second site for *FUL* silencing detection (Fig 2.3 E,F,G). These leaves looked similar to *CvPDS* silenced leaves and were classified as variegated. To validate *CvFUL* silencing at a molecular level, qRT-PCR analysis will be performed.

Erucaria erucarioides plants were also subjected to a pTRV2-*EeFUL* construct VIGS treatment. After 30 days post inoculation very few fruits were produced by the treated plants (<4) of which none displayed atypical development. For this reason no fruits were collected.

Discussion

Relatives of *Arabidopsis* are rich in morphological diversity and, as such, are ideal for investigating the genetic basis of morphological variation. This is traditionally done through comparative work between close relatives with the assumption that the variation of their morphology is due to modification of homologous loci (de Brujin et al., 2012). Such investigations require the combination of comparative developmental studies, comparative gene expression studies, and functional studies of focal taxa. Only once the candidate genes have been identified and examined within both systems can links to the functional evolution of those genes be made (de Brujin et al., 2012).

Here we have chosen two species to introduce the functional reverse genetic tool VIGS in two relatives of *Arabidopsis, C. violacea* and *E. erucarioides*, representing different phylogenetic distances. *Erucaria* is in same family as *Arabidopsis*, whereas *Cleome* more distantly related due to placement in sister family Cleomaceae. *Cleome violacea* serves as an ideal candidate for introducing genetic methodologies because of its relatively small genome size (525 Mb; Pires, unpublished data), its easiness to grow and inbred lines are accessible. Furthermore, a transcriptome library of putative genes has been assembled and annotated for *C. violacea* and genomic sequencing is underway, which will both be invaluable resources for facilitating future work. The monosymmetric flowers are of interest and can be used to analyze the genetic contributors to floral symmetry. The species *E. erucarioides* was also chosen as a close relative that displays a novel fruit morphology suitable for evolutionary

development analysis (Avino et al., 2012). Establishing VIGS as a tool accessible to these model systems will allow for genes of interest to be targeted for downregulation. By means of functional knock down, the roles of the candidate homologues associated with these morphologies can be collected.

Downregulation of *PDS* in two emerging models using both heterologous and endogenous constructs

VIGS continues to be a popular approach for functional knock down as demonstrated by the recent expansion in the number of species exposed to this methodology (Burch-Smith et al., 2004; Dinesh-Kumar et al., 2007; Purkayastha and Dasgupta, 2009; DiStilio, 2011). Unsurprisingly many species that are not amenable to more traditional transformation techniques and are being subjected to VIGS as an alternative for collecting functional data (Constantin et al., 2004; Hileman et al., 2005; Gould and Kramer, 2007; Wege et al., 2007; Di Stilio et al., 2010). However, VIGS does not work in all species and all new species must be empirically tested for suspectibility.

Here we have downregulated the carotenoid pathway marker, *PDS* in two species using both endogenous and heterologous constructs (Senthil-Kumar and Mysore, 2011). In addition, the MADS box fruit development gene *FUL* (Gu et al., 1998) was also downregulated in *C. violacea* using a hybrid construct. The success of this methodology demonstrates this technique as a feasible tool for future functional work, especially in *C. violacea*. Having downregulated *PDS* using both heterologous and endogenous constructs supports the accessibility to the VIGS methodology. Assembled pTRV2-*PDS* constructs are currently

available to order through the *Arabidopsis* Information Resource (TAIR) for multiple species including *Arabidopsis thaliana*, *Lycopersicon esculentum* and *Nicotiana tabacum*. Due to the bottleneck created by construct assembly, easy access to completed viral machinery is of great benefit to researchers attempting to develop a VIGS methodology. Our results indicate these vectors may be used for preliminary screening to determine the efficacy of this technique in a new plant system before investing time and resources into endogenous constructs.

The heterologous constructs produced a similar fold change reduction in *PDS* transcript abundance compared to their endogenous counterparts. This result is somewhat unsurprising because the degree of sequence similarity between *Arabidopsis* and both *C. violacea* and *E. erucarioides* is high (>85%) suggesting silencing was able to successfully occur by either construct type. In a similar study using a *Nicotiana benthamiana PDS* sequence for silencing other Solanaceae members, sequences with less than 80% similarity to the insert were only capable of decreasing *PDS* abundance by 25% or less (Senthil-Kumar et al., 2007). In this case, *Arabidopsis PDS* shared greater than 85% sequence similarity with both species (*C. violacea*, 86% and *E. erucarioides* 96%) and in both cases a reduction in transcripts of greater than 50% occurred. Thus, when establishing VIGS within a new system, using purchased constructs is an advisable strategy, especially if the endogenous sequence is greater than 85% similar in sequence to the construct insert sequence. In this case, the insert within the construct shares a degree of sequence similarity high enough to conclude it is capable of inducing downregulation results of similar strength to an endogenous construct.

Interestingly, *C. violacea*, whose sequence was less similar to the *AtPDS* construct and is phylogenetically more distant than *E. erucarioides* to *Arabidopsis* produced higher silencing efficiency (i.e. was able to induce silencing in more individuals) when treated with the *AtPDS* construct. In addition, the *PDS* fold change was notably greater in *C. violacea* using both heterologous and endogenous constructs then compared to *E. erucarioides*. As previously described, sequence similarity doesn't necessarily convey silencing efficiency indicating that individual species possess their own degree of innate resistance to this procedure (Senthil-Kumar et al., 2007). It has been generally accepted that a minimum nucleotide sequence stretch of 21bp shared between both the construct and the endogenous mRNA is required to induce downregulation within the target host (Burch-Smith et al., 2004; Senthil-Kumar et al., 2007). However, even if longer sequence stretches are present, silencing may still remain inefficient and the susceptibility of a new model to VIGS can only be established through completing VIGS trials (Senthil-Kumar et al., 2007).

Dowregulation of valve margin identity homologue *FUL* within *C. violacea*

Having now established VIGS as a methodology by knocking down the visual marker *PDS*, additional targets must be silencing in order to indicate this technique is amenable to developmental work in these plant systems (Gould and Kramer, 2007). To this pursuit the gene *FUL* which has shown to be involved in valve margin positioning (Dinneny et al., 2005; Dinneny and Yanofsky, 2005) of silique fruit was targeted for silencing within *C. violacea* using a hybrid TRV2 construct. Due to its ability to act as a visual marker, a fragment of the *PDS*

coding region was inserted along with a 444 bp fragment from the 3' end of the *FUL C. violacea* sequence into a TRV2 vector. Only the 3' end of *FUL* was chosen, to eliminate the inclusion of the MADS domain within the construct. The MADS domain is capable of inducing off target silencing with its conserved nucleotide sequence known to be shared with other members of the MADS family. This hybrid construct allowed for the simultaneous downregulation of both *PDS* and *FUL* simplifying the screening of treated plants for mutant *FUL* phenotypes.

Within *Arabidopsis FUL* is expressed in developing valve tissue and acts are a repressor of dehiscence zone identity genes (Dinneny et al., 2005; Dinneny and Yanofsky, 2005). Therefore, *FUL* maintains the integrity of the dehiscence zone by establishing the position of the valve margin (Dinneny et al., 2005; Dinneny and Yanofsky, 2005; Ripoll et al., 2011). Being that *Arabidopsis* is the closest relative with a well-characterized *FUL* function and relatively similar fruit morphology to Cleomaceae, we predicted that silenced *C. violacea* fruits would be similar to *ful* mutants. *Arabidopsis thaliana ful* mutants display shortened siliques due to the failure of the value tissue cells to grow and differentiate leading to a reduction in the size of these cells (Gu et al., 1998). The replum continues to develop as in wildtype fruit, which is unsurprising considering that *FUL* is only expressed in the valves of the fruit. However, the reduction in fruit length forces the replum into a zig-zag pattern (Gu et al., 1998).

After treatment with the pTRV2-*CvPDS-CvFUL* vector, *C. violacea* fruits were screened for both photobleaching and *ful* mutant symptoms. Using

stereomicroscopy we were able to find photobleached fruits with comparable morphological traits to those described by *Arabidopsis* mutant fruit. Fruits were stunted in length similar to *FUL;ful* heterozygous mutant *Arabidopsis* mutants (Gu et al., 1998). In addition, the valve tissue was tightly appressed against the seeds creating an overcrowded appearance of the fruit (Figure 2.3). The replum of the *C. violacea FUL* silenced fruit appeared engorged and lacked the sharp line of differentiation from the valve region as seen in untreated fruit.

Photographic data suggests that when treated with the pTRV2-*CvFUL-CvPDS* construct, photobleached fruit displayed atypical fruit development associated with valve growth. These findings are aligned with previously described *FUL* mutant analysis of *Arabidopsis thaliana* and support some degree of conserved homologue functioning between the two relatives (Gu et al., 1998). Silencing of *FUL* in *C. violacea* using the hybrid construct still requires molecular validation using qRT-PCR to show the degree of downregulation of *CvFUL* from viral silencing. Furthermore, SEM analysis of the silenced fruit is also required to determine if typical cell development and orientation is obscured as displayed by *Arabidopsis FUL* mutant fruits. With molecular data validation, we will be able to conclude that TRV-VIGS is capable of induced silencing phenotypes of loci acting within our target plant systems.

Silencing of valve margin identity homologue *FUL* with *E. erucarioides*

To facilitate further optimization of VIGS within *E. erucarioides* an additional target gene was chosen for downregulation. *Erucaria erucarioides* displays a derived fruit type known as heteroarthrocarpy. Heteroarthrocarpic fruits

possess a lateral joint with may or may not absice in addition to dividing the fruit into a distal and proximal segment (Hall et al., 2011). In this system, the function of the homologue *EeFUL1* is believed to facilitate the establishment of this unique dehiscence profile by parameterizing lines of dehiscence (Avino et al., 2012). By silencing this gene within heteroarthrocarpic fruit and identifying its contribution to this morphology we will be able to contribute function data for comparative work aiming to elucidate the evolutionary changes responsible for this novel fruit type.

A pTRV2-*EeFUL1* construct was assembled as previously described for treatment of *E. erucarioides* individuals. Similar to the *C. violacea* pTRV2-*CvFUL-CvPDS* construct, only the 3' end of the *EeFUL1* sequence was incorporated into the TRV2 construct to eliminate off target silencing. A marker sequence was not included into the construct. After treatment with the pTRV2-*EeFUL1* construct, silencing symptoms failed to manifest. Only a few individuals produced limited fruits that did not reach full maturity. These fruits did not differ in appearance from control unfertilized *E. erucarioides* fruit, suggesting that either silencing failed to occur or that the homologue targeted is functionally redundant with another loci (data not shown). *EeFUL2* is not expressed within developing valves, but is observed in ovules (Avino et al., 2012). In *Arabidopsis*, *ful* mutants also manifest atypical leaf symptoms which are visually distinct and thinner in appearance than wildtype leaves (Gu et al., 1998). It is unclear if *EeFUL1* was downregulated, as it is possible for silencing to have occurred within the leaves. However, no atypical leaf morphology was observed for *E.*

erucarioides when treated with the *EeFUL1* construct. The low silencing efficiency observed when *E. erucaridoides* was treated with *EePDS* suggests that a larger treatment sample size would be required for silencing to occur using the *EeFUL1* construct. More importantly, further optimization of the VIGS methodology is recommended before additional genes can be downregulated within *E. erucarioides* other than the visual marker *PDS*.

Conclusion

For *C. violacea* we have established VIGS as viable methodology by demonstrating its ability to downregulate *PDS* using two construct types. These experiments reveal that further investigation of *E. erucarioides* is needed to determine viability of VIGS. Our method involved silencing both individual and multiple genes simultaneously demonstrating the flexibility of VIGS targets. We also evaluated the application of readily available heterologous VIG constructs for the use of establishing VIGS within previously undocumented species. Based on these results, we advise this method as a viable option for initial establishment and optimization of this technique for species, preferably for which the endogenous sequence similarity is above 85% with the viral construct. Thus, using heterologous constructs can allow for optimization of experimental variables known to influence systemic spread of the virus such as temperature and infiltration method prior to investing in construct assembly. Introducing VIGS to these species offers a novel reverse genetic approach for studying gene function within a short time period. In the future this technique can be coupled with both

phylogenetic and expression data sets for comparative purposes and future evo-devo pursuits.

Figures

Table 2.1. Primers used for construct assembly. For both endogenous *PDS* constructs a primer set was used to originally amplify the PDS sequence prior to the amendment of restriction enzymes which was done with a second primer set. Constructs which lack an initial primer set used the primers with amendable restriction sites for the preliminary amplification.

Gene Construct	cDNA amplified region	Primers for cDNA amplification	Sequence 5'>3'	TRV2 Insert size	Primers for restriction amendment	Sequence 5'>3'
CvPDS	956	*PDS* F Brassicales	TGG AAG GAR CAC TCM ATG ATW TTY GCH ATG	444	*PDS* F XbaI	GGT CTA GAT AGT AGA TTT GAT TTC CCA GAT
		PDS R Brassicales	ACR ACA TGR TAC TTS AVD ATT TTW GCY TT		Cv*PDS* R2 BamHI	AAG GAT CCT AGA ATT TAG TCG TAC TTC CCC
EePDS	768	*PDS* F Brassicales	TGG AAG GAR CAC TCM ATG ATW TTY GCH ATG	444	*PDS* F2 XbaI	GGT CTA GAT AGT AGA TTT GAT TTC CCA GAT
		PDS R Brassicales	ACR ACA TGR TAC TTS AVD ATT TTW GCY TT		Ee*PDS* R2 BamHI	AAG GAT CCT TGA GTT AAG TCG TAC TTC CCC
CvFUL	N/A	N/A	N/A	195	cvFULex5xbaIf	CGG TCT AGA ACC AAG TCA TGT TCG AAT CCA TAG C

					cvFULex5bhamIr	GCT GGA TCC AAG CAG GAA GAA GAG AAT
EeFUL	N/A	N/A	N/A	195	FULex5xbaIf	CGG TCT AGA ACC AGG YYA TGT TCG AAT CCA TAT CDS C
					FULex5bamIr	GCT GGA TCC AAG CAG GAA GAA GAG AAT
CvTCP	N/A	N/A	N/A	507	TCPBamHIr	GCG GAT CCT CTC TAA TCG CCT T
					TCPxbaIF	GCT CTA GAT TAC AAT GGA GTG TAC CCT CT
CvFUL-Cv*PDS*	N/A	N/A	N/A	444	*PDS* F3 BamHiF	CGG GAT CCT AGT AGA TTT GAT TTC CCA GAT
					PDS xhoIRF3	AAC TCG AGT AGA ATT TAG TCG TAC TTC CCC

Table 2.2. Collection records of VIGS trails for *Cleome violacea*. The data collected represents seven VIGS trials with the number of individual plants treated grouped by treatment and then size. Mortality percentages were taken prior to 30 days post inoculation. Plants were categorized based on the number of true leaves: small (s) with 0-3 true leaves, medium (m) with 4-6 true leaves, and large (l) with greater than 7 true leaves.

	Total individual plants treated				% mortality				% phenotype (of total)				% Phenotype (of survivors)			
Construct	s	m	l	**total**	s	M	l	**total**	s	m	l	**total**	s	m	l	**total**
Untreated	19	14	39	**72**	5.4	21.4	2.6	**6.9**	0	0	0	**0**	0	0	0	**0**
pTRV2	35	44	0	**79**	40	63.6	0	**53.2**	0	0	0	**0**	0	0	0	**0**
pTRV2-*AtPDS*	42	25	15	**82**	31	16	73.3	**34.1**	59.5	0	20	**34.1**	86.2	0	75.0	**51.9**
pTRV2-*CvPDS*	16	54	37	**107**	87.5	72.2	64.9	**72.0**	0	14.8	29.7	**17.8**	0	53.3	84.6	**63.3**
pTRV2-*CvFUL-PDS*	0	2	60	**62**	0	50	5	**6.5**	0	0	6.7	**6.5**	0	0	35.7	**25.9**
pTRV2-*CvTCP*	7	48	46	**101**	100	66.7	8.7	**42.6**	0	0	32.6	**14.9**	0	0	7	**6.9**

Table 2.3. Statistical comparison of *Cleome violacea* VIGS treatments to untreated individuals at various inoculation maturities. One tailed student *t*-tests were conducted for all VIGS treatments including mock treated (empty pTRV2). Sample populations were obtained by grouping the observed mortality rate, silencing rate and silencing rate of survivors from each of the seven conducted VIGS trials by construct. Comparisons were made between the untreated group and a construct treatment population within common inoculation maturities (small, medium or large). – designates populations with insufficient variation or samples size for a comparison to be made. P-values < 0.05 have been displayed in red.

Small	df	mean	sd	Deaths t-stat	P-value	df	mean	sd	Silencing t-stat	P-value	df	mean	sd	Silencing survivors t-stat	P-value
pTRV2	7	0.284	0.170	0.858	0.210	-	-	-	-	-	-	-	-	-	-
AtPDS	8	0.774	0.024	0.049	0.481	7	0.198	0.118	1.528	0.085	8	0.216	0.186	1.265	0.121
CvPDS	7	0.880	0.016	6.085	0.0002	-	-	-	-	-	-	-	-	-	-
CvTCP	6	1.000	0.000	6.025	0.0009	-	-	-	-	-	-	-	-	-	-

medium	df	mean	sd	Deaths t-stat	P-value	df	mean	sd	Silencing t-stat	P-value	df	mean	sd	Silencing survivors t-stat	P-value
pTRV2	8	0.420	0.244	1.001	0.171	-	-	-	-	-	-	-	-	-	-
AtPDS	8	0.345	0.435	0.537	0.303	8	0.193	0.149	1.265	0.121	8	0.202	0.164	1.265	0.121
CvPDS	7	0.677	0.061	2.968	0.010	7	0.163	0.034	2.334	0.026	7	0.634	0.183	3.952	0.003
CvTCP	7	0.574	0.090	2.175	0.033	-	-	-	-	-	-	-	-	-	-

large	df	mean	sd	Deaths t-stat	P-value	df	mean	sd	Silencing t-stat	P-value	df	mean	sd	Silencing survivors t-stat	P-value
pTRV2	8	0.000	0.000	0.800	0.223	-	-	-	-	-	-	-	-	-	-
AtPDS	8	0.183	0.134	1.044	0.164	8	0.05	0.01	1.265	0.121	8	0.188	0.141	1.265	0.121
CvPDS	7	0.413	0.142	2.599	0.018	7	0.215	0.459	2.658	0.016	7	0.563	0.238	3.054	0.009
CvTCP	7	0.190	0.109	1.240	0.127	7	0.128	0.049	1.528	0.085	7	0.128	0.049	1.528	0.085

Table 2.4. Collection records of VIGS trails for *Erucaria erucarioides*. The data collected represents seven VIGS trials with the number of individual plants treated grouped by treatment and then size. Mortality percentages were taken prior to 30 days post inoculation. Plants were categorized based on the number of true leaves: small (s) with 0-3 true leaves, medium (m) with 4-6 true leaves, and large (l) with greater than 7 true leaves.

	N Treated				% mortality				% phenotype (of total)				% Phenotype (of survivors)			
Construct	s	m	l	**total**	s	m	l	**total**	s	m	l	**total**	s	m	l	**total**
Untreated	19	16	8	**43**	26.3	12.5	12.5	**18.6**	0	0	0	**0**	0	0	0	**0**
pTRV2	37	46	0	**83**	24.3	17.4	0	**20.5**	0	0	0	**0**	0	0	0	**0**
pTRV2-*AtPDS*	59	111	5	**175**	13.6	13.5	0	**13.1**	13.6	0	0	**4.6**	15.7	0	0	**5.3**
pTRV2-*EePDS*	67	40	5	**112**	31.3	15.0	20.0	**25.0**	7.5	10	0	**8.0**	10.9	11.8	0	**10.7**

Table 2.5. Statistical comparison of *Erucaria erucarioid*es VIGS treatments to untreated individuals at various inoculation maturities. One tailed student t-tests were conducted for all VIGS treatments including mock treated (empty pTRV2). Sample populations were obtained by grouping the observed mortality rate, silencing rate and silencing rate of survivors from each of the seven conducted VIGS trials by construct. Comparisons were made between the untreated group and a construct treatment population within common inoculation maturities (small, medium or large). – designates populations with insufficient variation or samples size for a comparison to be made. P-values < 0.05 have been displayed in red.

Small	df	mean	variance	Deaths t-stat	P-value	df	mean	sd	Silencing t-stat	P-value	df	mean	sd	Silencing survivors t-stat	P-value
pTRV2	8	0.308	0.092	0.313	0.381	-	-	-	-	-	-	-	-	-	-
AtPDS	7	0.368	0.302	0.448	0.339	7	0.047	0.007	1.528	0.085	7	0.053	0.008	1.528	0.085
EePDS	7	0.414	0.132	0.768	0.234	7	0.061	0.003	3.055	0.009	7	0.076	0.004	3.051	0.009

Medium	df	mean	sd	Deaths t-stat	P-value	df	mean	sd	Silencing t-stat	P-value	df	mean	sd	Silencing survivors t-stat	P-value
pTRV2	8	0.308	0.068	0.897	0.198	-	-	-	-	-	-	-	-	-	-
AtPDS	7	0.212	0.036	0.260	0.401	-	-	-	-	-	-	-	-	-	-
EePDS	7	0.103	0.008	0.554	0.298	7	0.048	0.007	1.538	0.085	7	0.056	0.009	1.528	0.085

Large	df	mean	sd	Deaths t-stat	P-value	df	mean	sd	Silencing t-stat	P-value	df	mean	sd	Silencing survivors t-stat	P-value
pTRV2	8	0.000	0.000	0.800	0.223	-	-	-	-	-	-	-	-	-	-
AtPDS	7	0.000	0.000	0.683	0.258	-	-	-	-	-	-	-	-	-	-
EePDS	7	0.067	0.013	0.860	0.209	-	-	-	-	-	-	-	-	-	-

Table 2.6. Primer sequences for quantitative reverse transcriptase polymerase chain reaction (qRT-PCR) analysis.

Primer set (Forward/Reverse)	Sequence 5'>3'
Cv*PDS*-F/Cv*PDS*-R	GTT GAG GCG CAA GAT GGT CTA/ CAT CGG TCA CAC GAT CAG GTA
Efai-f/Efai-r	AGG AGG CTG CTG AGA TGA ACA/ CGC TCG GCC TTA AGT TTG TC
CsFboxiii-f/CsFboxiii-r	AGG GTA TGG GAG CTG GAT CA/ CTC TGC CGA CAG TCT CAA CAG T
TCPC8-F/TCPC8-R	GCT CAA TAG GTA TCC GGG ACA A/ ACT GAC AAC CGG CCT TTT TG
CvFul-F/CvFul-r	CCT CAA CTC CAA GCC TCC AA/ CCA TCC GCC AAT CCA TTT C

Figure 2.1. *Cleome violacea* subjected to VIGS treatment using both heterologous and endogenous *PHYTOENE DESATURASE (PDS)* TRV2 constructs. A-B*: C. violacea* leaves after silencing using *AtPDS* displaying pale (A) and variegated (B) photobleaching. C-E: bracts silenced with *AtPDS* displaying pale (C) and variegated (D,E) photobleaching. F,G: leaves after treatment with *CvPDS* showing variegated (F) and strong (G) silencing. H-J: bracts silenced with *CvPDS* displaying variegated (H) and strong (I,J) photobleaching. K,L: untreated *C. violacea* leaf (K) and whole plant (L). M,N: whole plant views of *C. violacea* treated with *AtPDS* (M) and *CvPDS* (N). Scale bar = 2 mm.

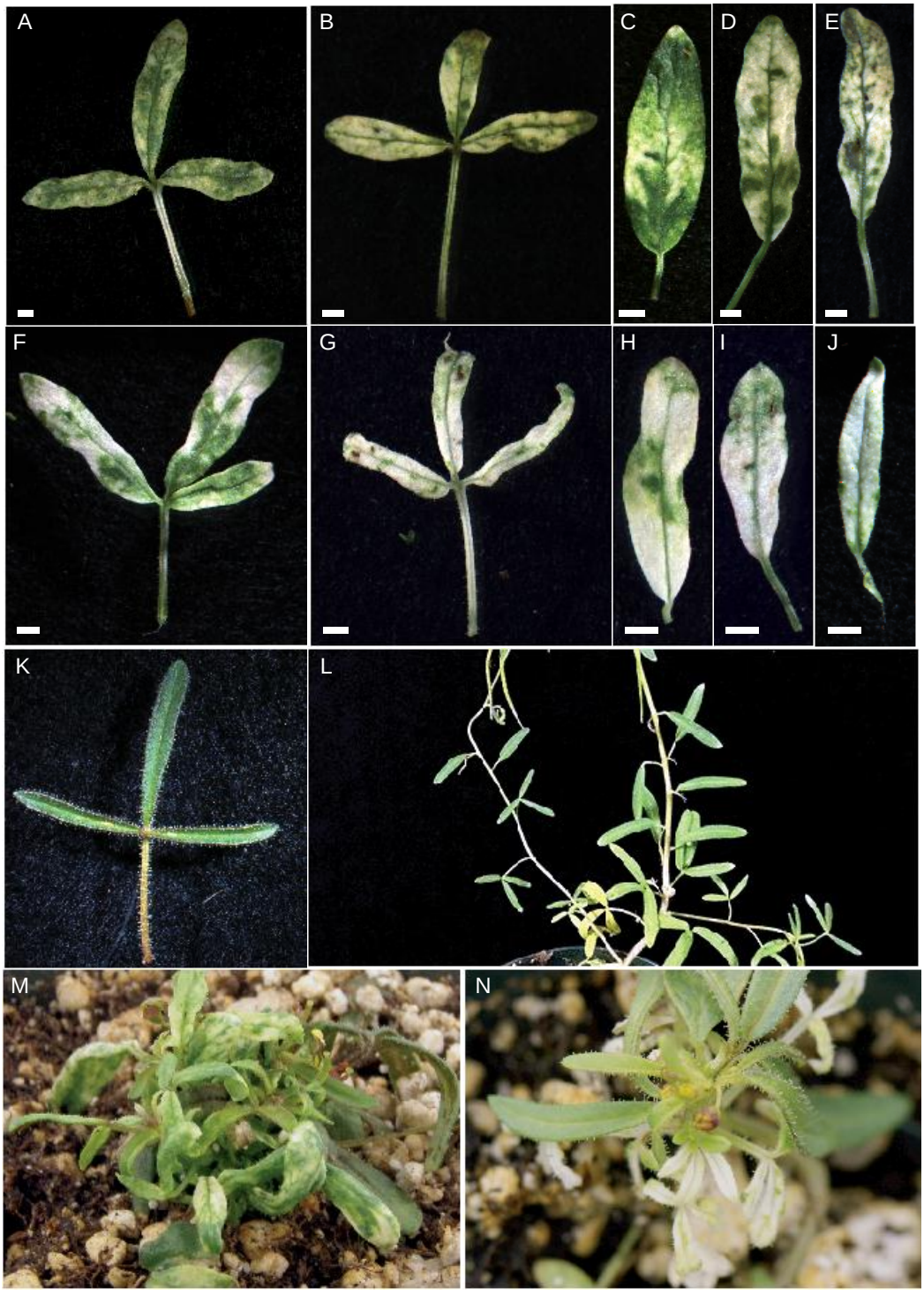
A
B
C
D
E
F
G
H
I
J
K
L
M
N

Figure 2.2. *Erucaria erucarioides* subjected to VIGS treatment using both heterologous and endogenous *PHYTOENE DESATURASE* (*PDS*) TRV2 constructs. A: an untreated *E. erucarioides* leaf. B: an *E. erucarioides* leaf after silencing using *AtPDS* displaying pale photobleaching. D-E: stems treated with At*PDS* showing variegated photobleaching symptoms. F-H: leaves treated with endogenous *EePDS* TRV2 constructs showing pale(F)and variegated (G,H) photobleaching. I-J: Whole plant views after *AtPDS* silencing (I) and *EePDS* (H) silencing of *E. erucarioides*. Scale bar= 2 mm.

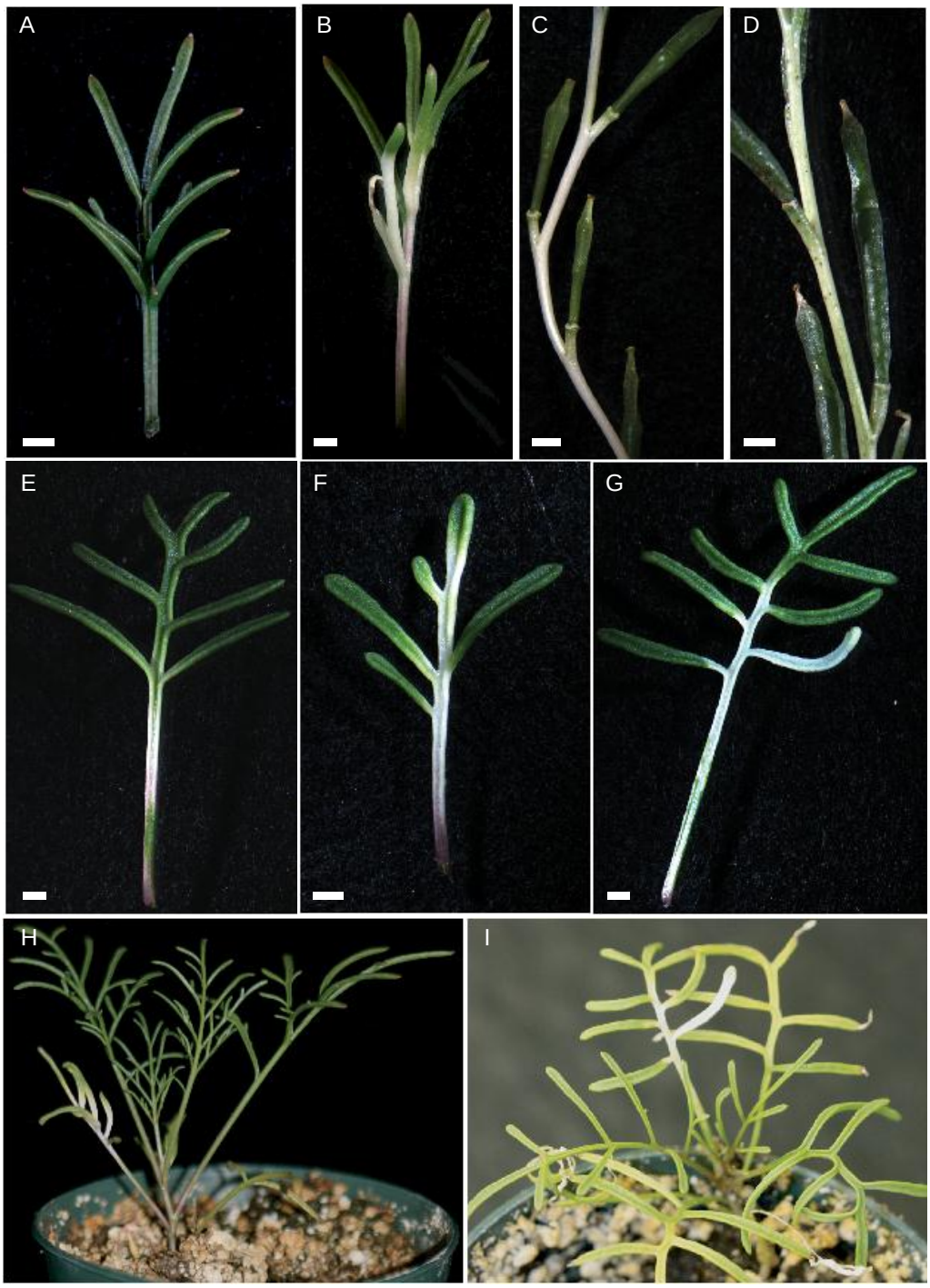
A
B
C
D
E
F
G
H
I

Figure 2.3. Quantitative reverse transcriptase polymerase chain reaction (qRT-PCR) analysis of *PDS* downregulation in *Cleome violacea* using a heterologous *AtPDS* VIGS construct. Average fold change of *PDS* expression between samples prepared from leaves of virus-induced gene silencing treated individuals. Bars represent average fold changes of three biological replicates. Error bars indicate ± standard deviation of the fold changes within a treatment group.

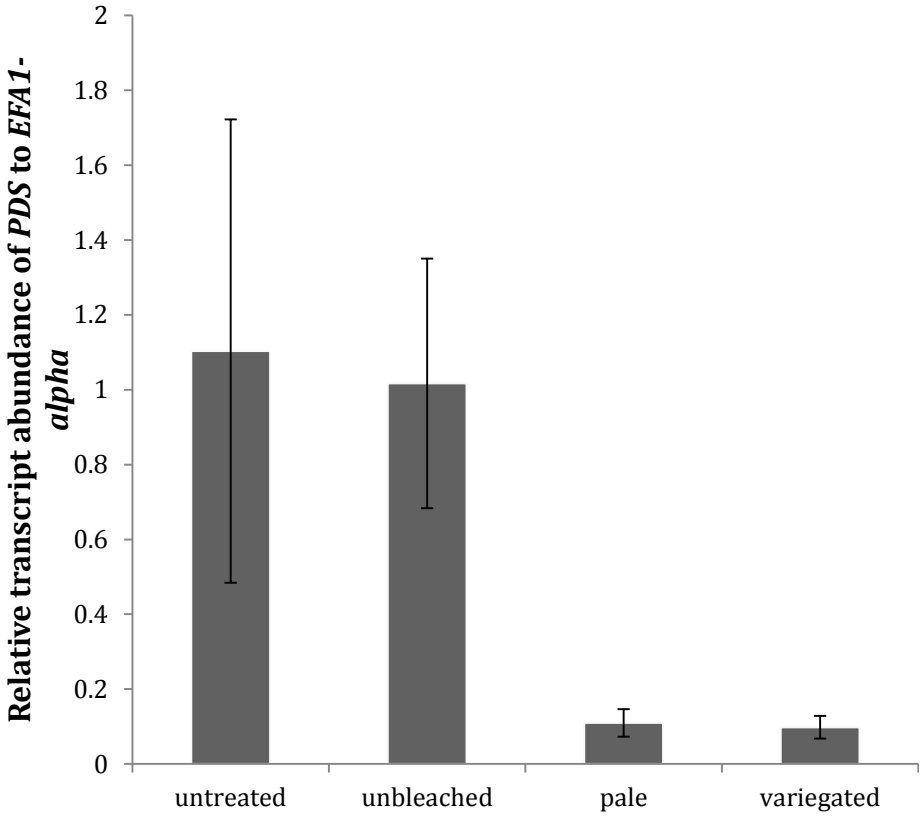

Figure 2.4. Quantitative reverse transcriptase chain reaction (qRT-PCR) analysis of *PDS* downregulation in *Cleome violacea* using an endogenous *CvPDS* VIGS construct. Average fold change of *PDS* expression between samples prepared from leaves of virus-induced gene silencing treated individuals. Bars represent average fold changes of three biological replicates for all groups except untreated where n=1. Error bars indicate ± standard error of the fold changes within a treatment group.

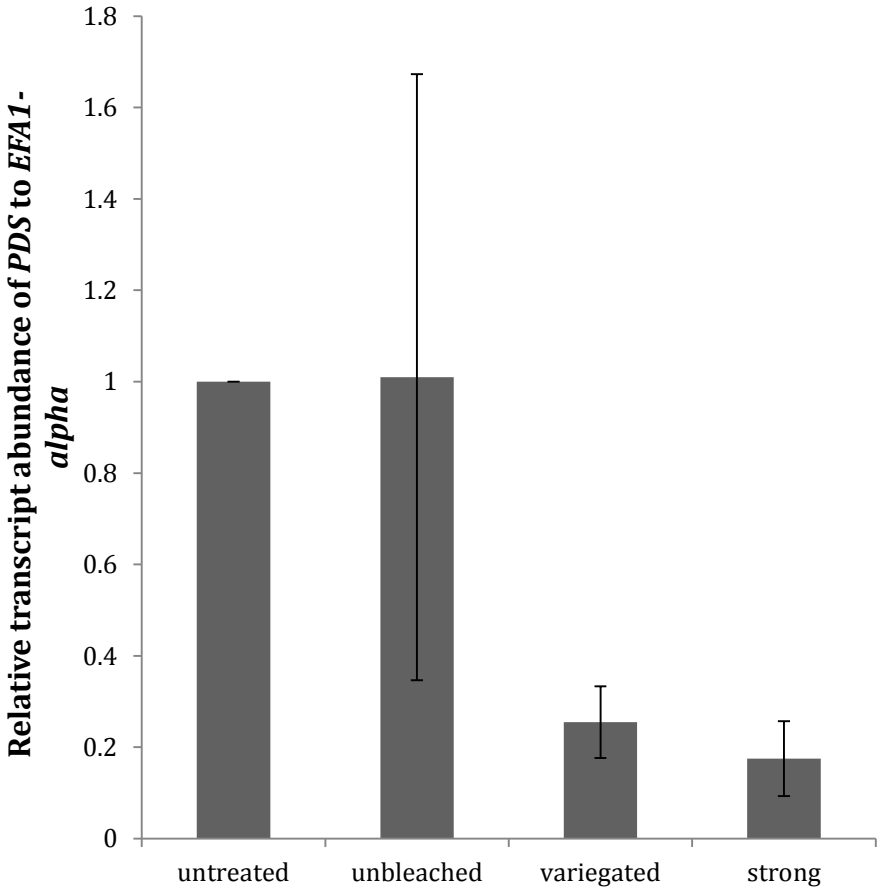

Figure 2.5. Quantitative reverse transcriptase polymerase chain reaction (qRT-PCR) analysis of *PDS* downregulation in *E. erucarioides*. Average fold change of *PDS* expression between samples prepared from leaves of virus-induced gene silencing treated individuals. Light gray bars represent *E. erucarioides* samples collected from individuals treated with a heterologous *AtPDS* construct. Dark gray bars represent *E. erucarioides* samples treated with an endogenous *EePDS* construct. Bars represent average fold changes of three biological replicates. Error bars indicate ± standard deviation of the fold changes within a treatment group.

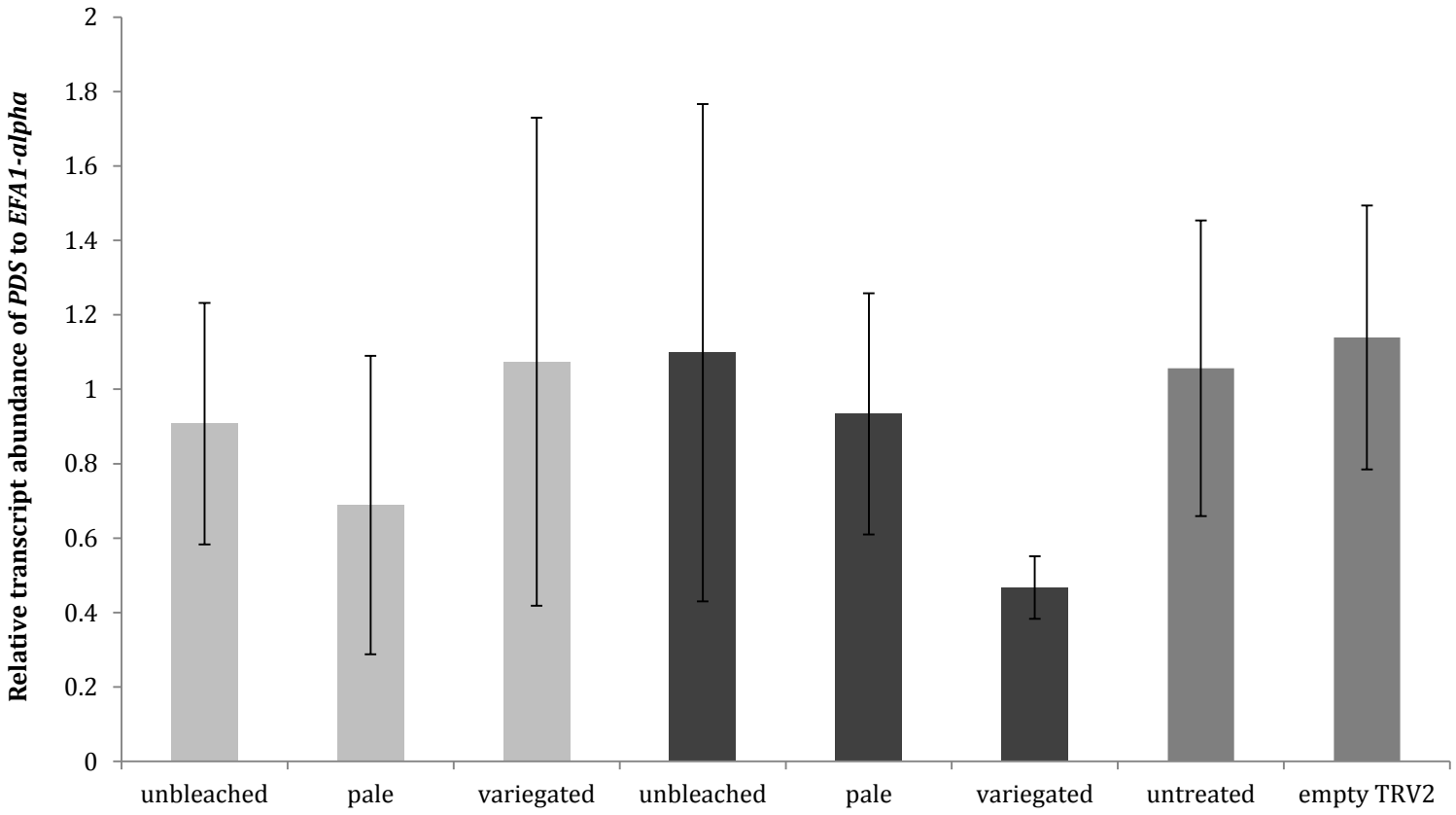
Relative transcript abundance of PDS to EFA1-alpha
2
1.8
1.6
1.4
1.2
1
0.8
0.6
0.4
0.2
0
unbleached
pale
variegated
unbleached
pale
variegated
untreated
empty TRV2

Figure 2.6. *Cleome violacea* subjected to VIGS treatment using a hybrid endogenous pTRV2-*PHYTOENE DESATURASE* (*PDS*)-*FRUITFULL* (*FUL*) construct. A-D; *C. violacea* fruit displaying photobleaching and atypical valve development after treated treatment with the pTRV2-*CvPDS*-*CvFUL*- VIGS construct. E,F,G: leaflets (E,F) and leaf (G) showing photobleaching. H, I: fruit from treated *C. violacea* resembling wildtype morphology. J-L: untreated *C. violacea* fruit (J,K) and leaf (L). Scale bar = 2 mm.


A
B
C
D
E
F
H
I
G
J
K
L

Figure 2.7. Replum and valve comparison of *Cleome violacea* subjected to VIGS treatment using a hybrid endogenous *PHYTOENE DESATURASE-FRUITFULL*-TRV2 construct. A-B; untreated *C. violacea* silique fruit displaying the valve (A) and replum (B) regions. C-D; fruit treated with the pTRV2-*CvFUL*-*CvPDS* construct showing photobleaching of the valve (C) and an irregular replum patterning (D). scale bars = 0.1 mm.

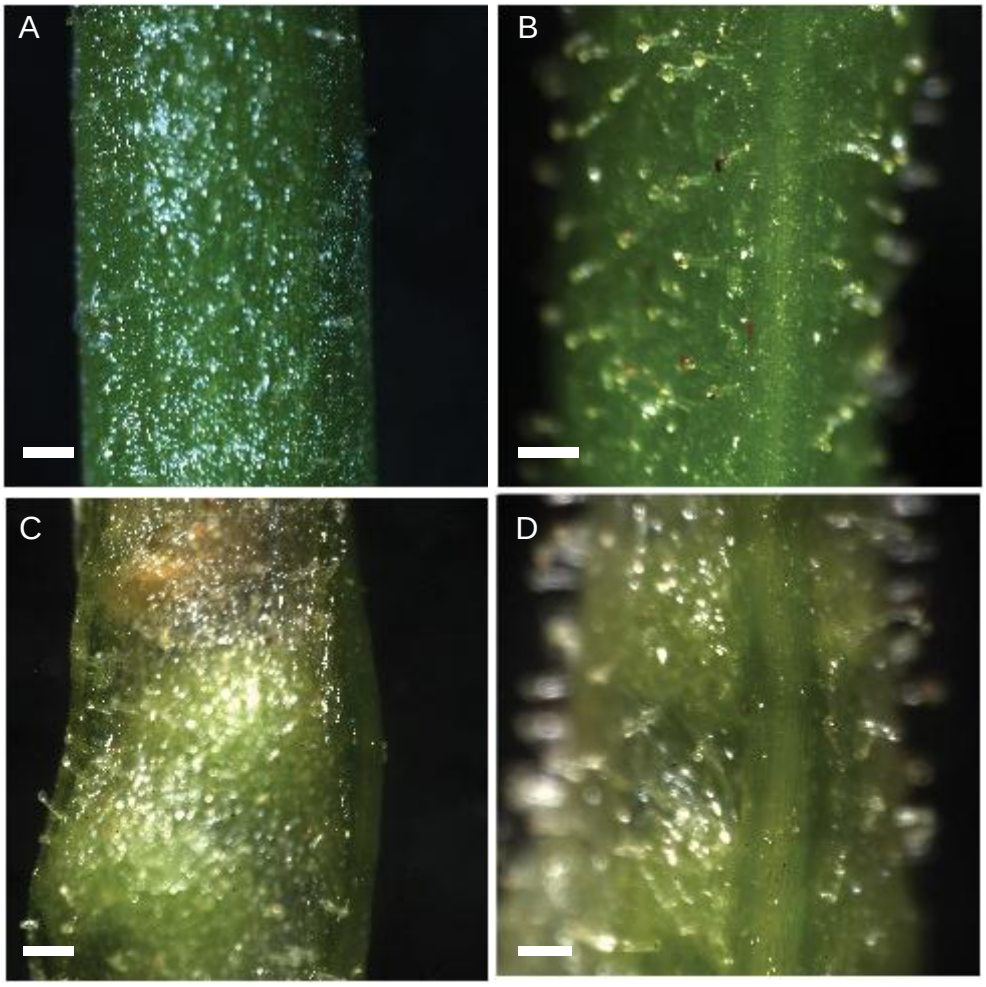

Figure 2.8. Scanning electron microscopy of replum and valve comparison of *Cleome violacea* subjected to VIGS treatment using a hybrid endogenous pTRV2-*FRUITFULL-PHYTOENE DESATURASE* construct. A-C; untreated *C. violacea* silique fruit displaying the replum (A),valve (B) regions and valve margin (C). D-F; fruit treated with the pTRV2-*CvFUL-CvPDS* construct showing photobleaching of the valve (D), irregular replum patterning (E) and the valve margin (F) . scale bars for A, B, D, E = 0.25 mm. scale bars for C, F = 0.10 mm.

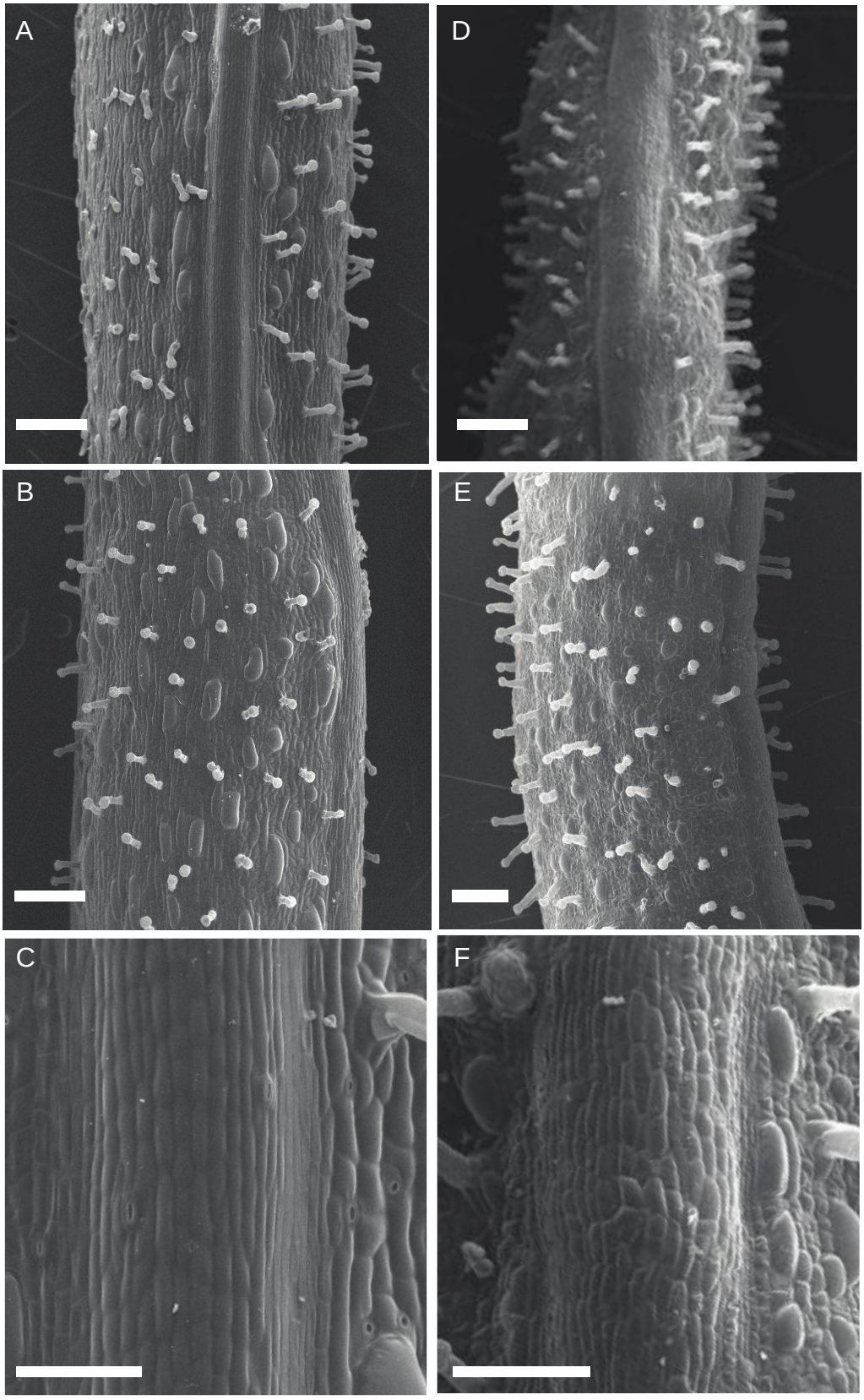
A
D
B
E
C
F

Table 2.7. Statistical comparison of *C. violacea* fruit dimensions between VIGS pTRV2-*CvFUL*-*CvPDS* treated and untreated individuals. Untreated and treated fruit were collected at approximately 30 days post inoculation to ensure similar developmental states. Length measurements are from the end of the petiole to the apex of the fruit. Width was measured half way down the valve as determined from the length measurement. P-values < 0.05 have been displayed in red. ± indicate variance.

	Untreated fruit	pTRV2-*CvGUL*-*CvPDS*
Sample size	12	12
Mean width	0.131 ± 0.002 cm	0.147 ± 0.002 cm
Df_{width}		22
$T\text{-}stat_{width}$		0.831
$P\text{-}value_{width}$		0.208
Mean length	5.542 ± 0.241 cm	4.400 ± 1.669 cm
Degrees of freedom		22
$T\text{-}stat_{length}$		2.862
$P\text{-}value_{length}$		0.005

Literature Cited

Abzhanov, A., Extavour, C.G., Groover, A., Hodges, S.A., Hoekstra, H.E., Kramer, E.M., and Monteiro, A. (2008). Are we there yet? Tracking the development of new model systems. Trends in Genetics **24,** 353-360.

Avino, M., Kramer, E.M., Donohue, K., Hammel, A.J., and Hall, J.C. (2012). Understanding the basis of a novel fruit type in Brassicaceae: conservation and deviation in expression patterns of six genes. EvoDevo **3,** 20.

Bachan, S., and Dinesh-Kumar, S.P. Tobacco Rattle Virus (TRV)-Based Virus-Induced Gene Silencing. Methods in Molecular Biology **894,** 83-92.

Barker, M.S., Vogel, H., and Schranz, M.E. (2009). Paleopolyploidy in the Brassicales: Analyses of the *Cleome* Transcriptome Elucidate the History of Genome Duplications in *Arabidopsis* and Other Brassicales. Genome Biology and Evolution **1,** 391-399.

Baulcombe, D.C. (1999). Fast forward genetics based on virus-induced gene silencing. Current Opinion in Plant Biology **2,** 109-113.

Becker, A., and Lange, M. (2010). VIGS - genomics goes functional. Trends in Plant Science **15,** 1-4.

Brown, N.J., Parsley, K., and Hibberd, J.M. (2005). The future of C-4 research - Maize, *Flaveria* or *Cleome*? Trends in Plant Science **10,** 215-221.

Burch-Smith, T.M., Anderson, J.C., Martin, G.B., and Dinesh-Kumar, S.P. (2004). Applications and advantages of virus-induced gene silencing for gene function studies in plants. Plant Journal **39,** 734-746.

Burch-Smith, T.M., Schiff, M., Liu, Y.L., and Dinesh-Kumar, S.P. (2006a). Efficient virus-induced gene silencing in Arabidopsis. Plant Physiology **142,** 21-27.

Burch-Smith, T.M., Schiff, M., Liu, Y., and Dinesh-Kumar, S.P. (2006b). Efficient virus-induced gene silencing in *Arabidopsis*. Plant Physiology **142,** 21-27.

Busch, A., and Zachgo, S. (2007). Control of corolla monosymmetry in the Brassicaceae *Iberis amara*. Proceedings of the National Academy of Sciences of the United States of America **104,** 16714-16719.

Busch, A., Horn, S., Muhlhausen, A., Mummenhoff, K., and Zachgo, S. (2012). Corolla Monosymmetry: Evolution of a Morphological Novelty in the Brassicaceae Family. Molecular Biology and Evolution **29,** 1241-1254.

Chang S., Puryear J., and J., C. (1993). A Simple and Efficient Method for Isolating RNA from Pine Trees. Plant Molecular Biology Reporter **11,** 113-116.

Constantin, G.D., Krath, B.N., MacFarlane, S.A., Nicolaisen, M., Johansen, I.E., and Lund, O.S. (2004). Virus-induced gene silencing as a tool for functional genomics in a legume species. Plant Journal **40,** 622-631.

Cubas, P. (2004). Floral zygomorphy, the recurring evolution of a successful trait. Bioessays **26,** 1175-1184.

de Bruijn, S., Angenent, G.C., and Kaufmann, K. (2012). Plant 'evo-devo' goes genomic: from candidate genes to regulatory networks. Trends in Plant Sciences **17,** 441-447.

Di Stilio, V.S. (2011). Empowering plant evo-devo: Virus induced gene silencing validates new and emerging model systems. Bioessays **33,** 711-718.

Di Stilio, V.S., Kumar, R.A., Oddone, A.M., Tolkin, T.R., Salles, P., and McCarty, K. (2010). Virus-Induced Gene Silencing as a Tool for Comparative Functional Studies in *Thalictrum*. PLOS One **5**.

Dinesh-Kumar, S.P., Anandalakshmi, R., Marathe, R., Schiff, M., and Liu, Y. (2003). Virus-induced gene silencing. Methods in Molecular Biology **236,** 287-294.

Dinesh-Kumar, S.P., Burch-Smith, T., Liu, Y., Schiff, M., Dong, Y., Zhu, X., and Mamillapalli, P. (2007). Virus-induced gene silencing (VIGS) for gene function studies in plants. Phytopathology **97,** S145-S145.

Dinneny, J.R., and Yanofsky, M.F. (2005). Drawing lines and borders: how the dehiscent fruit of *Arabidopsis* is patterned. Bioessays **27,** 42-49.

Dinneny, J.R., Weigel, D., and Yanofsky, M.F. (2005). A genetic framework for fruit patterning in *Arabidopsis thaliana*. Development **132,** 4687-4696.

DiStilio, V.S. (2011). Empowering plant evo-devo: Virus induced gene silencing validates new and emerging model systems. BioEssays **33,** 711-718.

Donaire, L., Barajas, D., Martinez-Garcia, B., Martinez-Priego, L., Pagan, I., and Llave, C. (2008). Structural and genetic requirements for the biogenesis of tobacco rattle virus-derived small interfering RNAs. Journal of Virology **82,** 5167-5177.

El Kayal, W., Allen, C.C.G., Ju, C.C-T., Adams, A., King-Jones, S., Zaharia, L.I., Abrams, S.R., Cookem J.E.K., (2011). Molecular events of apical

bud formation in white spruce, *Picea glauca*. Plant Cell environment **34**, 480-500.

Endress, P.K. (1992). Evolution and floral diversity: the phylogenetic surroundings of *Arabidopsis* and *Antirrhinum*. International Journal of Plant Sciences **153,** S106-S122.

Erbar, C., and Leins, P. (1997). Studies on the early floral development in Cleomoideae (Capparaceae) with emphasis on the androecial development. Plant Systematics and Evolution **206,** 119-132.

Feodorova, T.A., Voznesenskaya, E.V., Edwards, G.E., and Roalson, E.H. (2010). Biogeographic Patterns of Diversification and the Origins of C-4 in Cleome (Cleomaceae). Systematic Botany **35,** 811-826.

Fofana, I.B., Sangare, A., Collier, R., Taylor, C., and Fauquet, C.M. (2004). A geminivirus-induced gene silencing system for gene function validation in cassava. Plant Molecular Biology **56,** 613-624.

Franzke, A., Lysak, M.A., Al-Shehbaz, I.A., Koch, M.A., and Mummenhoff, K. (2011). Cabbage family affairs: the evolutionary history of Brassicaceae. Trends in Plant Science **16,** 108-116.

Gould, B., and Kramer, E.M. (2007). Virus-induced gene silencing as a tool for functional analyses in the emerging model plant *Aquilegia* (columbine, Ranunculaceae). Plant Methods **3,** 6.

Gu, Q., Ferrandiz, C., Yanofsky, M.F., and Martienssen, R. (1998). The *FRUITFULL* MADS-box gene mediates cell differentiation during *Arabidopsis* fruit development. Development **125,** 1509-1517.

Hall, J.C., Sytsma, K.J., and Iltis, H.H. (2002). Phylogeny of Capparaceae and Brassicaceae based on chloroplast sequence data. American Journal of Botany **89,** 1826-1842.

Hall, J.C., Tisdale, T.E., Donohue, K., Wheeler, A., Al-Yahya, M.A., and Kramer, E.M. (2011). Convergent evolution of a complex fruit structure in the tribe Brassiceae (Brassicaceae). American Journal of Botany **98,** 1989-2003.

Hayward, A., Padmanabhan, M., and Dinesh-Kumar, S.P. Virus-induced gene silencing in *Nicotiana benthamiana* and other plant species. Methods in Molecular Biology **678,** 55-63.

Hileman, L.C., Drea, S., de Martino, G., Litt, A., and Irish, V.F. (2005). Virus-induced gene silencing is an effective tool for assaying gene function in the basal eudicot species *Papaver somniferum* (opium poppy). Plant Journal **44,** 334-341.

Iltis, H.H., Hall, J.C., Cochrane, T.S., and Sytsma, K.J. (2011). Studies in the Cleomaceae I. in the separate recognition of Capparaceaem Cleomaceae, and Brassicaceae. Annals of the Missouri Botanical Garden **98,** 28-36.

Karrer, A.B. (1991). Blütenentwicklung und systematische stellung der Papaveraceae und Capparaceae (Zürich: University of Zürich).

Koch, M., Al-Shehbaz, I.A., and Mummenhoff, K. (2003). Molecular systematics, evolution, and population biology in the mustard family (Brassicaceae). Annals of the Missouri Botanical Garden **90,** 151-171.

Kramer, E.M. (2009). New model systems for the study of developmental evolution in plants. In Current Topics in Developmental Biology **86**, 67-105.

Kramer, E.M., Dorit, R.L., and Irish, V.F. (1998). Molecular evolution of genes controlling petal and stamen development: Duplication and divergence within the *APETALA3* and *PISTILLATA* MADS-box gene lineages. Genetics **149,** 765-783.

Liu, Y., Schiff, M., and Dinesh-Kumar, S.P. (2002). Virus-induced gene silencing in tomato. Plant Journal **31,** 777-786.

Livak, K.J., and Schmittgen, T.D. (2001). Analysis of relative gene expression data using real-time quantitative PCR and the $2^{-\Delta\Delta Ct}$ method. Methods **25,** 402-408.

Marshall, D.M., Muhaidat, R., Brown, N.J., Liu, Z., Stanley, S., Griffiths, H., Sage, R.F., and Hibberd, J.M. (2007). *Cleome*, a genus closely related to *Arabidopsis*, contains species spanning a developmental progression from C-3 to C-4 photosynthesism. Plant Journal **51,** 886-896.

Mummenhoff, K., Polster, A., Muhlhausen, A., and Theissen, G. (2009). Lepidium as a model system for studying the evolution of fruit development in Brassicaceae. Journal of Experimental Botany **60,** 1503-1513.

Patchell, M.J., Bolton, M.C., Mankowski, P., and Hall, J.C. (2011). Comparative floral development in Cleomaceae reveals two distinct

pathways leading to monosymmetry. International Journal of Plant Sciences **172,** 352-365.

Pavy, N., Boyle, B., Nelson, C., Giguere, I., Caron, S., Parsons, L.S., Dallaire, N., Bedon, F., Berube, H., Cooke, J., Mackay, J. (2008). Identification of conxerved core xylem gen sets: conifer cDNA microarray development, transcripto profiling and computational analyses. New Phytologist **180,** 766-786.

Purkayastha, A., and Dasgupta, I. (2009). Virus-induced gene silencing: A versatile tool for discovery of gene functions in plants. Plant Physiology and Biochemistry **47,** 967-976.

Ratcliff, F., Martin-Hernandez, A.M., and Baulcombe, D.C. (2001). Technical Advance. Tobacco rattle virus as a vector for analysis of gene function by silencing. Plant J **25,** 237-245.

Ripoll, J.J., Roeder, A.H.K., Ditta, G.S., and Yanofsky, M.F. (2011). A novel role for the floral homeotic gene *APETALA2* during *Arabidopsis* fruit development. Development **138,** 5167-5176.

Rotenberg, D., Thompson, T.S., German, T.L., and Willis, D.K. (2006). Methods for effective real-time RT-PCR analysis of virus-induced gene silencing. Journal of Virology Methods **138,** 49-59.

Ruiz, M.T., Voinnet, O., and Baulcombe, D.C. (1998). Initiation and maintenance of virus-induced gene silencing. Plant Cell **10,** 937-946.

Schranz, M.E., and Mitchell-Olds, T. (2006). Independent ancient polyploidy events in the sister families Brassicaceae and Cleomaceae. Plant Cell **18,** 1152-1165.

Senthil-Kumar, M., and Mysore, K.S. (2011). New dimensions for VIGS in plant functional genomics. Trends in Plant Science **16,** 656-665.

Senthil-Kumar, M., Hema, R., Anand, A., Kang, L., Udayakumar, M., and Mysore, K.S. (2007). A systematic study to determine the extent of gene silencing in *Nicotiana benthamiana* and other Solanaceae species when heterologous gene sequences are used for virus-induced gene silencing. New Phytologist **176,** 782-791.

Voznesenskaya, E.V., Koteyeva, N.K., Chuong, S.D.X., Ivanova, A.N., Barroca, J., Craven, L.A., and Edwards, G.E. (2007). Physiological, anatomical and biochemical characterisation of photosynthetic types in genus Cleome (Cleomaceae). Functional Plant Biology **34,** 247-267.

Wang, C.C., Cai, X.Z., Wang, X.M., and Zheng, Z. (2006). Optimisation of tobacco rattle virus-induced gene silencing in *Arabidopsis*. Functional Plant Biology **33,** 347-355.

Wege, S., Scholz, A., Gleissberg, S., and Becker, A. (2007). Highly efficient virus-induced gene silencing (VIGS) in california poppy (*Eschscholzia californica*): An evaluation of VIGS as a strategy to obtain functional data from non-model plants. Annals of Botany **100,** 641-649.

Weigel, D., and Glazebrook, J. (2002). *Arabidopsis*: A Laboratory Manual. (Cold Spring Harbor Laboratory Press).

Chapter 3. Functional assessment of the homologue *TCP1* and its contribution to monosymmetry in *Cleome violacea*

Peter Mankowski

Introduction

Monosymmetric flowers have evolved many times from radially symmetric ancestors across angiosperms. Surprisingly, the same gene family appears to be involved in all investigated independent shifts in floral symmetry (Rosin and Kramer, 2009; Preston et al., 2011). Multiple comparative genetic studies have implicated class II *TCP* proteins within the *CYC*-like subclade to the development of floral monosymmetry (Luo et al., 1996; Cubas et al., 2001; Hileman et al., 2003; Jabbour et al., 2009; Martin-Trillo and Cubas, 2010; Zhang et al., 2010). The name of *TCP* is based on the first four proteins in which the *TCP* domain was identified: teosinte branched1 (*TB1*) from maize (*Zea mays*), *CYCLOIDEA* (*CYC*) from snapdragon (*Antirrhinum majus*), and *PROLIFERATING CELL FACTORS 1* and *2 (PCF1* and *PCF2*) from rice (*Oryza sativa*). The independent recruitment of these genes has occurred in multiple plant orders (Jabbour et al., 2009; Rosin and Kramer, 2009). The role of *TCP* in floral symmetry is mostly based on comparative gene expression studies of families such as Malpighiaceae (Zhang et al., 2010), Gesneraceae (Zhou et al., 2008), Brassicaceae (Busch et al., 2012), Papaveraceae (Damerval et al., 2007), and Dipsacaceae (Howarth and Donoghue, 2009). Functional data demonstrating a *TCP*-like gene is responsible for monosymmetry is more limited and includes model species *Antirrhinum majus* (Plantaginaceae) (Luo et al., 1999), *Lotus japonicus* (Fabaceae) (Feng et al., 2006; Zhou et al., 2008), *Cysticapnos vesicaria* (Ranunculaceae) (Hidalgo et al.), and *Iberis amara* (Brassicaceae) (Busch and Zachgo, 2007). It is clear that to better understand how this gene family has been

involved in transitions to monosymmetry across angiosperms, more species need to be investigated using functional approaches.

The independent recruitment of monosymmetry has led to a divergence in the gene regulation utilized by these clades (Busch and Zachgo, 2007; Rosin and Kramer, 2009). Furthermore, multiple duplication and diversification events of *CYC*-like genes have altered the functions between individual homologues (Rosin and Kramer, 2009). This resulting variability in the roles of monosymmetric machinery has made extrapolation of this process to non model species difficult (Hileman and Cubas, 2009; Rosin and Kramer, 2009; Martin-Trillo and Cubas, 2010). In some species *CYC*-like homologues have shown to be promoters of growth but in others they act as growth repressors (Busch and Zachgo, 2007; Rosin and Kramer, 2009; Martin-Trillo and Cubas, 2010). Two explanations have been proposed as possible mechanisms for this variation in *CYC*-like *TCP* gene activity. The first is that the functions of *TCP* proteins are being conserved while downstream targets have accumulated modifications altering their binding relationships with transcription factors (Martin-Trillo and Cubas, 2010). The second explanation suggests specific *TCP* homodimers and heterodimers of *TCP* proteins occur in unique combinations between developmental stages and cell types facilitating highly specific roles with various contexts (Martin-Trillo and Cubas, 2010).

RNA interference and loss of function techniques are promising for identifying mechanisms underlying the establishment of monosymmetry (Galego and Almeida, 2002; Hidalgo et al., 2012). One method, virus-induced gene

silencing (VIGS) is a RNAi technique which can produce a transient knock down phenotype of a specific gene target (Baulcombe 1999, Ruiz et al., 1998). VIGS has becoming increasing utilized due to its dependency on a virus mechanism allowing the methodology to be applied to many non model and emerging model organisms. VIGS involves introducing a viral vector into a plant system what contains the target gene sequence from the plant host. When the viral construct is replicated it produces a double stranded RNA sequence of the target gene. This elicits a plant defense mechanism known as post transcriptional gene silencing when degrades the dsRNA molecule and matching endogenous mRNA molecules causing a silenced phenotype at the transcriptional level (Burch-Smith et al., 2004; Becker and Lange, 2010).

Loss of function analysis has been traditionally used to accumulate knowledge of the molecular mechanisms behind monosymmtry in model species (Busch and Zachgo, 2007; Hidalgo et al.). VIGS is a promising technique for functional analysis of class II TCP genes due to its ability to alter the specificity of the gene target for silencing and has previously been shown as a tool amenable to floral symmetry studies (Burch-Smith et al., 2004; Di Stilio, 2011; Hidalgo et al.). VIGS can be catered to be either highly specific for single gene or gene copy or more general by silencing multiple genes simultaneously (Burch-Smith et al., 2004; Becker and Lange, 2010). This variability lies in the nature of the post-transcription gene silencing (PTGS) (Ruiz et al., 1998; Baulcombe, 1999). The mechanism by which PTGS occurs involves cutting a dsRNA template into 24-mers which then act as a template for degradation of like molecules. If the

sequence inserted into the viral construct is highly conserved it can target many genes and copies as long as they share that sequence. Likewise, if the sequence in the construct is highly specific (e.g. UTR sequence) only a single target will be silenced.

Using VIGS for evolutionary developmental studies on monosymmetric flowers will help determine regulators of floral symmetry for comparative work against dissymmetric relatives (Hidalgo et al. 2012). Loss of function *tcp1* mutants in *Arabidopsis thaliana* have unaffected flowers making it difficult to assess the role of *TCP1* in this model organism (Cubas, 2004; Preston et al., 2009). This is perhaps not surprising given that *A. thaliana* has dissymmetric flowers. However, *AtTCP1* is expressed transiently in the adaxial portion of developing floral buds which suggests a role in dorsal-ventral identity (Cubas et al., 2001). More recently, *TCP1* has been implicated in independent origins of floral monosymmery in Brassicaceae (Busch and Zachgo, 2007; Busch et al., 2012). In all examined monosymmetric species of Brassicaceae, the abaxial petals are significantly larger than the adaxial and monosymmetry appears to be due to later expression of TCP in developing corolla.

Cleomaceae, the sister family to Brassicaceae, provides an excellent opportunity to outline the role of *TCP1*. Most species have monosymmetric flowers, the ancestral character state for the family, in contrast to the dissymmetric species that dominate Brassicaceae (Hall et al., 2002). Specifically, flowers in Cleomaceae are monosymmetric due to the upward curvature of petals and stamens near anthesis. In flowers of some species, such as *Cleome violacea*,

there are shape, color and size differences between the adaxial and abaxial petals. These morphological characteristics are notably divergent from the nature of all other species in which the role of *TCP* has been investigated. Importantly, the developmental trajectory of monosymmetry has been characterized in *C. violacea* (Patchell et al., 2011), a transcriptome library is available, and a VIGS protocol has been established (Chapter 2). Thus, the tools are in place to investigate whether *TCP1* has been recruited for the development of monosymmetry in this taxon.

Current *TCP* models include examples of duplication followed by divergence as well as modification in gene regulation (Rosin and Kramer, 2009). Both mechanisms have been previously linked as causes for novel morphological development (Abzhanov et al., 2008). Studies of *Cleome TCP* orthologues indicate that more than one copy is present and they may represent possible contributors to monosymmetry (Patchell, unpublished). Taking advantage of the ability for VIGS to target both specific and multiple genes allows for this methodology to support the individual role of *TCP1* and its homologues within the Cleomaceae.

In this study, a *CvTCP1* homologue was targeted for silencing by VIGS determine its contribution to floral monosymmetry. A range of floral morphologies was observed in *CvTCP1*-TRV2 treated plants and quantitative reverse transcriptase PCR (qRT-PCR) was used to support that these morphologies were due to this downregulation of *TCP1*. This work represents a

critical step in understanding the roles of *TCP*-like genes in contributing to floral monosymmetry in Cleomaceae.

Methods

Construct design and VIGS

Construct design and viral inoculation was carried out as described previously (Chapter 2) and in accordance with previous VIGS works (Kramer and Schluter, 2003; Gould and Kramer, 2007; Sharma et al., 2011).

TCP1-like genes were amplified from *Cleome violacea* DNA and cDNA using primers designed from *Iberis amara* (Busch and Zachgo, 2007)**.** Amplification was done using *rTaq* DNA polymerase (Takara Co., Tokyo, Japan) and the recommended polymerase chain reaction (PCR) parameters. The amplified PCR products were gel-extracted and purified using a min-elute PCR product purification kit (Qiagen) prior to cloning into TOPO-TA plasmid vector (Invitrogen) using the manufacture instructions. Multiple clones were sequenced using BigDye Terminator Sequencing (Applied Biosystems, Foster City, CA) and vector-specific primers M13F and M13R (5'-GTA AAA CGA CGG CCA G-3'/ 5'-CAG GAA ACA GCT ATG AC-3'). Sequence identity was confirmed using a BLAST search as well as phylogenetic analyses (Bernard and Patchell, unpublished data). A cDNA sequence of the *CvTCP1* gene chosen for VIGS is listed Patchell (2012). One copy was examined for this study as an initial test of whether *TCP1* plays a role in floral symmetry. The copy chosen was one for which complementary gene expression data is available (Patchell, 2012).

Once the identity was confirmed, primers were designed (TCPXbaIf and TCPBamHIr; See chapter 2, Table 2.1) to amplify a fragment from the TCP1 homologue which would add the flanking restriction enzyme sites, XbaI and BamHI. A 507bp size fragment was amplified using the previously cloned PCR product as a template and then cloned into a TOPO-TA plasmid vector (Invitrogen). The large proportion of the *TCP1* coding sequence was including into the construct to support strong silencing of *TCP1* which is believed to function in a dosage-dependent manner in Brassicaceae (Busch et al., 2012). Because CYC-like TCP genes may remain undetected in the Cleomaceae, a larger sequence insert was chosen capable which could simultaneously silence conserved homologues. This approach should prevent genetic redundancy from recovering wildype phenotypes in VIGS-treated plants. To obtain a large amount of insert for digestion, *E.coli* containing the cloned PCR product was grown for 2 days in 200ml LB followed by midiprep using a Nucleobond Xtra kit (Nucleobond) in accordance to the manufactures instructions. *E.coli* containing the TRV2 vector was also grown and subjected to the same midi prep treatment.

To assemble the *TCP1* construct both the TRV2 vector and TOPO-TA vector containing the *TCP1* homologue were individually double digested using XbaI and BamHI restriction enzymes (New England BioLabs). The fragments were then ligated together using T4 DNA ligase in an over night reaction at 14^{o}C. Construct identity was confirmed using BigDye Terminator sequencing (Applied Biosystems, Foster City, CA) and primers which span the TRV2 cloning site, 156F (5'-TTA CTC AAG GAA GCA CGA TGA GC-3') and 156R (5'-GAA

CCG TAG TTT AAT GTC TTC GGG-3'). Sequences were obtained with an ABI-3730 DNA Analyzer (Applied Biosystems, Foster City, California, USA) after being cleaned with a Performa DTR V# 96-well Short Plate Kit (Edge BioSystems, Gaithersburg, MD). Chromatograms were edited in Sequencher v. 4.10.1.

Construct transformation into *Agrobacterium*, VIGS inoculation, infected plant RNA extraction and cDNA synthesis as well as QRT-PCR analysis was carried out as previously described (Chapter 2). A total of 101 *C. violacea* plants were treated with the *CvTCP1*-TRV vector during VIGS trials which also included other treatment groups (Chapter 2). Control and mock treated (empty TRV2) plants were to other. Control and mock-treated *C. violacea* were established within each trial to compared against the treated groups (See Chapter 2 Table 2.2 for trial composition).

Morphological characterization

Floral development and mature morphology of *C. violacea* has been described previously (Karrer, 1991; Erbar and Leins, 1997; Patchell et al., 2011) and provided foundation for morphological comparison between wildtype and VIGS plants. Mature flowers have enlarged abaxial sepals, differences in size, shape and colour between abaxial and adaxial petals, and presence of a large adaxial gland (Figure 3.1A). Adaxial petals are smaller and dominated by a yellow spot. To better characterize potential VIGS-induced phenotypes, measurements were taken from both wildtype and potentially down-regulated

flowers. Petal width and length were taken from 12 untreated flowers. The same measurements were taken from irregular flowers in VIGS treated plants.

Results

Cleome violacea plants were subject to silencing using the *CvTCP1*-construct. Symptoms of downregulation of *TCP1* did not arise until after 30 days in order for the treated seedlings to reach the flowering state. Treated *C. violacea* plants displayed curled stems, a symptom typical of TRV2 viral infection. (Chapter 2). Flowers in control and mock-treated plants displayed no atypical viral symptoms suggesting that the virus is not responsible for atypical floral morphology in the treated group.

In order to detect changes in floral morphology, measurements were recorded for both the control and viral-treated individuals (Table 3.1). For each flower chosen to be measured, the length and width of all four petals were recorded (two adaxial, two abaxial). The length of each petal was measured along the midvein and the width was taken from the widest section of the petal. Control flowers display two abaxial petals with an average width of 3.10 ± 0.12 cm and a length of 3.44 ± 0.14 cm (n =12 flowers, ± sample variance). These petals were completely maroon unlike the two adaxial petals which display yellow spots (Figure 3.1A). The adaxial petals were also oblong in shape with an average width of 1.69 ± 0.10 cm and a length of 3.2 ± 0.12 cm (Figure 3.1A and Table 3.1).

A range of silenced phenotypes was observed in VIGS treated plants. Transformations which noticeably deviated from typical wildtype morphology were categorized into three groups: uniform maroon (Figure 3.1B-D), uniform

yellow (Figure 3.1F), and reduced adaxial petals (Figure 3.1E). For each atypical phenotype, the length and width of each petal was measured. Measurements were then grouped into abaxial width, abaxial length, adaxial width and adaxial length. Each group was compared to the by means of a one-tailed students *t*-test to the respective untreated group (e.g. untreated adaxial width with uniform maroon adaxial width) (Table 3.2). In every case, the adaxial and abaxial dimensions for each mutant phenotype were significantly different than the untreated petal dimentsion (Table 3.2)

Uniform maroon flowers displayed four petals similar in size and an absence of the wildtype adaxial yellow spots. The petal dimensions were similar across all four petals. Abaxial petals had an average diameter of 1.72 ± 0.36 cm and a length of 2.5 ± 0.24 cm while adaxial petals averaged a diameter of 1.70 ± 0.41 cm with a length of 2.85 ± 0.29 cm (Table 3.1). The similarity between both the abaxial and adaxial petals of this silenced phenotype suggests that the adaxial petals morphologically resemble the abaxial petals. This was the most commonly observed phenotype (n=5 flowers).

The second silencing category, uniform yellow flowers displayed yellow pigmentation on all four petals (Figure 3.1F). The average width of the abaxial petals was width 2.38±1.0 cm and the average length was length 2.75 ± 0.80 cm. (Table 3.1) For the abaxial petals, the width average was 1.06±0.38 cm and the length average was 2.88 ± 0.76 cm (Table 3.1). A sample size of two flowers was observed.

The third group (Figure 3.1E), reduced adaxial petals displayed wildtype coloration of the petals however, adaxial petals had shortened width and length average measurements when compared to the control (1.03 ± 0.13 cm, 2.69 ± 0.38 cm). The abaxial dimensions of this phenotypic category were similar to wildtype with an average width of 2.06 ± 0.47 cm and average length of 2.56±0.35 cm (n = 4 flowers) (Table 3.1).

A variety of other differences were observed in pTRV2-*CvTCP* treated plants, including loss of nectaries and reduction in stamen number (Figure 3.1). In some cases apex of the adaxial petals failed to curve outwards as seen in control *C. violacea* flowers (Figure 3.1A, C). Adaxial petals that failed to curve were always completely maroon and there grouped into the uniform maroon category.

In a single case, petal position of a treated flower deviated from wildtype morphology (Figure 3.1B, n=1). Control flowers produce petals with an upward orientation will the lamina of each petal above the horizontal central axis (Figure 3.1A). However, for this one mutant the petals were distributed evenly around the reproductive whorls in a similar pattern to dissymmetric flowers (Figure 3.1B).

After collection, qRT-PCR analysis will be used to determine the degree of *CvTCP1* downregulation in these mutants.

Discussion

The *CYC2* clade of the *TCP* gene family repeatedly has been found to include multiple transcription factors that function in establishing floral symmetry (Rosin and Kramer 2009). However, a large degree of molecular divergence of the floral symmetry machinery throughout flowering plants indicates that the

recruitment of these genes has occurred multiple times independently and that a large degree of molecular novelty may be involved for maintaining monosymmetry within the Brassicales compared to other monosymmetric groups (Rosin and Kramer, 2009; Busch et al., 2012). In this study, I provide functional data that demonstrates that *CvTCP1* is involved in floral symmetry of *C. violacea*.

CvTCP1-TRV2 treated plants had flowers with dramatic changes in floral symmetry. Interestingly, these flowers showed both adaxialization and abaxialization of petals. In other words, in some treated flowers all petals appear like adaxial petals of wildtype (Figure 3.1F), whereas in other flowers the petals were more abaxial-like (Figure 3.1B-D). This pattern is different from what is known from *Antirrhinum* and Fabaceae, but shares similarities with comparative work in Brassicaceae. In *Antirrhinum*, two TCP genes, *CYCLOIDEA* (*CYC*) and *DICHOTOMA* (*DICH*) are expressed in the adaxial portion of the flower and promote adaxial identity of the petals (Luo et al., 1996; Luo et al., 1999). This is similar to what has been observed in the Fabaceae, where *TCP*-like homologues promote adaxial identity and are expressed only in the adaxial portion of the developing flowers (Feng et al., 2006; Wang et al., 2008). In these instances, when the genes are knocked-out, a complete abaxialization is observed in all petals. Thus, based on our putative knock-down phenotypes, it appears that *CvTCP1* is functioning in a divergent manner such that there is not a clear role in promoting either adaxial or abaxial identity.

While there are no knock-out or knock-down phenotypes in Brassicaceae species examined, comparative expression data provides a potential testable

hypothesis to explain our putative knock-down data. In disymmetric *Arabidopsis thaliana AtTCP1* is transiently expressed in the dorsal portion of the flower at the floral bud stage (Cubas et al., 2001). Recent work involving one of the few monosymmetric Brassicaceae species *Iberis amara* identified a CYC-like homologue *IbTCP1* as responsible for establishing dorsal-ventral identity by inhibiting growth within the adaxial petals (Busch and Zachgo, 2007; Busch et al., 2012). However, *IaTCP1* is expressed broadly throughout the developing floral bud early in development and only becomes restricted to adaxial petals closer to anthesis (Busch and Zachgo, 2007; Busch et al., 2012). This expression pattern is consistent across multiple species: broad expression of *TCP1* genes early in development, with greater expression in adaxial petals later in development in monosymmetric species (Busch et al., 2012). Moreover, it is hypothesized that *TCP1* controls monosymmetry through repressing cell division in a dosage-dependent manner. The copy of *CvTCP1* examined in this study exhibits a broad expression pattern throughout floral development in *C. violacea* (Patchell, unpublished data). Thus, expression patterns indicate Cv*TCP1* may function similar to Brassicaceae, which is consistent with functional data presented here.

Only one *TCP1* copy has been recovered from all Brassicaceae examined to date (Busch and Zachgo, 2007; Busch et al., 2012), whereas two to three copies have been identified in all Cleomaceae species examined (Patchell and Bernard, unpublished data). The presence of multiple copies is likely due to a recent polyploidy event at the base of the Cleomaceae (Schranz and Mitchell-Olds, 2006). The maintenance of multiple copies in Cleomaceae suggests that a greater

degree of complexity is involved in regulating monosymmetry in this family as compared to Brassicaceae. This hypothesis is supported by morphological data. Monosymmetry in Brassicaceae is achieved by smaller adaxial than abaxial petals. In other words, monosymmetry may result from one difference (size) in one whorl (corolla). Monosymmetry in Cleomaceae, in *C. violacea* specifically, is the result of multiple differences in many whorls. Not only are there differences in size, shape, and corolla of adaxial versus abaxial petals, there are size differences in sepals as well as curvature of reproductive whorl. In other words, floral morphology itself provides a testable hypothesis that multiple gene copies are involved in promoting floral monosymmetry in *C. violacea.*

A major limitation in my ability to hypothesize how *CvTCP1* promotes floral monosymetry is having minimal data from only one copy. I assembled a TRV2 construct containing a 507bp insert of the 5' coding region of our *TCP1* homologue. Because VIGS induces silencing with variable penetrance it is likely that silenced flowers are expressing varying degrees of mRNA downregulation. Thus this range of phenotypic categories has arisen due to variable *TCP1* activity between biological replicates. In other words, we cannot eliminate the possibility that variable copy and gene combinations are being silenced within individual replicates. The insert used in the *TCP1* construct was large enough that it is highly possible for additional gene copies to have been targeted. If so, any gene which shares a region of approximately 23bp continuous similarity may have been downregulated by this VIGS construct (Burch-Smith et al., 2004; Senthil-Kumar et al., 2007). If multiple *TCP* genes were targeted and each is acting in a dosage-

dependent manner the combinations of silencing are multiplicative making it difficult to identify any individual gene candidate as being responsible for *TCP* maintenance.

In order to determine the contribution of this VIGS targeted *CvTCP1* homologue to floral symmetry qRT-PCR analysis is required. Silenced *C. violacea* flowers were pooled into the described phenotypic categories which will then be subjected to qRT-PCR analysis. Our initial goal was to determine the degree of downregulation of the targeted *CvTCP1* that has occurred. However, due to the size of the insert used for silencing, additional genes which possess high amounts of sequence similarity need to be assessed for possible downregulation by off target silencing as well. Therefore, primer sets for additional *TCP* homologues need to be designed for quantification within these collected phenotypes. Only once the degree of *CvTCP1* downregulation within each phenotypic pool has been identified in combination with other TCP gene family members will we be able to determine how this gene or genes function in promoting floral monosymmetry.

The relative fold change of each downregulated *TCP* homologue must further be analyzed. Because *TCP* transcription factors are believed to function in a dosage-dependent manner in Brassicaceae, the downregulation strength of each homologue targeted by the construct has the potential to be responsible for producing multiple phenotypic categories. Therefore the ability to correlate a specific locus with the regulation of monosymmetry will prove to be challenging since phenotypic categories may be the result of a shared reduction in transcript

abundance of multiple loci. This complexity reinforces the importance of detecting additional *TCP* homologues and their copies by qRT-PCR within each collected samples to identify possible contributors to the monosymmetric morphology.

Conclusion

Although it remains unclear if our identified *CvTCP1* homologue contributes to floral monosymmetry within the Cleomaceae the photographic data suggests some degree of *CYC2* homologue silencing has occurred. Here we have shown the use of VIGS as a functional methodology capable of being utilized to produce a variety of mutant phenotypes for future forward genetic work. To regulate off target silencing future construct assembly involving software to analyze the potential for shared sequence homology with the construct will be utilized (Senthil-Kumar and Mysore, 2011). Once individual *CvTCP* homologue silencing has been assessed, the variable penetrance of VIGS will allow for the quantification of candidate loci and outline their dosage-dependent expression.

Figures

Figure 3.1. *Cleome violacea* subjected to VIGS treatment using endogenous pTRV2-*CvTCP* construct displaying a range of silenced phenotypes. A: untreated *C. violacea* flower. B-F: treated *C. violacea* flowers displaying a range of phenotypes including uniform maroon (B,C,D), reduced adaxial petals (E), and uniform yellow (F). Scale bar = 1 mm.

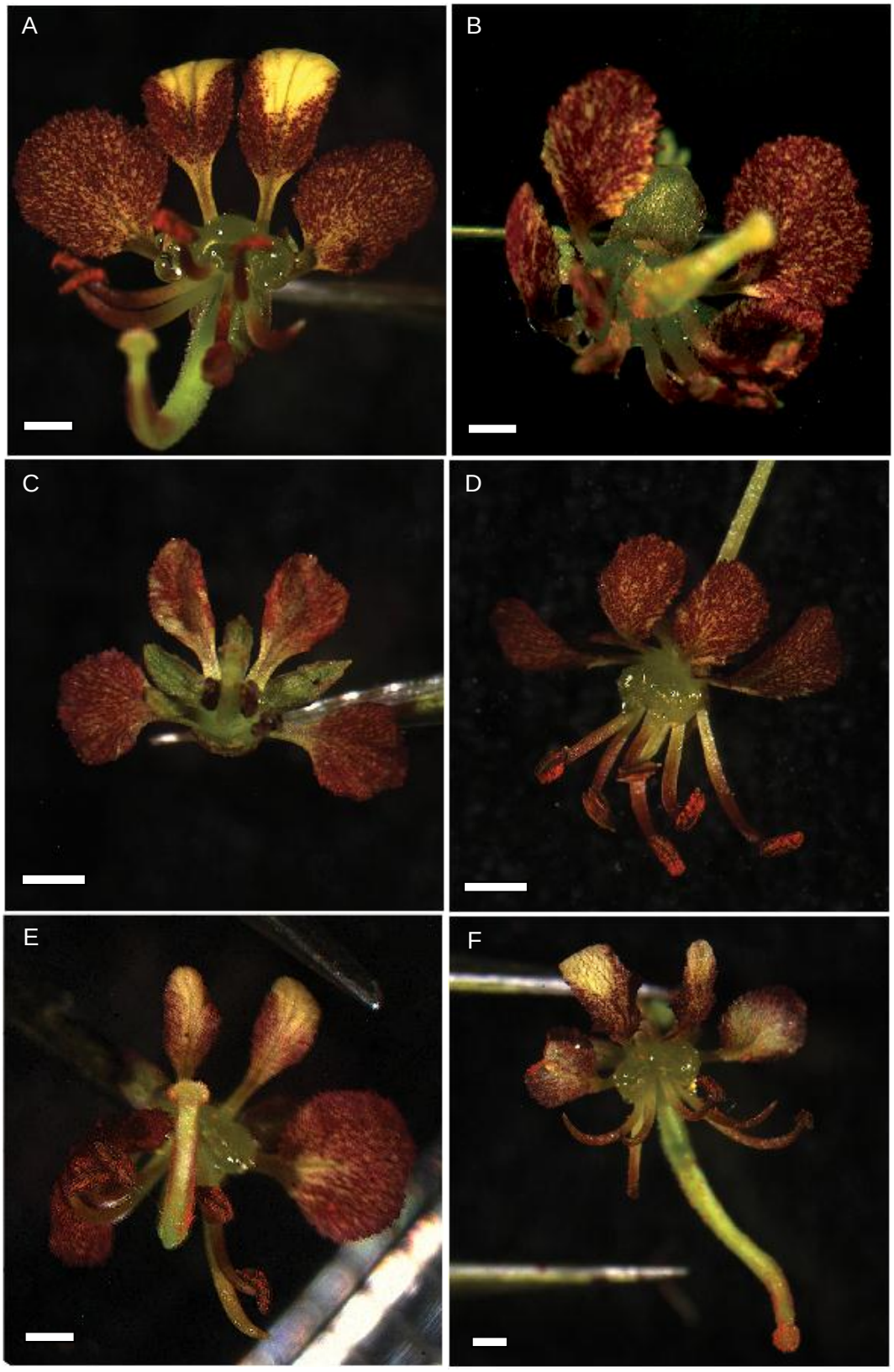
A
B
C
D
E
F

Table 3.1. Petal dimensions of untreated and pTRV2-*CvTCP* treated *Cleome violacea* after 30 days post VIGS inoculation. For each flower chosen all four petals were measured: 2 adaxial and 2 abaxial. The length of each petal was measured along the midvein and the width was taken from the widest section of the petal. Measurement averages were reported with ± one standard error.

Phenotypic category	Sample size	Average abaxial width (cm)	Average abaxial length (cm)	Average adaxial width (cm)	Average adaxial length (cm)
Control	12	3.10±0.12	3.44±0.14	1.69±0.10	3.2±0.12
Uniform maroon	5	1.72±0.36	2.5± 0.24	1.70± 0.41	2.85±0.29
Uniform yellow	2	2.38±1.0	2.75±0.80	1.06±0.38	2.88±0.76
Reduced adaxial petals	4	2.06 ±0.47	2.56±0.35	1.03± 0.13	2.69± 0.38

Table 3.2. Statistical comparison of petal dimensions between untreated and pTRV2-*CvTCP* treated populations after 30 days post VIGS inoculation. For each flower chosen all four petals were measured: 2 adaxial and 2 abaxial. Comparisons were made between the untreated population and a mutant phenotype population within a common location (abaxial or adaxial) and measurement (length or width). P-valves > 0.05 have been designated in bold.

	Df	Ave. Ab. Length T_{ST}	P-value	Ave. Ab. Width T_{ST}	P-value	Ave. Ad. Length T_{ST}	P-value	Ave. Ad. width T_{ST}	P-value
Maroon	32	7.369	**1.108 E -8**	10.001	**1.131E-11**	2.886	**0.003**	0.090	**0.466**
Yellow	26	3.517	**0.0008**	3.862	**0.0003**	1.925	**0.040**	4.697	**3.736 E-5**
Reduced ad. petals	30	5.964	**7.718 E -7**	6.812	**7.381 E -8**	3.775	**0.0004**	6.991	**4.540 E -8**

Literature Cited

Abzhanov, A., Extavour, C.G., Groover, A., Hodges, S.A., Hoekstra, H.E., Kramer, E.M., and Monteiro, A. (2008). Are we there yet? Tracking the development of new model systems. Trends in Genetics **24,** 353-360.

Baulcombe, D.C. (1999). Fast forward genetics based on virus-induced gene silencing. Current Opinion in Plant Biology **2,** 109-113.

Becker, A., and Lange, M. (2010). VIGS - genomics goes functional. Trends in Plant Science **15,** 1-4.

Burch-Smith, T.M., Anderson, J.C., Martin, G.B., and Dinesh-Kumar, S.P. (2004). Applications and advantages of virus-induced gene silencing for gene function studies in plants. Plant Journal **39,** 734-746.

Busch, A., and Zachgo, S. (2007). Control of corolla monosymmetry in the Brassicaceae *Iberis amara*. Proceedings of the National Academy of Sciences of the United States of America **104,** 16714-16719.

Busch, A., Horn, S., Muhlhausen, A., Mummenhoff, K., and Zachgo, S. (2012). Corolla monosymmetry: evolution of a morphological novelty in the Brassicaceae family. Molecular Biology and Evolution **29,** 1241-1254.

Cubas, P. (2004). Floral zygomorphy, the recurring evolution of a successful trait. Bioessays **26,** 1175-1184.

Cubas, P., Coen, E., and Zapater, J.M.M. (2001). Ancient asymmetries in the evolution of flowers. Current Biology **11,** 1050-1052.

Damerval, C., Le Guilloux, M., Jager, M., and Charon, C. (2007). Diversity and evolution of *CYCLOIDEA*-like TCP genes in relation to flower development in Papaveraceae. Plant Physiology **143,** 759-772.

Di Stilio, V.S. (2011). Empowering plant evo-devo: Virus induced gene silencing validates new and emerging model systems. Bioessays **33,** 711-718.

Kramer, E.M., and Schluter, P.M. (2003). Complex patterns of gene duplication in the *APETALA3* and *PISTILLATA* lineages of the Ranunculaceae. International Journal of Plant Science **164,** 1-11.

Feng, X.Z., Zhao, Z., Tian, Z.X., Xu, S.L., Luo, Y.H., Cai, Z.G., Wang, Y.M., Yang, J., Wang, Z., Weng, L., Chen, J.H., Zheng, L.Y., Guo, X.Z., Luo, J.H., Sato, S.S., Tabata, S., Ma, W., Cao, X.L., Hu, X.H., Sun, C.R., and Luo, D. (2006). Control of petal shape and floral zygomorphy in Lotus japonicus. Proceedings of the National Academy of Sciences of the United States of America **103,** 4970-4975.

Galego, L., and Almeida, J. (2002). Role of *DIVARICATA* in the control of dorsoventral asymmetry in *Antirrhinum* flowers. Genes & Development **16,** 880-891.

Gould, B., and Kramer, E.M. (2007). Virus-induced gene silencing as a tool for functional analyses in the emerging model plant *Aquilegia* (columbine, Ranunculaceae). Plant Methods **3,** 6.

Hall, J.C., Sytsma, K.J., and Iltis, H.H. (2002). Phylogeny of Capparaceae and Brassicaceae based on chloroplast sequence data. American Journal of Botany **89,** 1826-1842.

Hidalgo, O., Bartholmes, C., and Gleissberg, S. (2012). Virus-induced gene silencing (VIGS) in *Cysticapnos vesicaria*, a zygomorphic-flowered Papaveraceae (Ranunculales, basal eudicots). Annals of Botany **109,** 911-920.

Hileman, L.C., and Cubas, P. (2009). An expanded evolutionary role for flower symmetry genes. Journal of Biology (London) **8,** 90.

Hileman, L.C., Kramer, E.M., and Baum, D.A. (2003). Differential regulation of symmetry genes and the evolution of floral morphologies. Proceedings of the National Academy of Sciences of the United States of America **100,** 12814-12819.

Howarth, D.G., and Donoghue, M.J. (2009). Duplications and Expression of *DIVARICATA*-Like Genes in Dipsacales. Molecular Biology and Evolution **26,** 1245-1258.

Jabbour, F., Nadot, S., and Damerval, C. (2009). Evolution of floral symmetry: a state of the art. Comptes Rendus Biologies **332,** 219-231.

Luo, D., Carpenter, R., Vincent, C., Copsey, L., and Coen, E. (1996). Origin of floral asymmetry in *Antirrhinum*. Nature **383,** 794-799.

Luo, D., Carpenter, R., Copsey, L., Vincent, C., Clark, J., and Coen, E. (1999). Control of organ asymmetry in flowers of *Antirrhinum*. Cell **99,** 367-376.

Martin-Trillo, M., and Cubas, P. (2010). TCP genes: a family snapshot ten years later. Trends in Plant Science **15,** 31-39.

Patchell, M.J., Bolton, M.C., Mankowski, P., and Hall, J.C. (2011). Comparative floral development in Cleomaceae reveals two distinct Pathways Leading to Monosymmetry. International Journal of Plant Sciences **172,** 352-365.

Patchell, M.J. (2012) Evolutionary developmental genetics of floral monosymmetry in *Cleome violacea* (Cleomaceae). University of Alberta. Edmonton, Alberta.

Preston, J.C., Kost, M.A., and Hileman, L.C. (2009). Conservation and diversification of the symmetry developmental program among close relatives of snapdragon with divergent floral morphologies. New Phytologist **182,** 751-762.

Preston, J.C., Hileman, L.C., and Cubas, P. (2011). Reduce, reuse and recycle: Developmental evolution of train diversificiation. American Journal of Botany **98,** 397-403.

Rosin, F.M., and Kramer, E.M. (2009). Old dogs, new tricks: Regulatory evolution in conserved genetic modules leads to novel morphologies in plants. Developmental Biology **332,** 25-35.

Ruiz, M.T., Voinnet, O., and Baulcombe, D.C. (1998). Initiation and maintenance of virus-induced gene silencing. Plant Cell **10,** 937-946.

Schranz, M.E., and Mitchell-Olds, T. (2006). Independent ancient polyploidy events in the sister families Brassicaceae and Cleomaceae. Plant Cell **18,** 1152-1165.

Senthil-Kumar, M., and Mysore, K.S. (2011). New dimensions for VIGS in plant functional genomics. Trends in Plant Science **16,** 656-665.

Senthil-Kumar, M., Hema, R., Anand, A., Kang, L., Udayakumar, M., and Mysore, K.S. (2007). A systematic study to determine the extent of gene silencing in *Nicotiana benthamiana* and other Solanaceae species when heterologous gene sequences are used for virus-induced gene silencing. New Phytologist **176,** 782-791.

Sharma, B., Guo, C., Kong, H., and Kramer, E.M. (2011). Petal-specific subfunctionalization of an *APETALA3* paralog in the Ranunculales and its implications for petal evolution. New Phytologist **191,** 870-883.

Wang, Z., Luo, Y.H., Li, X., Wang, L.P., Xu, S.L., Yang, J., Weng, L., Sato, S.S., Tabata, S., Ambrose, M., Rameau, C., Feng, X.Z., Hu, X.H., and Luo, D. (2008). Genetic control of floral zygomorphy in pea (*Pisum sativum* L.). Proceedings of the National Academy of Sciences of the United States of America **105,** 10414-10419.

Zhang, W.H., Kramer, E.M., and Davis, C.C. (2010). Floral symmetry genes and the origin and maintenance of zygomorphy in a plant-pollinator mutualism. Proceedings of the National Academy of Sciences of the United States of America **107,** 6388-6393.

Zhou, X.R., Wang, Y.Z., Smith, J.F., and Chen, R.J. (2008). Altered expression patterns of TCP and MYB genes relating to the floral developmental transition from initial zygomorphy to actinomorphy in *Bournea* (Gesneriaceae). New Phytologist **178,** 532-543.

Chapter 4 Conclusion

Functional analysis and VIGS contribution to Evo-devo research

Functional data is required to determine the genes and regulatory changes responsible for the establishment of specific traits. Specifically, these data are essential to understanding the evolution of a particular process and provide insight into morphological novelty (Rosin and Kramer, 2009; de Bruijn et al., 2012). The majority of evolutionary developmental research has looked at candidate genes and their expression patterns to link their functions with morphological evolution through comparative work (Abzhanov et al., 2008; de Bruijn et al., 2012). Strong hypotheses regarding the evolutionary origins of particular morphologies can be established by combining phylogenetic analyses of organisms and genes, comparative gene expression data, and functional experiments in species with variable morphologies (Abzhanov et al., 2008; de Bruijn et al., 2012).

The genomic era has focused on determining the role of individual genomic sequences and their contribution to the makeup of a cellular organism (Stratmann and Hind, 2011). While obtaining sequence data has rapidly progressed, correlating sequences with a function has lagged behind (de Bruijn et al., 2012). To determine how genes are interacting and how they contribute toward a particular phenotype functional data is required (Abzhanov et al., 2008).

Many gene sequences still have obscure functions, even within models whose genomes have been completely sequenced (Stratmann and Hind, 2011; Fitzgerald et al., 2012). Model organisms offer extensive information about gene functions however, many homologues must be studied endogenously to elucidate their function within the context of their expression (Stratmann and Hind, 2011).

It is clear that evo-devo studies require tools which can be applied to the systems possessing morphologies and traits of interest. A minimum of one functional methodology is required to establish a new system as an emerging evo-devo model (Abzhanov et a; 2008). Here, I met this criterion by introducing the reverse genetic functional technique virus-induced gene silencing (VIGS) into two potential plant systems: *Cleome violacea* (Cleomaceae) and *Erucaria erucarioides* (Brassicaceae). However, these data show that *C. violacea* is clearly more amenable to the VIGS methodology than *E. erucarioides*.

This thesis represents an essential contribution to the development of *C. violacea* as an emerging model system. More importantly, there is a larger research community that is interested in the development of *C. violacea* has a model organism. In collaboration with C. Pires (University of Missouri), we have generated a transcriptome library. The comparative Brassicaceae genomic community is proposing to sequence the genome, which would complement the current genome sequenced for *C. spinosa*.

Future VIGS optimization in *Cleome violacea* and *Erucaria erucarioides*

As with model systems studied, optimization of the VIGS methodology is required for each new system (Dinesh-Kumar et al., 2003; Burch-Smith et al., 2006; Wang et al., 2006). The susceptibility of VIGS appears to be species specific and nucleotide homology does not always correlate with silencing efficiency (Senthil et al., 2007; Chapter 2). Therefore, an initial VIGS trial using available heterologous constructs is advisable to identify if endogenous constructs have the potential to be successful. That is, I demonstrate in chapter 2 that using

readily available heterologous constructs from *Arabidopsis* is a viable option as a first-pass to determine whether a relative may be amenable to VIGS. While endogenous constructs were more effective, results from using the *Arabidopsis* construct in VIGS experiments were a good indicator of success with endogenous constructs in our focal species. That is, *PDS* downregulation and photobleaching was much stronger for *C. violacea* that *E. erucarioides* regardless of construct. These data shows the potential for continued VIGS experiments in focal species. For both *C. violacea* and *E. erucarioides* optimization of the VIGS methodology can now occur in order to strengthen future experiments.

To increase efficiency and penetrance of silencing symptoms, alternate experimental variables should be tested. For example, vacuum infiltration was chosen because previous studies indicate it the most efficacious infiltration method (Wang et al., 2006). However, silencing genes only identified from transcriptomes of mature organs (i.e. flowers) can be difficult to do with this approach (Sharma et al., 2011). Specifically for *Erucaria*, flowers are produced after a long vegetative growth stage and vacuum infiltration becomes difficult due to individual plant size. The timing for infiltration is particularly important given interest in fruit characteristics. In this case, syringe injection (Gould and Kramer, 2007; Sharma et al., 2011) or toothpick inoculation (Senthil-Kumar and Mysore, 2011b) may be a more favourable option. Alternatively, infiltration at later stages or in detached fruits could be attempted as these approaches were effective in tomato (Fu et al., 2005; Romero et al., 2011).

Future optimization of *C. violacea* and *E. erucarioides* must also aim to improve silencing penetrance which was found to be highly variable. Previous reports using *Arabidopsis* found silencing as high as 90% in treated individuals (Wang et al., 2006) with similar efficacy's being reported in *Nicotiana benthamiana* (Senthil-Kumar and Mysore, 2011a). Here silencing efficacy fell on average below 40% (37%) between 4 constructs for *C. violacea* and at 8% for *E. erucarioides* between 2 constructs, although it is not clear if this is due to variable experimental conditions or due to the susceptibility of these non-model organisms. Host genotype can also effect the performance of a viral construct indicating that optimal silencing levels in these two systems may be lower than other previously reported hosts (Senthil-Kumar and Mysore, 2011b). Simultaneous reporter gene expression assays during VIGS infection has proven beneficial for determining viral activity and to localize silencing in order to quantify silencing efficiency (Zhang et al. 2010; Burch-Smith et al., 2006; Senthil-Kumar and Mysore, 2011b). To counter decreased silencing rates, many trials with numerous individuals were completed to collect enough biological replicates for analysis with qRT-PCR. However, this approach is not ideal since it contradicts a major benefit of VIGS application, namely, its short time requirement (Senthil-Kumar and Mysore, 2011b). In order for this technique to fulfill its role as a rapid functional assessment of candidate loci, increased silencing efficacy is of paramount importance.

Growth conditions of the post-innoculated seedlings play a predominant role in establishing silencing symptoms (Wang et al., 2006). For both *Nicotiana*

and *Arabidopsis*, silencing was most effective when plants were grown at 22^{o}C a deviation from their optimal growing temperature (Wang et al., 2006; Senthil-Kumar and Mysore, 2011a). Temperatures above 22^{o}C displayed a rapid decay in silencing efficacy demonstrating that new model systems must be flexible in their growing conditions to produce strongly silenced symptoms. Favoring temperatures which promote the systemic spread of the virus can increase viral movement throughout the targeted hosts. In future *C. violacea* and *E. erucarioides* VIGS treatments, temperature should be manipulated to identify the most effective condition for post inoculation plant maintenance (Senthil-Kumar and Mysore, 2011b). It is important to take the natural growing conditions of the focal plants in consideration when planning these experiments.

To further improve phenotypic characterization of VIGS using *C. violacea*, atypical vegetative symptoms which arise from viral infection should be reduced. In previous work, choosing a new viral strain for construct assembly has been a viable solution, however, the TRV2 strain (YL156) used in this work has shown to be the most efficacious strain for targeting Brassicaceous species. If VIGS work using *C. violacea* is to proceed with this viral strain, it is advisable not to target genes associated with stem development since the stunting of treated plants will make phenotypic characterization extremely difficult. Strategies such as immunocapture RT-PCR can be used to parameterize viral levels and symptomology within treated groups as a way to isolate silencing phenotypes (Senthil-Kumar and Mysore, 2011a).

Fruit development in heteroarthrocarpic species *Erucaria erucarioides*

After continued optimization of VIGS in *E erucarioides*, future work may utilize this methodology for additional functional analysis. The molecular mechanisms responsible for the establishment of the novel fruit morphology heteroarthrocarpy remains unknown and therefore, it is an ideal pursuit for future *E. erucarioides* VIGS application (Hall et al., 2011; Avino et al., 2012). Fruit morphology is under intensive evolutionary pressure due to its association with plant fitness and offers a potential manipulation site for regulating species success (Hall and Donohue, in press). Although heteroarthrocarpy is a derived fruit type within Brassicaceae, its attributes (indehiscence, segmentation, and indehiscence) are found in fruits across angiosperms (Imbert, 2002). Thus, additional VIGS experiments would provide insight in the genetic basis of differences in seed dispersal as well as natural variation in dehiscence capabilities. This is particularly important as close relatives of *E. erucarioides* include canola, a crop for which early fruit opening has significant negative impact (Price et al., 1996).

After optimization to increase the silencing efficiency and duration within *E. erucarioides*, fruit development and dehiscence genes can be targeted for downregulation. Currently, six homologous loci have been identified and are believed to contribute to the establishment of heteroarthrocarpy (Avino et al., 2012). By targeting these genes individually with VIGS and establishing their function, we can potentially dissect aspects of the regulatory network responsible for the molecular development of this fruit type. Specifically, we can directly test which components of the pathway have been conserved as well as test how this pathway may have been modified to produce segmentation and indehiscence. The

candidate gene *FRUITFULL* remains a prime initial target for silencing within *Erucaria*.

Floral development in monosymmetric *Cleome violacea*

I have now established VIGS as a viable methodology for functional analysis within *C. violacea*. After silencing with *PDS* was achieved, promising results were obtained for two additional knock downs, *FUL* and a *CYC-like* homologue *CvTCP1*. As originally predicted, a variety of phenotypes displaying variable alterations to floral symmetry were obtained in *CvTCP1*-VIGS plants. Thus, I have clearly shown that *TCP* contributes towards monosymmtry in *C. violacea*. However, these experiments were not as informative in how *TCP* generates monosymmetry. The construct utilized in this work most likely targeted multiple *CYC*-like genes due to the length of the coding sequence used. Therefore, in order to better elucidate the contributions of individual *TCP* genes to floral symmetry within the Cleomaceae, additional constructs targeting individual genes and copies need to be assembled and tested. Moreover, previous research on monosymmetric Brassicaceae species suggests that there is at least one *TCP* homolog responsible for establishing dorsal-ventral floral identity within the Brassicales (Busch and Zachgo, 2007; Busch et al., 2012). This research has shown that monosymmetry is correlated with different expression levels in abaxial versus adaxial petals. VIGS is an ideal methodology due to its variable penetrance to establish a set of individuals exhibiting a range of downregulation and subsequent ability to correlate their phenotypes to a specific quantity of mRNA transcript abundance. In sum, future VIGS experiments complemented by

comparative expression data should address two important issues: (1) the relative contribution of different loci to monosymmetry and (2) whether these contributions are dosage dependent, as observed in Brassicaceae.

This work as well as previous research on monosymmetric Brassicaceae species suggests that there is at least one *TCP* homolog responsible for establishing dorsal-ventral floral identity within the Brassicales . However, independent genomic duplications have occurred within the Cleomeaceae, likely generating additional paralogues and copies of *CYC*-like genes. These additional candidate *TCP* targets must also be targeted for VIGS downregulation in order to establish the contribution of individual loci to monosymmetry and the novel machinery utilized by the Cleomeaceae to maintain floral monosymmetry.

Conclusion

With the post-genomic era occurring, molecular techniques that are capable of producing high throughput results and complete data sets within a short time frame are in high demand (Becker and Lange, 2010; Stratmann and Hind, 2011). VIGS is one of the few techniques capable of meeting this demand as both a forward or reverse genetic tool (Becker and Lange, 2010; Senthil-Kumar and Mysore, 2011b). As I have shown, VIGS can selectively downregulate genes to induce a mutant phenotype for reverse genetic purposes. However, VIGS is also amenable to forward genetic applications in which entire cDNA libraries are used to produce viral construct libraries which can infect the treated group with a variety of silencing outcomes (Becker and Lange, 2010). These individuals can be screened and analyzed to identity novel candidates associated with particular

traits. Being that VIGS is a methodology capable of contributing to such a diversity of pursuits reinforces its importance to emerging models.

Here we have utilized VIGS for reverse genetic functional analysis however future work using either *C. violacea* or *E. erucarioides* may be able to take advantage of other VIGS applications now that the technique is accessible. Specifically for the Cleomaceae family, other genomic resources are being established for the group (Schranz and Mitchell-Olds, 2006; Schranz et al., 2007). Stable *Agrobacterium* transformation mediated by callus development has been success in two species, *C. gynandra* and *C. spinosa* (Newell et al. 2010; Tsai et al., 2012). Now, VIGS offers an additional methodology invaluable for its rapid ability to identify gene function. Specifically for our purposes this new technique is capable of contributing to evolutionary-developmental comparative work and ideally will be used to support the mechanisms by which select novel morphologies arose.

Literature Cited

Abzhanov, A., Extavour, C.G., Groover, A., Hodges, S.A., Hoekstra, H.E., Kramer, E.M., and Monteiro, A. (2008). Are we there yet? Tracking the development of new model systems. Trends Genet. **24,** 353-360.

Avino, M., Kramer, E.M., Donohue, K., Hammel, A.J., and Hall, J.C. (2012). Understanding the basis of a novel fruit type in Brassicaceae: conservation and deviation in expression patterns of six genes. EvoDevo **3,** 20.

Becker, A., and Lange, M. (2010). VIGS - genomics goes functional. Trends in Plant Science **15,** 1-4.

Burch-Smith, T.M., Schiff, M., Liu, Y., and Dinesh-Kumar, S.P. (2006). Efficient virus-induced gene silencing in Arabidopsis. Plant Physiol **142,** 21-27.

Busch, A., and Zachgo, S. (2007). Control of corolla monosymmetry in the Brassicaceae Iberis amara. Proceedings of the National Academy of Sciences of the United States of America **104,** 16714-16719.

Busch, A., Horn, S., Muhlhausen, A., Mummenhoff, K., and Zachgo, S. (2012). Corolla monosymmetry: Evolution of a morphological novelty in the Brassicaceae family. Molecular Biology and Evolution **29,** 1241-1254.

de Bruijn, S., Angenent, G.C., and Kaufmann, K. (2012). Plant 'evo-devo' goes genomic: from candidate genes to regulatory networks. Trends in Plant Science **17,** 441-447.

Dinesh-Kumar, S.P., Anandalakshmi, R., Marathe, R., Schiff, M., and Liu, Y. (2003). Virus-induced gene silencing. Methods in Molecular Biology **236,** 287-294.

Fitzgerald, T.L., Kazan, K., and Manners, J.M. (2012). The application of reverse genetics to polyploid plant species. Critical Reviews in Plant Sciences **31,** 181-200.

Fu, D.Q., Zhu, B.Z., Zhu, H.L., Jiang, W.B., and Luo, Y.B. (2005). Virus-induced gene silencing in tomato fruit. Plant Journal **43,** 299-308.

Gould, B., and Kramer, E.M. (2007). Virus-induced gene silencing as a tool for functional analyses in the emerging model plant *Aquilegia* (columbine, Ranunculaceae). Plant Methods **3,** 6.

Hall, J.C., and Donohue, K. (in press). Genetics of Plant Dispersal. In Dispersal: causes and consequences, J. Clobert, M. Baguette, T. Benton, and J. Bullock, eds (Oxford University Press).

Hall, J.C., Tisdale, T.E., Donohue, K., Wheeler, A., Al-Yahya, M.A., and Kramer, E.M. (2011). Convergent evolution of a complex fruit structure in the tribe Brassiceae (Brassicaceae) American Journal of Botany **98,** 1989-2003.

Imbert, E. (2002). Ecological consequences and ontogeny of seed heteromorphism. Perspectives in Plant Ecology Evolution and Systematics **5,** 13-36.

Newell, C.A., Brown, N.J., Liu, Z., Pflug, A., Gowik, U., Westhoff, P., and Hibberd, J.M. (2010). *Agrobacterium tumefaciens*-mediated

transformation of *Cleome gynandra* L., a C-4 dicotyledon that is closely related to *Arabidopsis thaliana*. Journal of Experimental Botany **61,** 1311-1319.

Price, J.S., Hobson, R.N., Neale, M.A., and Bruce, D.M. (1996). Seed losses in commercial harvesting of oilseed rape. Journal of Agricultural Engineering Research **65,** 183-191.

Romero, I., Tikunov, Y., and Bovy, A. (2011). Virus-induced gene silencing in detached tomatoes and biochemical effects of phytoene desaturase gene silencing. Journal of Plant Physiology **168,** 1129-1135.

Rosin, F.M., and Kramer, E.M. (2009). Old dogs, new tricks: regulatory evolution in conserved genetic modules leads to novel morphologies in plants. Dev Biol **332,** 25-35.

Schranz, M.E., and Mitchell-Olds, T. (2006). Independent ancient polyploidy events in the sister families Brassicaceae and Cleomaceae. Plant Cell **18,** 1152-1165.

Schranz, M.E., Song, B.H., Windsor, A.J., and Mitchell-Olds, T. (2007). Comparative genomics in the Brassicaceae: a family-wide perspective. Current Opinion in Plant Biology **10,** 168-175.

Senthil-Kumar, M., and Mysore, K.S. (2011a). Virus-induced gene silencing can persist for more than 2 years and also be transmitted to progeny seedlings in *Nicotiana benthamiana* and tomato. Plant Biotechnology Journal **9,** 797-806.

Senthil-Kumar, M., and Mysore, K.S. (2011b). New dimensions for VIGS in plant functional genomics. Trends in Plant Science **16,** 656-665.

Sharma, B., Guo, C., Kong, H., and Kramer, E.M. (2011). Petal-specific subfunctionalization of an *APETALA3* paralog in the Ranunculales and its implications for petal evolution. New Phytol **191,** 870-883.

Stratmann, J.W., and Hind, S.R. (2011). Gene silencing goes viral and uncovers the private life of plants. Entomologia Experimentalis Et Applicata **140,** 91-102.

Tsai, Y.T., Chen, P.Y., and To, K.Y. (2012). Plant regeneration and stable transformation in the floricultural plant *Cleome spinosa*, a C-3 plant closely related to the C-4 plant *C-gynandra.* Plant Cell Reports **31,** 1189-1198.

Wang, C.C., Cai, X.Z., Wang, X.M., and Zheng, Z. (2006). Optimisation of tobacco rattle virus-induced gene silencing in *Arabidopsis*. Functional Plant Biology **33,** 347-355.

Zhang, C., Bradshaw, J.D., Whitham, S.A., and Hill, J.H. (2010). The development of an efficient multipurpose bean pod mottle virus viral vector set for foreign gene expression and RNA silencing. Plant Physiology **153,** 52-65.

Appendix

Appendix 1. Sequence alignment of *PHYTOENE DESATURASE* cDNA inserts from both *Erucaria erucarioides* and *Cleome violacea* to *Arabidopsis thaliana PDS* fragment. Primers used to amplify the construct inserts have been aligned 5' to 3'.

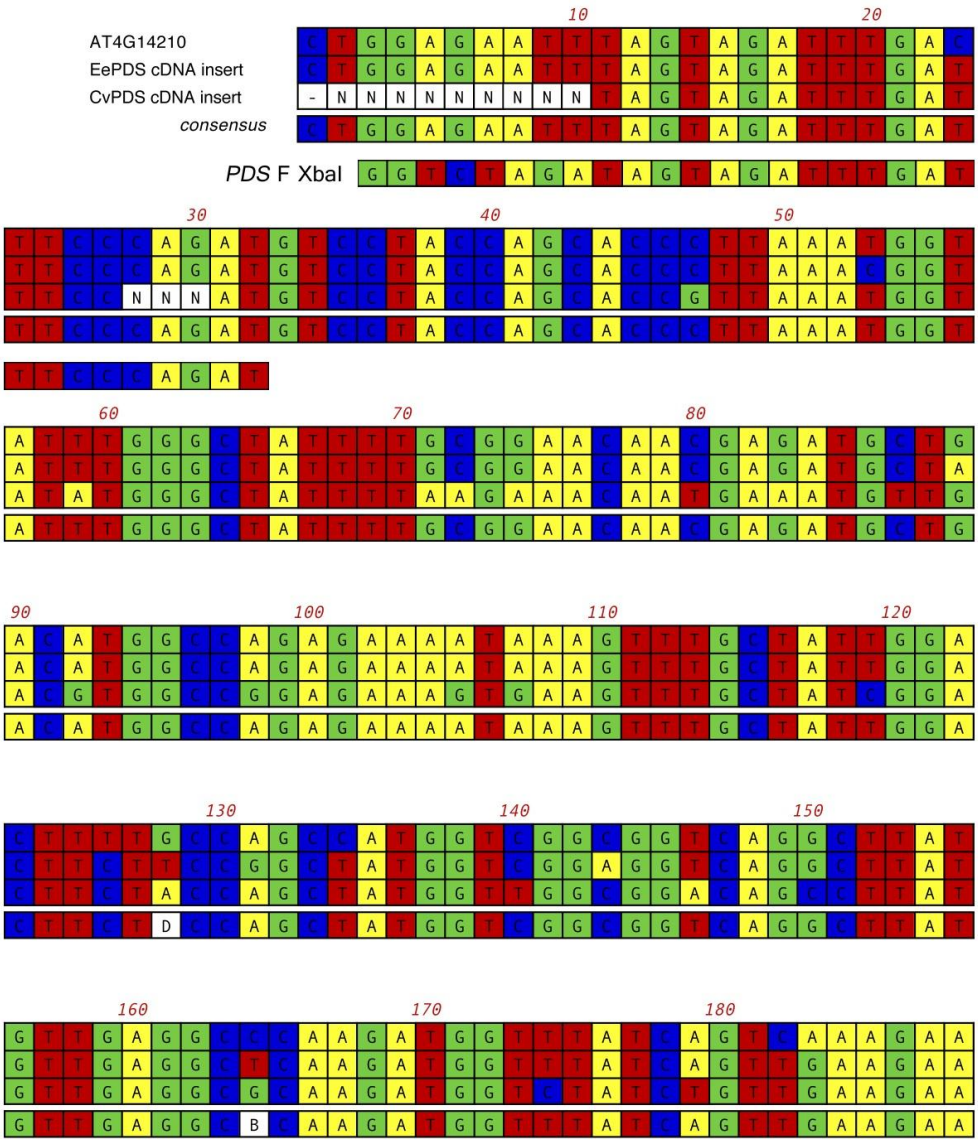
AT4G14210
EePDS cDNA insert
CvPDS cDNA insert
consensus
PDS F XbaI

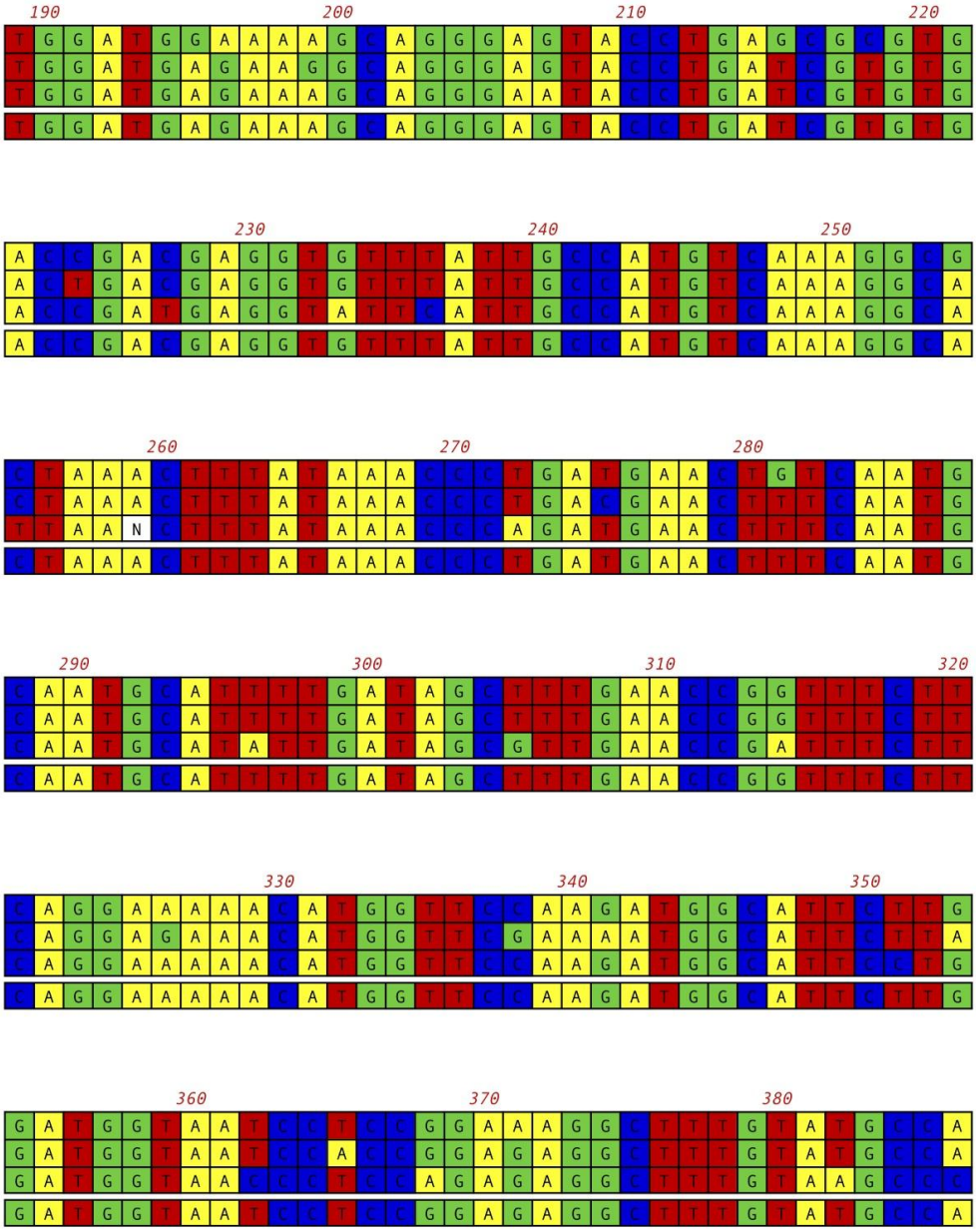
190
200
210
220
230
240
250
260
270
280
290
300
310
320
330
340
350
360
370
380

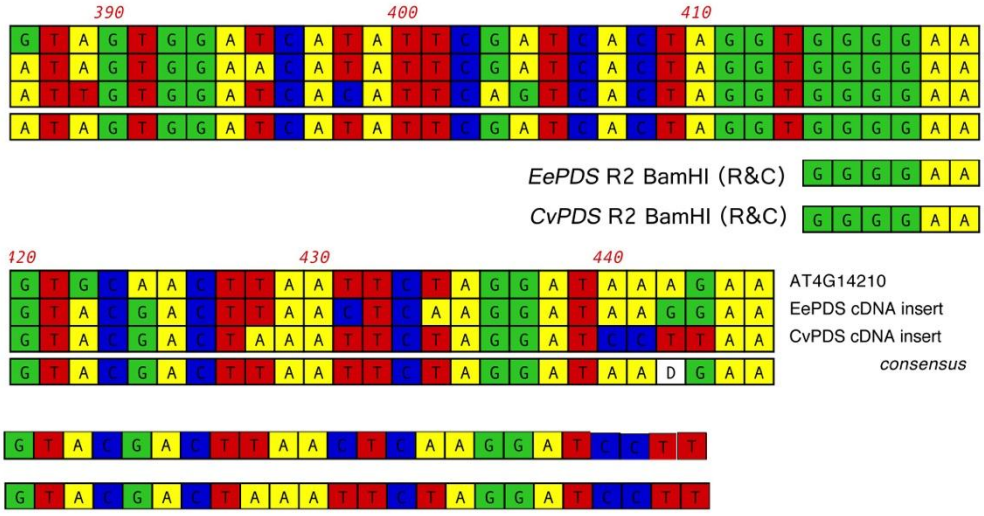
390
400
410
EePDS R2 BamHI (R&C)
CvPDS R2 BamHI (R&C)
120
430
440
AT4G14210
EePDS cDNA insert
CvPDS cDNA insert
consensus

Appendix 2. Sequence alignment of *FRUITFULL* cDNA inserts from both *Erucaria erucarioides* and *Cleome violacea* to *Arabidopsis thaliana FUL* fragment. Primers used to amplify the construct inserts have been aligned 5' to 3'.

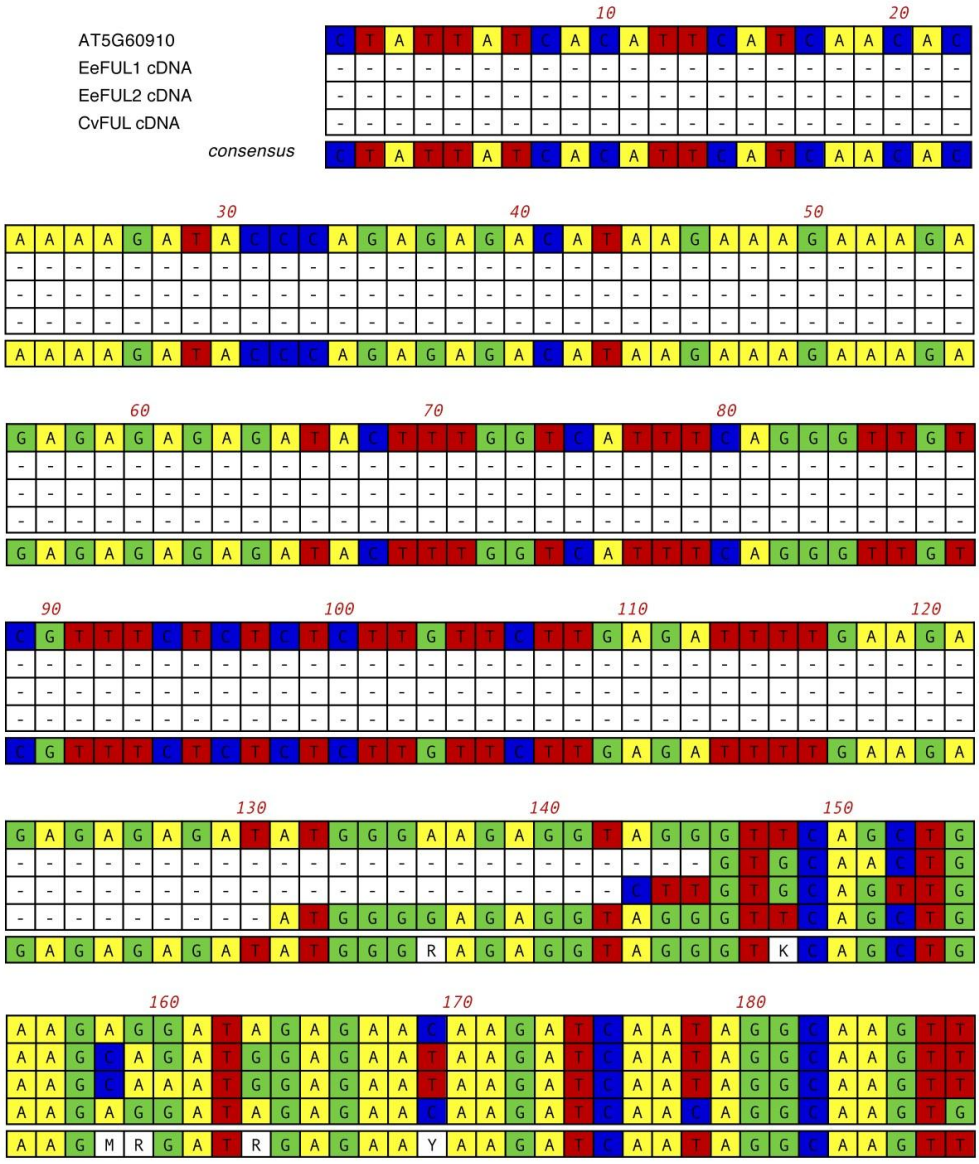
AT5G60910
EeFUL1 cDNA
EeFUL2 cDNA
CvFUL cDNA
consensus
10
20
30
40
50
60
70
80
90
100
110
120
130
140
150
160
170
180

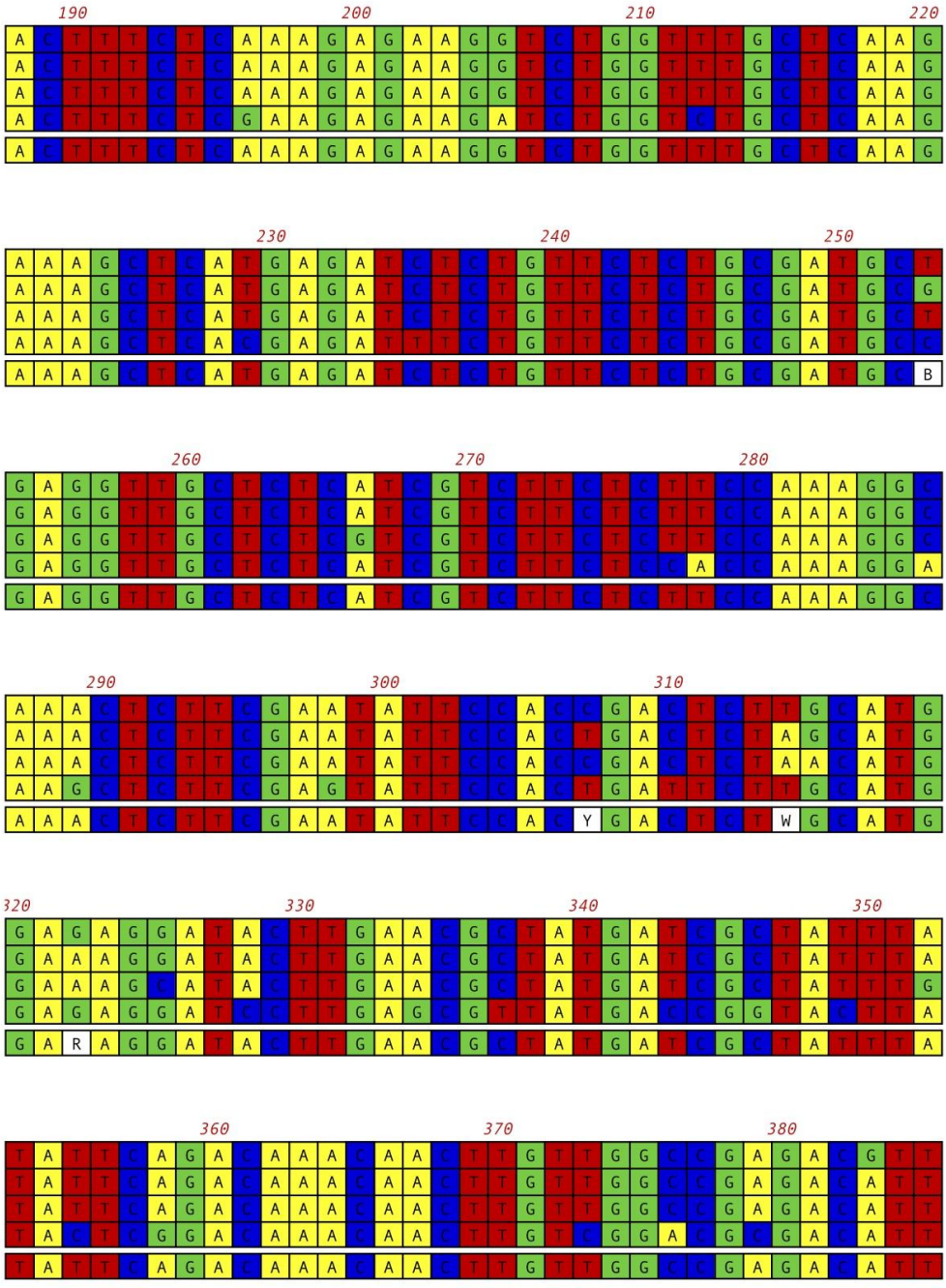
190
200
210
220
230
240
250
260
270
280
290
300
310
320
330
340
350
360
370
380

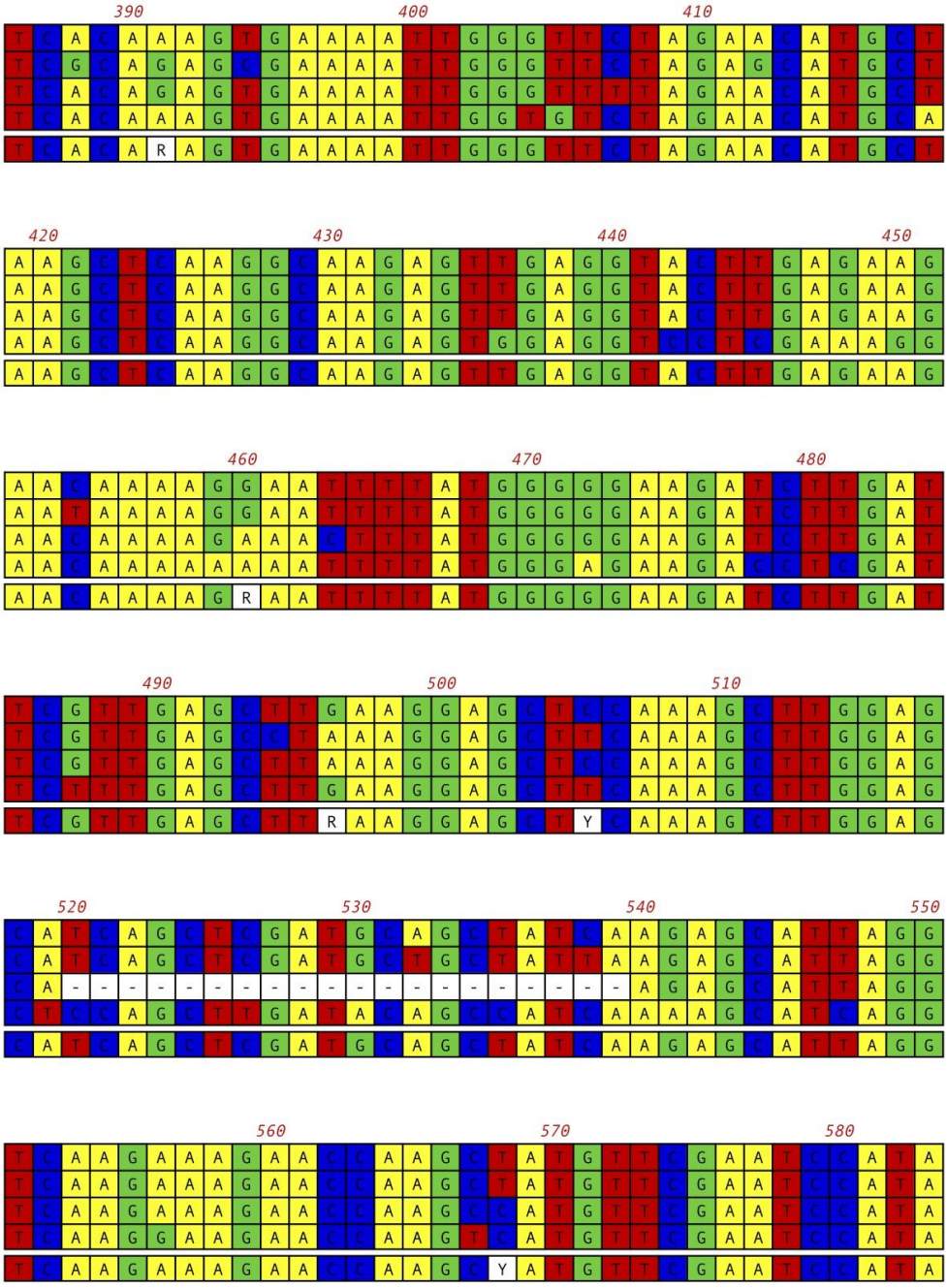
390
400
410
420
430
440
450
460
470
480
490
500
510
520
530
540
550
560
570
580

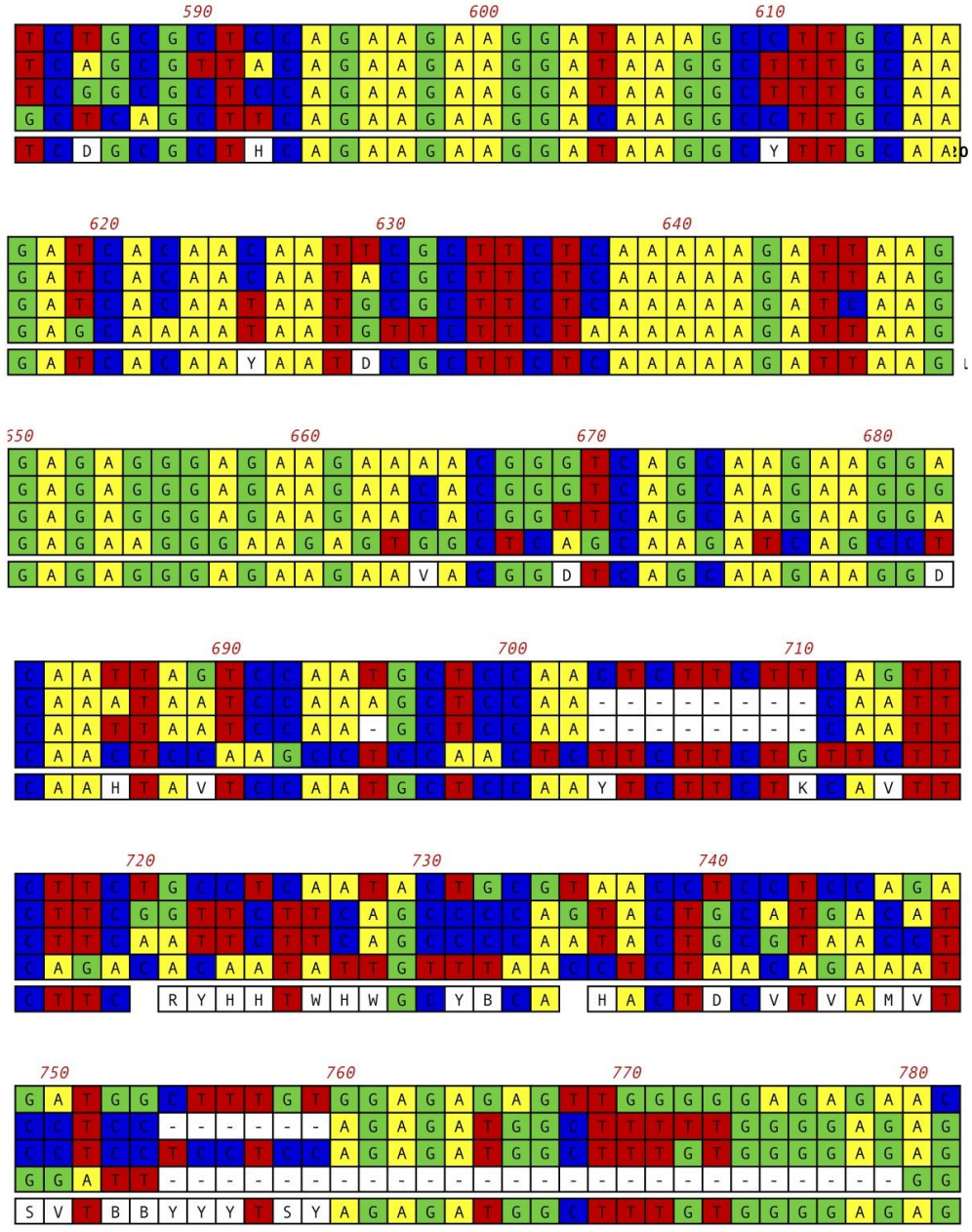
590
600
610
620
630
640
550
660
670
680
690
700
710
720
730
740
750
760
770
780

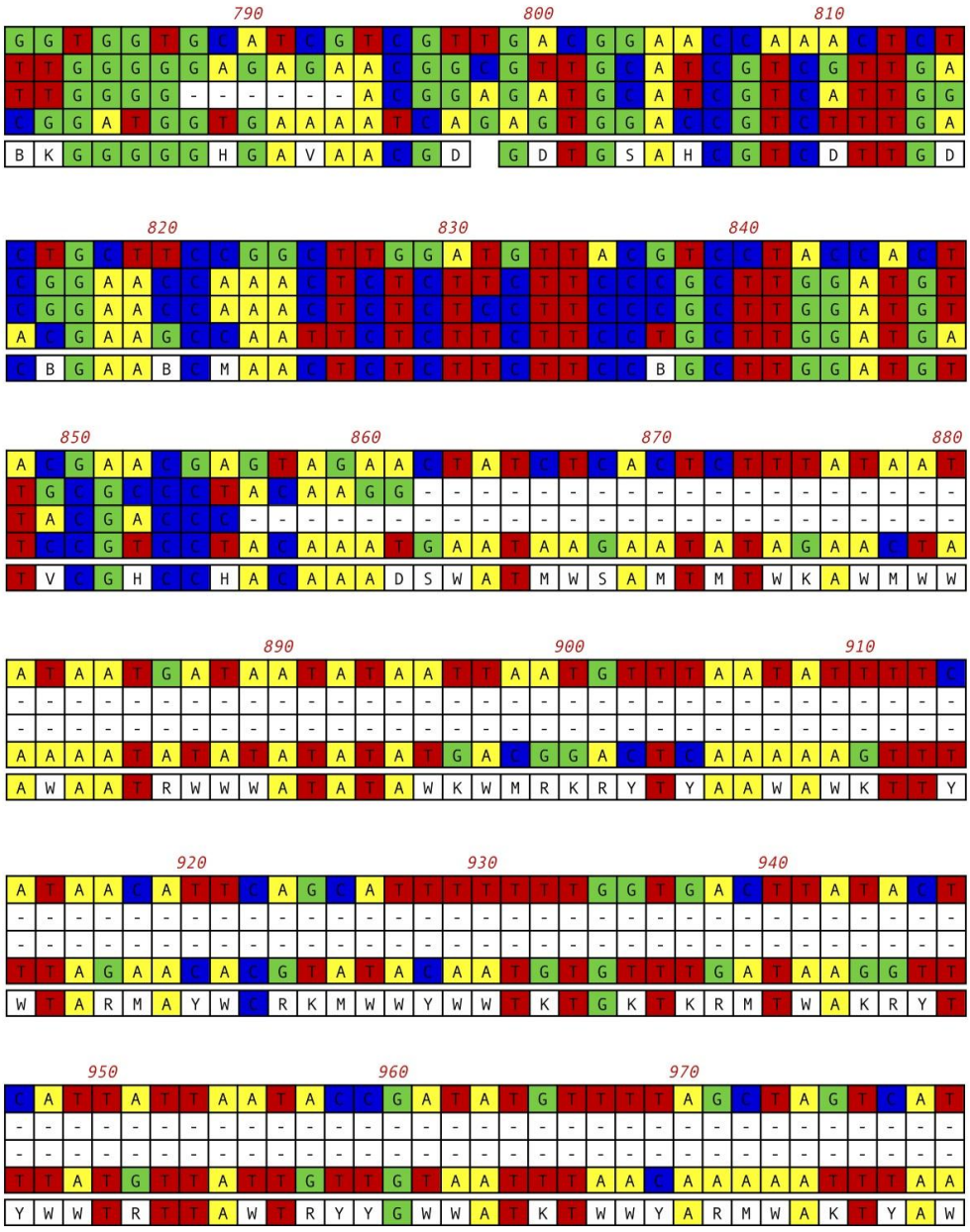
790
800
810
820
830
840
850
860
870
880
890
900
910
920
930
940
950
960
970

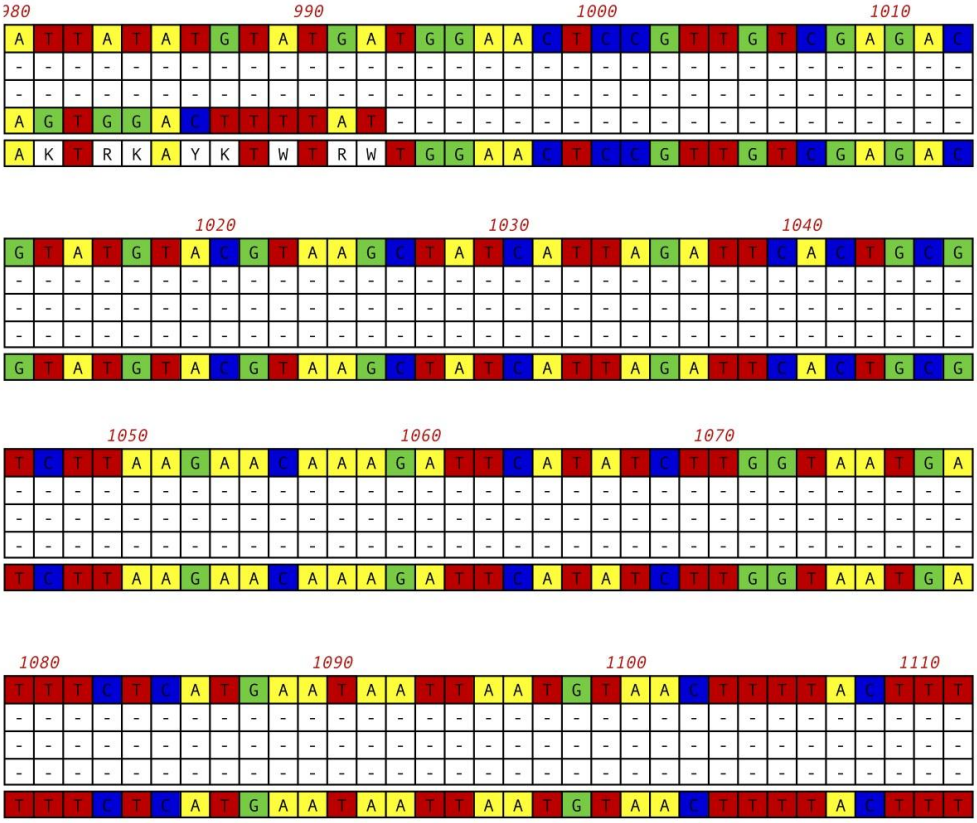
980
990
1000
1010
ATTATATGTATGATGGAACTCCGTTGTCGAGAGAC
AKTRKAYKTWTRWTGGAACTCCGTTGTCGAGAGAC
1020
1030
1040
GTATGTACGTAAGCTATTCATTAGATTTCACTGCG
GTATGTACGTAAGCTATTCATTAGATTTCACTGCG
1050
1060
1070
TCTTAAGAAACAAAGATTCATATCTTGGTAATGA
TCTTAAGAAACAAAGATTCATATCTTGGTAATGA
1080
1090
1100
1110
TTTCTCATGAAATAATTAATTGTAACTTTTTACTT
TTTCTCATGAAATAATTAATTGTAACTTTTTACTT

Appendix 3. Standard curve for primer efficiency calculation. A dilution series was created and amplified using four different primer sets. The obtained C_t values were then plotted against the log of their respective dilution factors to produce a standard curve.

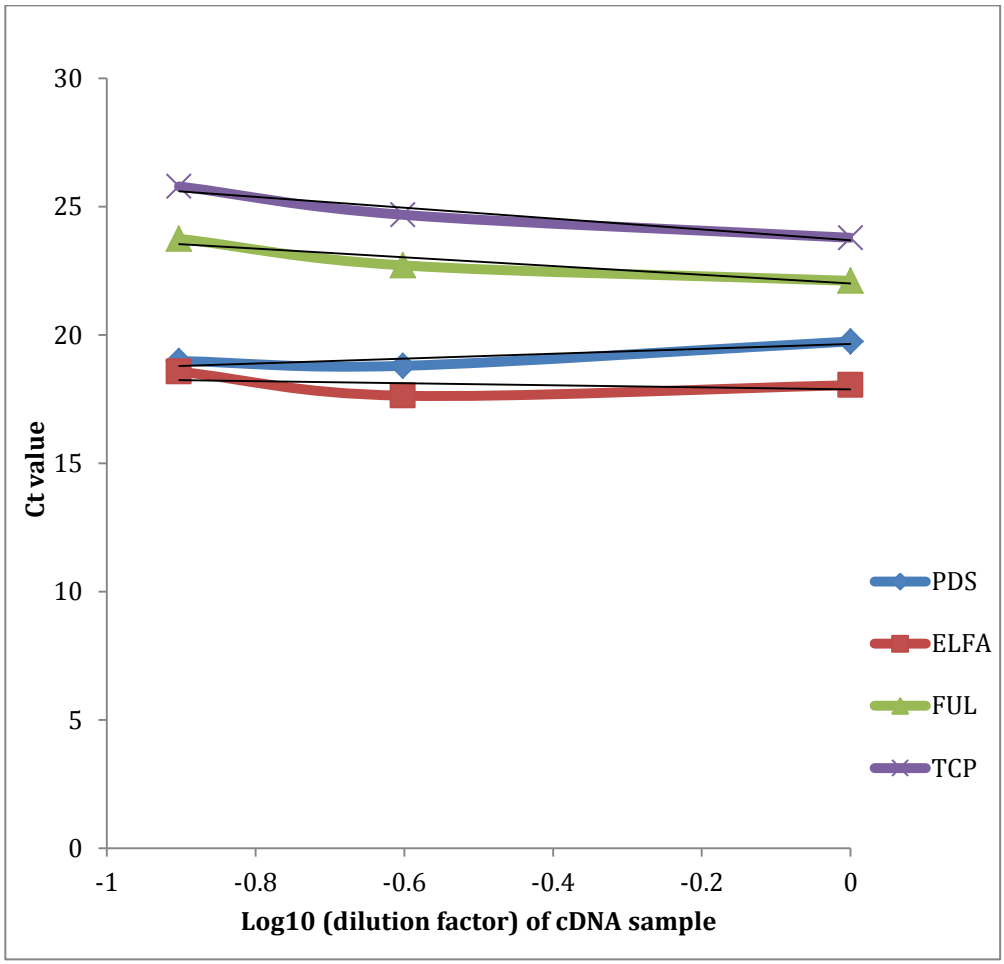

Appendix 4. Primer efficiency and slope analysis for qRT-PCR primer sets. Primer efficiencies were calculated using the slope of the standard curve produced from a dilution series of 3 samples for each primer set. The slope of each dilution series was then used to calculate efficiency with the formula $E_x = 10^{(-1/slope)} - 1$.

	Slope	Primer Efficiency (%)
EFA1	-0.400	31,366.66
PDS	0.949	-91.17
TCP1	-2.111	197.59
FUL	-1.699	287.65

Appendix 5. Summary of modifications and corrections recommended for the basis of future VIGS data collection using *Cleome violacea* and *Erucaria erucarioides*.

For the purposes of future work within the Hall lab, the inaccuracies of these experiments and how they can be corrected will be highlighted here.

Experiment modifications to be made:

Primer quality and design

Primer sets to be used for qRT-PCR detection of induced transcript downregulation by VIGS must display a specific set of characteristics:

i. The primers must detect an amplicon that is representative of only the loci of interest.

ii. The chosen reference gene(s) must be consistently expressed across all compared treatments.

iii. The primers must have amplification efficiencies high enough to meet the assumptions required for the $2^{-\Delta\Delta Ct}$ method.

iv. The primers must meet all other parameters required to be effective under the reaction conditions for qRT-PCR.

The above criteria were not satisfied by the four primers sets used during the qRT-PCR detection component of these experiments (Chapter 2). For the first criterion, our primers were designed to detect a region of the targeted gene that was also incorporating into the viral construct. Therefore, our primer sets detected the endogenous transcripts of the gene of interest (e.g. *PDS, FUL, TCP)* as well as the viral constructs and any associated viral transcripts (Rottenberg et al., 2006).

Due to the conserved sequence used to design our primer sets, they could not accurately represent the degree of downregulation of the endogenous transcript. The first step to correct this is to redesign primers that fall outside of the viral construct region (i.e. at least one of the primers is situated outside of the construct sequence) but still target the gene of interest. All primer sets with the exception of the reference gene (*EFA-1*) need to be redesigned.

Once new primers have been designed, they each need to be evaluated for their primer efficiency. The primer efficiencies failed to approach 100% for all four primer sets used here. Ideally, the primer sets detecting a target loci and the reference gene should have primer efficiencies within 5% of each other. The reference gene primer set can be re-evaluated for its efficiency without designing a new primer.

To determine primer efficiency, a standard curve using each primer set must be obtained. In this case, the primer efficiency was assessed using a 3 point dilution series. In the future, a minimum of a 5 point standard curve should to be created using standard samples of known concentrations over a dilution series with a concentration range of 5-log (Applied Biosystems). PCR products should be used to create the dilution series as opposed to cDNA samples in order to create a dilution range of this magnitude. A larger concentration range will provide a more accurate reporting of the individual primer efficiencies. Primer efficiencies can be obtained using the method previously described (Chapter 2). For each primer set that does not display an efficiency approaching 100% after the evaluation plate is and a standard curve based calculation of the efficiency has

been obtained, a new primer set must be designed. This is to be repeated until a high primer efficiency is obtained for each primer set.

In additional to primer redesign and efficiency assessment, the reference gene primer set must be evaluated across all the treatment groups to demonstrate that the gene itself displays consistent expression and remains unaltered during the course of the experiment. To do this, the reference gene must be quantified using multiple technical replicates over multiple biological replicates from each treatment group. Once C_t values are obtained across the treatments, the variance of the average C_t level between biological replications must be calculated. Only if the variance is low (approximately 0.1) can the chosen reference gene be supported as a reliable standard for comparison. This must be done for all reference gene primers sets that are to be used for qRT-PCR.

Once these errors in primer design have been accounted for, additional qRT-PCR can be carried out. It is likely that the inaccuracies in primer location and efficiency are responsible for the large error bars obtained within the qRT-PCR data sets presented here (Chapter 2). By following the previously described criteria, it is likely that these margins will be reduced.

Once new primers for *PDS* and a reference gene primer set have been shown to be both efficient and reliable, both the *Cleome violacea* and *Erucaria erucarioides* qRT-PCR data sets should be rerun and reanalyzed.

Experimental control for *FRUITFULL* downregluation within *C. violacea*

Currently *C. violacea* individuals targeted with the pTRV2-*CvFUL-CvPDS* construct are being compared to untreated individuals. This comparison

does not allow for morphological differences caused by the presence of the viral vector to be distinguished from those caused by the downregulation of *PDS* and *FUL*. Therefore, a new control, pTRV2-*CvPDS* treated *C. violacea,* must be incorporated to identify the phenotypic characteristics that differentiate the treatment with pTRV2-*CvFUL*-*CvPDS* from the pTRV2-*CvPDS* treatment. Only then can the phenotypic characteristics displayed by pTRV2-*CvFUL*-*CvPDS* individuals be associated with the downregulation of *FUL.* This comparison should also be carried out with qRT-PCR analysis.

Future Experimental goals:

qRT-PCR support for *CvFUL* downregulation

With the methodology of VIGS and qRT-PCR detection now elucidated, the following experiments should be completed in order to better support the work presented here.

First, a qRT-PCR data set which supports the downregulation of *FUL* within *C. violacea* must be obtained. Ideally, this will be completed using newly designed primers and will include the following *C. violacea* treatment groups:

i. untreated fruit

ii. untreated leaves

ii. mock treated fruit (pTRV2 only)

iii. mock treated fruit (pTRV2 only)

iv. pTRV2-*CvFUL*-*CvPDS* leaves, non photobleached

v. pTRV2-*CvFUL*-*CvPDS* leaves, photobleached

vi. pTRV2-*CvFUL*-*CvPDS* fruit, non photobleached

vii. pTRV2-*CvFUL-CvPDS* fruit, photobleached

While the purpose of this qRT-PCR data set is to demonstrate *FUL* downregulation, *PDS* should be simultaneously assessed in order to demonstrate its use as a screening marker. It is likely that individuals with a notable fold change reduction of *CvPDS* will also have decreased *CvFUL* transcript abundance.

These treatment groups should be analyzed using at least 4 biological replicates from each treatment with a minimum of three technical replicates each. This must be repeated for each primer set: *CvPDS, CvFUL,* and a minimum of one reference gene.

qRT-PCR support for *CvTCP1* downregulation

A qRT-PCR data set must be obtained to support the downregulation of *CvTCP1* within *C. violacea* target individuals. Currently, three mutant phenotypic categories have been identified from VIGS target downregulation. All three of these should be assessed for their degree of *CvTCP1* silencing. Ideally, this data set will support the hypothesis that the various phenotypes reflect different silencing profiles. The data should be run using new primers and the following treatment groups:

i. untreated flower

ii. mock treated flowers (empty pTRV2)

iii. pTRV2-*CvTCP* flowers, uniform maroon

iv. pTRV2-*CvTCP* flowers, uniform yellow

v. pTRV2-*CvTCP* flowers, reduced adaxial petals.

Each treatment group must be run using a primer set for *CvTCP1* as well as at least one reference gene. Each primer set must include at least 4 biological replicates for each treatment with a minimum of three technical replicates per biological replicate.